THE JOURNAL OF CHEMICAL PHYSICS

VOLUME 11 NUMBER 3

MARCH, 1943

Published by the
AMERICAN INSTITUTE OF PHYSICS
LANCASTER, PA., AND NEW YORK, N. Y.

THE JOURNAL OF CHEMICAL PHYSICS

ADVISORY EDITORIAL BOARD

R. T. BIRGE
A. H. COMPTON
JAMES FRANCK
IRVING LANGMUIR
JOHN T. TATE
HAROLD C. UREY

BOARD OF EDITORS

JOSEPH E. MAYER, *Editor*

Associate Editors

Term ending December 31, 1943

SIDNEY FERED
MAURICE L. HUGGINS
J. G. KIRKWOOD
GEORGE SCATCHARD
J. H. VAN VLECK

Term ending December 31, 1944

CHARLES O. BECKMAN
BRYCE L. CRAWFORD, JR.
P. DEBYE
DAVID HARKER
FRANK H. WESTHEIMER

Term ending December 31, 1945

L. O. BROCKWAY
RONALD W. GURNEY
KENNETH S. PITZER
ALFRED L. SKLAR
E. W. R. STACIE
HUGH S. TAYLOR

THE JOURNAL OF CHEMICAL PHYSICS is published monthly by the American Institute of Physics. Its purpose is to bridge a gap between journals of physics and journals of chemistry. The artificial boundary between physics and chemistry has now been in actual fact completely eliminated, and a large and active group is engaged in research which is as much the one as the other. It is to this group that the Journal is rendering its principal service and makes its greatest appeal, both as a prompt and efficient medium for publication of research and as a convenient and carefully edited assemblage of pertinent information.

Manuscripts for publication should be submitted to Joseph E. Mayer, Havemeyer Hall, Columbia University, New York, New York.

Proof and all correspondence concerning papers in the process of publication should be addressed to the Publication Manager, American Institute of Physics, 175 Fifth Avenue, New York, New York.

Subscriptions and orders for single copies should be addressed to Prince and Lemon Streets, Lancaster, Pennsylvania, or to the American Institute of Physics, 175 Fifth Avenue, New York, New York.

Changes of address should be addressed to the Publication Manager.

Subscription Price

The United States and Possessions, Canada and Mexico $10.00
Elsewhere 11.00

Back Numbers

Complete set: Vol 1, 1933—Vol 10, 1942 ..... $100.00
Yearly rate: $11.00.
Single copies: $1.00 each.

The Journal of Chemical Physics is published monthly at Prince and Lemon Streets, Lancaster, Pennsylvania.

Entered as second class matter December 30, 1932, at the Post Office at Lancaster, Pa., under the Act of August 24, 1912. Acceptance for mailing at special rate of postage prescribed in the Act of February 28, 1925, embodied in paragraph 4, Section 538, P. L. & R., authorized

THE JOURNAL
OF
CHEMICAL PHYSICS

VOLUME 11, NUMBER 3 MARCH, 1943

Vibrational Frequencies of the Isotopic Water Molecules; Equilibria with the Isotopic Hydrogens

W. F. LIBBY*
Department of Chemistry, University of California, Berkeley, California
(Received December 12, 1942)

The fundamental frequencies, anharmonicities, and vibrational modes for the molecules HDO, HTO, DTO, and T_2O are calculated on the basis of Dennison's and Darling's recent analysis of the vibrational spectrum of the H_2O molecule. The equilibrium constants for nine equilibria involving these molecules are given. Experimental values for the reactions $HD+H_2O=H_2+HDO$ and $HT+H_2O=H_2+HTO$ are compared with those calculated. It is concluded that the vibrational potential function is essentially unaltered by isotopic substitution.

THE recent work of Dennison and Darling[1a,1b] on the vibrational levels of the water molecule has considerably improved our knowledge of the detailed nature of the potential function in the ground state.[1c] As a consequence, an improvement in the calculated levels for the isotopic water molecules should result. Several authors[2–6] have given results for HDO and D_2O on the older analyses of the vibration-rotation spectrum of H_2O. The agreement between the results of this research and those previously published is correlated directly with the analysis of the H_2O molecule spectrum adopted in most of the papers.

The discovery of tritium[7] (radioactive hydrogen) has made possible further tests of the fundamental assumption of all such calculations, namely, that the potential function of a molecule shall be independent of the isotopic composition of its constituent elements. The new molecules which are subject to experimental investigation at present are HTO and DTO. The other, T_2O, has not been obtained in sufficient amounts or purity to allow examination, due to the radioactivity of tritium (half-life approximately 30 years[8]).

I. FUNDAMENTAL MODES AND FREQUENCIES

Since substitution of one of the hydrogen atoms of H_2O by D or T destroys the symmetry of the molecule, the form and interactions of the normal modes are altered rather seriously (cf. Fig. 1). In particular the secular equations for

* This research was completed during tenure of a John Simon Guggenheim Fellowship.
[1a] B. T. Darling and D. M. Dennison, Phys. Rev. **57**, 128 (1940).
[1b] D. M. Dennison, Rev. Mod. Phys. **12**, 175 (1940).
[1c] Harald H. Nielsen, Phys. Rev. **62**, 422 (1942), has recently given values for the frequencies and anharmonicities slightly different from those of Dennison and Darling. The differences are so small, however, as to have little effect on the considerations in the present paper.
[2] T. Förster, Zeits. f. physik. Chemie **B27**, 1 (1934).
[3] A. Farkas and L. Farkas, Proc. Roy. Soc. (London) **A144**, 467 (1934).
[4] R. H. Crist and G. A. Dalin, J. Chem. Phys. **2**, 735 (1934).
[5] B. Topley and H. Eyring, J. Chem. Phys. **2**, 217 (1934).
[6] T. Jones and A. Sherman, J. Chem. Phys. **5**, 375 (1937).
[7] L. W. Alvarez and R. Cornog, Phys. Rev. **56**, 613 (1939).
[8] R. D. O'Neal and M. Goldhaber, Phys. Rev. **58**, 574 (1940).

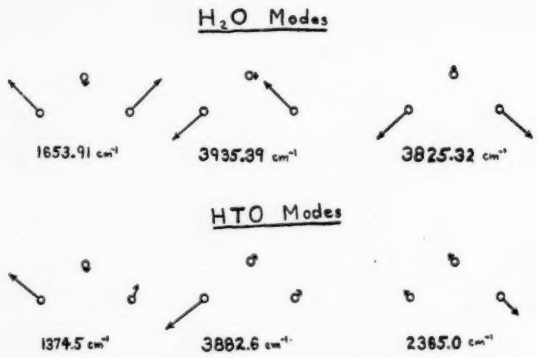

FIG. 1. Normal modes for isotopic water molecules.

the frequencies must be cubics. Cross and Van Vleck[9] have discussed the problem for the general triatomic molecule, arriving at simplified general expressions leading to the secular cubic.

Dennison's and Darling's[1a,1b] analysis gave as the expression for the first-order or simple harmonic potential energy of the water molecule

$$\begin{aligned}2V(\text{ergs}) &= 8.428\times10^5(\delta r_1)^2 \\ &+8.428\times10^5(\delta r_2)^2+0.7676\times10^5(R\delta\alpha)^2 \\ &-2(0.1051)\times10^5(\delta r_1\delta r_2) \\ &+2(0.2521)\times10^5(R\delta\alpha)(\delta r_1\delta r_2)^*\end{aligned} \quad (1)$$

where δr_1 and δr_2 are the differences in cm between the actual distances between the O atom and each of the two hydrogen atoms and the corresponding equilibrium distance, R, and $\delta\alpha$ is the difference in radians between the actual angle between the two lines joining the O atoms to the hydrogens and its equilibrium value. The equilibrium values of R and α are 0.9580A and 104° 31′, respectively.

The fundamental frequencies for the six isotopic molecules based on the above potential are given in Table I. The hydrogen masses used were 1.00813, 2.01473, and 3.01705 for the H, D, and T atoms, respectively.

The normal modes are represented in Table II, where δr_1 always refers to the distance between the O atom and the heavier of the two hydrogen atoms in the molecule. The dimensionless variables, x_i, related to the normal coordinates, Q_i, by

$$x_i = 2\pi(\nu_i/h)^{\frac{1}{2}}Q_i \quad (2)$$

are used. The coefficients are adjusted to give the δr_1, δr_2, and $R\delta\alpha$ values in Angstroms. For classical vibrations x_i ranges from 0 to $\pm\sqrt{2}$.

An interesting characteristic of the normal modes for the asymmetric molecules is that the two stretching vibrations approximate vibrations of the hydroxyl groups with respect to the remaining hydrogen atoms, the two frequencies being separated because of the different masses. This is illustrated in Fig. 1.

The results of the application of the Teller,[10] Redlich[11] product rule are presented in Table III. The rule rigorously requires that insofar as two molecules have identical potential energies for motions of the constituent atoms they must have identical values for the expression

$$\frac{(\pi\nu_i)^2(\pi m_i)^3}{M^3 I_A I_B I_C},$$

in which $\pi\nu_i$ is the product of the frequencies, πm_i is the product of the masses of the constituent atoms, M is the molecular weight, and $I_A I_B I_C$ is the product of the principal moments of inertia. Column 4 of the table contains these values. The check appears to be satisfactory.

II. ANHARMONICITIES

A. Values Uncorrected for Kinetic Energy Perturbations

Dennison and Darling[1] have shown from experimental data that the anharmonicities, X_{ij},

TABLE I. Fundamental frequencies of isotopic water molecules.

Molecule	Frequencies (cm^{-1}) ω_3	ω_1	ω_2
H_2O	3935.59	3825.32	1653.91
HDO	3883.8	2820.3	1449.4
D_2O	2883.79	2758.06	1210.25
DTO	2830.7	2357.1	1117.9
T_2O	2436.12	2296.63	1017.89
HTO	3882.6	2365.0	1374.5

in the energy expression

$$\begin{aligned}W &= \omega_1(n_1+\tfrac{1}{2})+\omega_2(n_2+\tfrac{1}{2})+\omega_3(n_3+\tfrac{1}{2}) \\ &+X_{11}(n_1+\tfrac{1}{2})(n_1+\tfrac{1}{2})+X_{12}(n_1+\tfrac{1}{2})(n_2+\tfrac{1}{2}) \\ &+X_{22}(n_2+\tfrac{1}{2})(n_2+\tfrac{1}{2})+X_{23}(n_2+\tfrac{1}{2})(n_3+\tfrac{1}{2}) \\ &+X_{13}(n_1+\tfrac{1}{2})(n_3+\tfrac{1}{2})+X_{33}(n_3+\tfrac{1}{2})(n_3+\tfrac{1}{2})\end{aligned} \quad (3)$$

[9] Cross and Van Vleck, J. Chem. Phys. 1, 357 (1933).

* Note: The expression (1) differs from that given in reference 1*b* in the sign of the fourth term on the right, apparently because of a typographical error in reference 1*b*.

[10] W. R. Angus, C. R. Bailey, J. B. Hale, C. K. Ingold, A. H. Leckie, C. G. Raisin, J. W. Thompson, and C. L. Wilson, J. Chem. Soc. (London), 971 (1936).

[11] O. Redlich, Zeits. f. physik. Chemie **B28**, 371 (1935).

for the H_2O and D_2O molecules are nearly in the direct ratio $(\omega_i'\omega_j'/\omega_i\omega_j)^{\frac{1}{2}}$ where the primes refer to the H_2O frequencies, a result strictly true for H_2O^{16} *vs.* D_2O^{32}. Since both the H_2O and D_2O molecules are symmetrical, doubts arise that the method is applicable strictly to the asymmetrical molecules HDO, HTO, and DTO when compared with H_2O or D_2O. This point appears to deserve further consideration.

Expressing the potential energy in terms of the dimensionless variables x_i,

$$\begin{aligned}2V=&h\nu_1x_1^2+h\nu_2x_2^2+h\nu_3x_3^2+\alpha_1x_1^3+\alpha_2x_2^3\\&+\alpha_3x_3^3+\alpha_{12}x_1^2x_2^1+\alpha_{21}x_2^2x_1+\alpha_{13}x_1^2x_3\\&+\alpha_{31}x_3^2x_1+\alpha_{23}x_2^2x_3+\alpha_{32}x_3^2x_2+\alpha_{123}x_1x_2x_3\\&+\beta_1x_1^4+\beta_2x_2^4+\beta_3x_3^4+\beta_{12}x_1^2x_2^2+\beta_{13}x_1^2x_3^2\\&+\beta_{23}x_2^2x_3^2+\epsilon_1x_1x_2^3+\epsilon_2x_2x_1^3+\end{aligned}\quad(4)$$

other odd powers of fourth order, standard perturbation theory gives expressions for the anharmonicities in terms of the potential constants. These are given in Appendix I.

Certain small adjustments in the numerical constants in these expressions were made to insure that the expression for the energy W remain a power series in $(n_i+\frac{1}{2})$. Dennison's and Darling's[1] discussion of this point is completely applicable here.

The procedure adopted has been to calculate the α_i and β_i constants for each isotopic water molecule in terms of those for the H_2O molecule and substitute them in the above expressions. Using the expressions in Table II and equating the deformations δr_1, δr_2, and $R\delta\alpha$ for the two molecules leads to a linear relation between the x_i for the isotopic molecule and the x_i' for the H_2O molecule, $x_i'=\sum\gamma_{ij}x_j$.

Substitution in Eq. (4) gives expressions for the α_i and β_i for the isotopic molecule in terms of those for H_2O, α_i' and β_i'. These expressions are given in Appendix II.

Table IV gives the potential constants, those for H_2O being those from Dennison and Darling.

Table V gives the anharmonicities calculated from these constants and the equations in Appendix I.

TABLE II. Normal modes of isotopic water molecules.

Molecule		Modes		
H_2O	$\delta r_1=$	$0.0676x_1$	$-0.00647x_2$	$-0.0690x_3$
	$\delta r_2=$	$0.0676x_1$	$-0.00647x_2$	$+0.0690x_3$
	$R\delta\alpha=$	$0.000946x_1$	$+0.209x_2$	$+\ 0x_3$
HDO	$\delta r_1=$	$0.0824x_1$	$-0.00537x_2$	$+0.0063x_3$
	$\delta r_2=$	$0.00480x_1$	$-0.00559x_2$	$-0.0965x_3$
	$R\delta\alpha=$	$-0.00295x_1$	$+0.196x_2$	$+0.00104x_3$
D_2O	$\delta r_1=$	$0.0573x_1$	$-0.00614x_2$	$-0.0591x_3$
	$\delta r_2=$	$0.0573x_1$	$-0.00614x_2$	$+0.0591x_3$
	$R\delta\alpha=$	$0.0050x_1$	$+0.179x_2$	$+\ 0x_3$
DTO	$\delta r_1=$	$0.0748x_1$	$-0.00371x_2$	$+0.0116x_3$
	$\delta r_2=$	$0.0104x_1$	$-0.00387x_2$	$-0.0820x_3$
	$R\delta\alpha=$	$-0.00895x_1$	$+0.172x_2$	$+0.00486x_3$
T_2O	$\delta r_1=$	$0.0524x_1$	$-0.00623x_2$	$-0.0542x_3$
	$\delta r_2=$	$0.0524x_1$	$-0.00623x_2$	$+0.0542x_3$
	$R\delta\alpha=$	$0.0090x_1$	$+0.1638x_2$	$+\ 0x_3$
HTO	$\delta r_1=$	$0.0754x_1$	$-0.00479x_2$	$+0.00408x_3$
	$\delta r_2=$	$0.00400x_1$	$-0.00509x_2$	$-0.0965x_3$
	$R\delta\alpha=$	$-0.00474x_1$	$+0.191x_2$	$+0.00160x_3$

TABLE III. Product rule check on fundamental frequencies.

Molecule	$\left(\frac{m_1m_2m_3}{M}\right)^3\frac{1}{I_AI_BI_C}$	$(\nu_1\nu_2\nu_3)^2$	$\left(\frac{m_1m_2m_3}{M}\right)^3\frac{(\nu_1\nu_2\nu_3)^2}{I_AI_BI_C}$
H_2O	$\frac{1}{7.9625}$	6.1992	0.7783
HDO	$\frac{1}{3.2405}$	2.5204	0.7777
D_2O	$\frac{1}{1.1928}$	0.92659	0.7764
DTO	$\frac{1}{0.71640}$	0.55636	0.7764
T_2O	$\frac{1}{0.41721}$	0.32433	0.7776
HTO	$\frac{1}{2.0482}$	1.5930	0.7777

B. Kinetic Energy Perturbations

These values for the X_{ij}'s are not quite correct because the motions of the atoms contribute zero angular momentum with respect to axes defined in terms of the equilibrium positions of the atoms only at the instant that the atoms are in these equilibrium positions. The actual motions constitute an oscillatory vibrational motion with respect to these axes. These energies are to be calculated as perturbations of the levels derived on the basis of the axes established with respect to the equilibrium positions. Weinberg and Eckart[12] have discussed this calculation, and Dennison and Darling[1] describe its application

[12] A. Weinberg and C. Eckart, J. Chem. Phys. **5**, 517 (1937).

TABLE IV.

Constant	H_2O	HDO	D_2O	DTO	T_2O	HTO
α_1	−322	−272.2	−197.4	−203.7	−149.7	−208.2
α_2	−47	−36.9	−30.85	−22.7	−24.79	−34.0
α_3	0	431.8	0	264.0	0	433.7
α_{12}	1	45.66	13.08	14.5	20.58	31.45
α_{21}	216	124.7	134.4	101.25	99.1	109.9
α_{13}	0	−34.39	0	−67.0	0	−19.5
α_{31}	−909	−96.48	−562.6	−127.0	−431.1	−72.4
α_{23}	0	−126.4	0	−75.9	0	−121.8
α_{32}	160	74.07	107.9	45.7	86.97	71.8
α_{123}	0	127.2	0	96.74	0	120.9
β_1	39	37.91	20.28	25.79	14.02	26.46
		$-4.57\times10^{-3}\epsilon_2$	$+0.0123\epsilon_2$	$-0.01002\epsilon_2$	$+1.83\times10^{-2}\epsilon_2$	$-0.00497\epsilon_2$
		$+0.00705\epsilon_1$	$-0.00553\epsilon_1$	$+0.0124\epsilon_1$	$-0.00824\epsilon_1$	$+0.00944\epsilon_1$
β_2	2	1.54	1.073	0.908	0.748	1.383
β_3	35	70.44	18.8	36.43	13.37	71.02
		$-2.35\times10^{-3}\epsilon_2$		$-0.00352\epsilon_2$		$-0.00332\epsilon_2$
		$-0.0290\epsilon_1$	$+0.0375\epsilon_1$	$-0.0535\epsilon_1$	$+0.056\epsilon_1$	$-0.0362\epsilon_1$
β_{12}	−116	−72.0	−61.3	−46.45	−42.55	−56.8
		$+0.01002\epsilon_2$	$-0.0163\epsilon_2$	$0.0216\epsilon_2$	$-0.0242\epsilon_2$	$+0.0115\epsilon_2$
β_{13}	212	5.22	112.2	8.62	78.6	4.2
		$-0.0212\epsilon_2$		$-0.0373\epsilon_2$		$-0.0275\epsilon_2$
		$-0.0140\epsilon_1$		$-0.0271\epsilon_1$		$-0.0177\epsilon_1$
β_{23}	−108	−97.4	−57.9	−54.5	−40.8	−92.6
		$+0.0107\epsilon_2$		$+0.0148\epsilon_2$		$+0.0177\epsilon_2$

TABLE V. Anharmonicities (uncorrected for KEP).

	H_2O	HDO	D_2O	DTO	T_2O	HTO
X_{11}	−43.89	−42.27	−22.65	−27.84	−15.71	−29.43
		$-0.00686\epsilon_2$	$+0.0184\epsilon_2$	$-0.0150\epsilon_2$	$0.02745\epsilon_2$	$-0.00746\epsilon_2$
		$+0.0106\epsilon_1$	$-0.0083\epsilon_1$	$+0.0186\epsilon_1$	$-0.0124\epsilon_1$	$+0.0141\epsilon_1$
X_{22}	−19.50	4.1*	−15.92	−13.7*	−8.212	−5.91
X_{33}	−46.37	−77.39	−25.27	−41.77	−18.39	−77.70
		$-0.00353\epsilon_2$		$-0.00528\epsilon_2$		$-0.00498\epsilon_2$
		$-0.0290\epsilon_1$	$+0.0375\epsilon_1$	$-0.0535\epsilon_1$	$+0.056\epsilon_1$	$-0.0362\epsilon_1$
X_{12}	−20.02	−93.7*	−6.76	13.53*	−4.27	−22.45
		$+0.01002\epsilon_2$	$-0.0163\epsilon_2$	$+0.0216\epsilon_2$	$-0.0242\epsilon_2$	$+0.0115\epsilon_2$
X_{13}	−155.06	−16.00	−79.13	−9.01	−56.79	−11.63
		$-0.0212\epsilon_2$		$-0.0373\epsilon_2$		$-0.0275\epsilon_2$
		$-0.0140\epsilon_1$		$-0.0271\epsilon_1$		$-0.0177\epsilon_1$
X_{23}	−51.1	−40.03	−24.32	−20.00	−17.41	−38.35
		$+0.0107\epsilon_2$		$+0.0148\epsilon_2$		$0.0177\epsilon_2$

* Values corrected for resonance splitting of $2\omega_2$ and ω_1 states. New value for $2\omega_2-\omega_1$ is $[(2\omega_2-\omega_1)^2+\alpha_{22}{}^2]^{\frac{1}{2}}$; cf. Section on Resonance Splitting.

to the symmetrical water molecule. The Wilson and Howard[13] Hamiltonian is used.

In general for triatomic molecules the first-order perturbation energy due to this approximate but very simplifying choice of axes is of the form $(1/2C)\bar{P}_z{}^2$ where C is the moment of inertia about the axis perpendicular to the plane of the molecule and $\bar{P}_z{}^2$ is the average square of the angular momentum parallel to this axis.

TABLE VI. Corrections to X_{ij} for kinetic energy perturbations (cm^{-1}).

	H_2O	HDO	D_2O	DTO	T_2O	HTO
X_{12}	0	4.4	0	2.7	0	3.5
X_{13}	0	0	0	0	0	0
X_{23}	31.3	14.5	16.2	8.7	11.2	11.4

[13] E. B. Wilson and J. B. Howard, J. Chem. Phys. **4**, 260 (1936).

TABLE VII. Anharmonicities (fully corrected).

	H_2O	HDO	D_2O	DTO	T_2O	HTO
X_{11}	−43.89	−42.27 $-0.00686\epsilon_2$	−22.65 $+0.0184\epsilon_2$	−27.84 $-0.0150\epsilon_2$	−15.71 $+0.0275\epsilon_2$	−29.43 $-0.00746\epsilon_2$
		$+0.0106\epsilon_1$	$-0.0083\epsilon_1$	$+0.0186\epsilon_1$	$-0.0124\epsilon_1$	$+0.0141\epsilon_1$
X_{22}	−19.50	4.1	−15.92	−13.7	−8.212	−5.91
X_{33}	−46.37	−77.39 $-0.00353\epsilon_2$	−25.27	−41.77 $-0.00528\epsilon_2$	−18.39	−77.70 $-0.00498\epsilon_2$
		$-0.0290\epsilon_1$	$+0.0375\epsilon_1$	$-0.0535\epsilon_1$	$+0.056\epsilon_1$	$-0.0362\epsilon_1$
X_{12}	−20.02	−89.3 $+0.0100\epsilon_2$	−6.76 $-0.0163\epsilon_2$	13.53 $+0.0216\epsilon_2$	−4.27 $-0.0242\epsilon_2$	−18.95 $+0.0115\epsilon_2$
X_{13}	−155.06	−16.00 $-0.0212\epsilon_2$	−79.13	−9.01 $-0.0373\epsilon_2$	−56.79	−11.63 $-0.0275\epsilon_2$
		$-0.0140\epsilon_1$		$-0.0271\epsilon_1$		$-0.0177\epsilon_1$
X_{23}	−19.8	−25.53 $+0.0107\epsilon_2$	−8.12	−11.3 $+0.0148\epsilon_2$	−6.21	−26.95 $+0.0177\epsilon_2$
		$-0.0081\epsilon_1$	$+0.0073\epsilon_1$	$-0.0155\epsilon_1$	$+0.011\epsilon_1$	$-0.00995\epsilon_1$
$\frac{1}{4}\Sigma X_{ij}$	−76.16	−61.6 $-0.00272\epsilon_2$	−39.45 $+0.0005\epsilon_2$	−21.86 $-0.0053\epsilon_2$	−25.34 $+0.0008\epsilon_2$	−42.67 $-0.0027\epsilon_2$

TABLE VIII. Anharmonicities by product method.

	H_2O	HDO	D_2O	DTO	T_2O	HTO
X_{11}	− 43.89	− 23.86	−22.81	−16.65	−15.80	−16.79
X_{22}	− 19.50	− 14.98	−10.44	− 8.90	− 7.37	−13.48
X_{33}	− 46.37	− 45.1	−24.90	−23.9	−17.75	−45.2
X_{12}	− 20.02	− 13.00	−10.56	− 8.32	− 7.37	−10.28
X_{13}	−155.06	−113.0	−81.92	−68.6	−57.45	−94.6
X_{23}	− 19.81	− 17.12	−10.62	− 9.61	− 7.53	−16.23
$\frac{1}{4}\Sigma X_{ij}$	− 76.1	− 56.8	−40.3	−34.0	−28.3	−49.15

TABLE IX. Resonance splitting parameters for symmetrical water molecules.

Molecule	(cm^{-1}) (calc.)	(cm^{-1}) (experimental)
H_2O	+71.7	+74.8
D_2O	+38.5	
T_2O	+27.4	

TABLE X. Resonance splitting parameters for asymmetrical water molecules.

Molecule	(cm^{-1}) calc.
HDO	88.2
DTO	71.8
HTO	77.8

Other first-order terms exist but are negligible for the water molecules. The second-order terms are negligible also for these molecules. The calculation of $\bar{P}_z^2$ is made by expressing P_z, the perpendicular component of the "internal angular momentum," as $(-aQ_2-cQ_3)P_1+(aQ_1+bQ_3)P_2+(cQ_1-bQ_3)P_3$, where the P_i's are the momenta conjugate to the Q_i's. Integrating

$$\int \psi^*_{i,j,k} P_z^2 \psi_{i,j,k} d\tau$$

gives the result. Weinberg and Eckart[12] showed this to be

$$\left(\frac{h}{2\pi}\right)^2 \left\{ \begin{array}{l} a^2(n_1+\frac{1}{2})(n_2+\frac{1}{2})\left(\dfrac{\nu_1}{\nu_2}+\dfrac{\nu_2}{\nu_1}\right) \\ \quad +b^2(n_1+\frac{1}{2})(n_3+\frac{1}{2})\left(\dfrac{\nu_1}{\nu_3}+\dfrac{\nu_3}{\nu_1}\right)-\frac{1}{4} \\ \quad +c^2(n_2+\frac{1}{2})(n_3+\frac{1}{2})\left(\dfrac{\nu_2}{\nu_3}+\dfrac{\nu_3}{\nu_2}\right) \end{array} \right\}$$

where $a^2+b^2+c^2=1$.

The corrections to the anharmonicities therefore are

$$\Delta X_{12}=\frac{1}{2c}\left(\frac{h}{2\pi}\right)^2 a^2\left(\frac{\nu_1}{\nu_2}+\frac{\nu_2}{\nu_1}\right),$$

$$\Delta X_{13}=\frac{1}{2c}\left(\frac{h}{2\pi}\right)^2 \left(\frac{\nu_1}{\nu_3}+\frac{\nu_3}{\nu_1}\right),$$

$$\Delta X_{23}=\frac{1}{2c}\left(\frac{h}{2\pi}\right) c^2\left(\frac{\nu_2}{\nu_3}+\frac{\nu_3}{\nu_2}\right),$$

if the constant term is neglected to preserve the form of the expression for the energy as a power

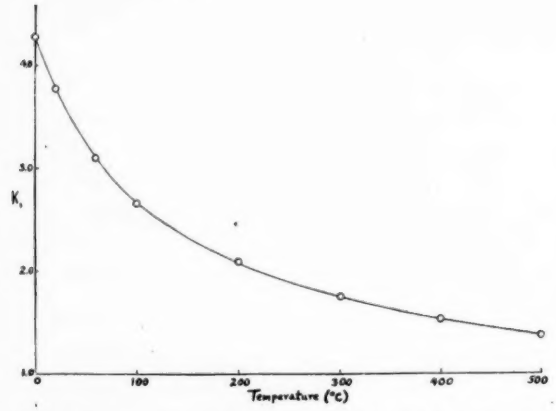

FIG. 2. Theoretical values for $(HDO)(H_2)/(H_2O)(HD)$.

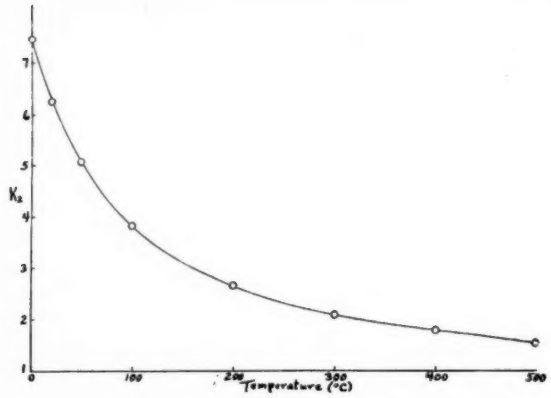

FIG. 3. Theoretical values for $(HTO)(H_2)/(H_2O)(HT)$.

TABLE XI. Frequencies and anharmonicities of hydrogen molecules.

H_2	HD	D_2	DT	T_2	HT
4405.30	3817.09	3117.07	2845.64	2546.50	3598.14
62.66	47.01	31.36	26.14	20.94	41.80

TABLE XII. H_0^0 (calories per mole).

Molecule	H_2O	HDO	D_2O	DTO	T_2O	HTO
H_0^0	13,241	11,480	9,682	8,951	8,148	10,771
Molecule	H_2	HD	D_2	DT	T_2	HT
H_0^0	6,253	5,423	4,433	4,049	3,625	5,114

TABLE XIII. $(F-H_0^0)/T$ values (calories/degree).

Molecules	25°C	100°C	200°C	300°C	400°C	500°C
H_2O	−37.20	−39.00	−40.88	−42.40	−43.70	−44.90
HDO	−39.80	−41.55	−43.50	−45.10	−46.40	−47.50
D_2O	−39.42	−41.15	−43.10	−44.65	−46.00	−47.20
DTO	−41.55	−43.20	−45.20	−46.80	−48.15	−49.40
T_2O	−41.02	−42.64	−44.58	−46.20	−47.57	−48.72
HTO	−40.45	−42.30	−44.10	−45.70	−47.05	−48.30
H_2	−24.37	−25.90	−27.48	−28.78	−29.85	−30.88
HD	−27.48	−29.06	−30.60	−31.88	−33.00	−34.00
D_2	−27.72	−29.26	−30.80	−32.15	−33.25	−34.25
DT	−30.07	−31.64	−33.35	−34.60	−35.67	−36.65
T_2	−29.70	−31.26	−32.82	−34.18	−35.26	−36.20
HT	−28.55	−30.10	−31.66	−32.94	−34.08	−35.03

series in $(n_i+\frac{1}{2})$. This point was discussed in a preceding paragraph.

Table VI gives the corrections and Table VII the final values for the X_{ij}.

Table VIII gives the X_{ij} values calculated by the method used by Darling and Dennison[1] for D_2O. The agreement for individual X_{ij}'s is quite good for the symmetrical molecules and poor for the asymmetric ones, though the contributions to the zero-point energy, $\frac{1}{4}\sum X_{ij}$, are in fair agreement in all cases. The coefficients ϵ_1 and ϵ_2 are taken to be of the same order as the other quartic coefficients, the β's. With this assumption their effects on $\frac{1}{4}\sum X_{ij}$ are of the order of 1 cm^{-1} which is quite small. More accurate experimental investigation will require their evaluation, of course. Since the ϵ's refer to bending coordinates, considerations of the type used by Redlich[14] further justify the expectation that they are small.

III. INFRA-RED SPECTRA AND RESONANCE INTERACTIONS

A valuable check on the results discussed above would be afforded by an experimental determination of the infra-red and Raman spectra of HDO by subtraction of the H_2O and D_2O spectra from the composite obtained for a 50 percent solution of H_2O and D_2O.

Fuson, Randall, and Dennison[15] have given values for about eighty lines of the infra-red spectrum of HDO obtained in this way. An attempt was made to check the frequencies and anharmonicities calculated above against these lines. All lines definitely known to belong to HDO were attributable to relatively probable transitions in the calculated infra-red spectrum. The fit usually was as close as 1 or 2 cm^{-1}. In the absence of intensity data, however, a completely conclusive test can hardly be obtained with so few lines.

The expression (3) for the energy levels is

[14] O. Redlich, J. Chem. Phys. **9**, 298 (1941).
[15] N. Fuson, H. M. Randall, and D. M. Dennison, Phys. Rev. **56**, 982 (1939).

directly applicable, except for the Fermi[16] resonance effect arising in the cases of certain overtones. Dennison and Darling have discussed this problem for the symmetrical H_2O, and D_2O molecules. They found serious interaction between the levels (n_3, n_1, n_2) and (n_3+2, n_1-2, n_2). The levels are split symmetrically, the new separation being $(\delta_0^2+\delta_1^2)^{\frac{1}{2}}$ where δ_0 is the separation for no resonance interaction and δ_1 is given by

$$\delta_1 = 2b^{n_3, n_1, n_2}_{n_3+2, n_1-2, n_2} = hc[n_1(n_1-1)(n_3+1)(n_3+2)]^{\frac{1}{2}}\gamma$$

where

$$\gamma = \tfrac{1}{2}\beta_{13} - \frac{\alpha_{13}^2}{\omega_1} + \frac{\alpha_1\alpha_{31}}{2\omega_1} + \frac{\alpha_{12}\alpha_{32}}{4(2\omega_1-\omega_2)} - \frac{\alpha_{12}\alpha_{32}}{4(2\omega_1+\omega_2)}.$$

TABLE XIV. Masses and moments of inertia.

Molecule	Mass	$I_{ABC}\cdot 10^{120}$ (g cm²)
H_2O	18.01626	5.869
D_2O	20.02946	40.67
T_2O	22.03410	120.5
HDO	19.02286	16.6
DTO	21.03178	70.84
HTO	20.02518	29.40
		I 0.10^{40}
H_2	2.01626	0.4599
D_2	4.02946	0.9191
T_2	6.03410	1.376
HD	3.02286	0.6131
DT	5.03178	1.102
HT	4.02518	0.6894

Table IX contains γ values for the symmetrical molecules.

For the molecules HDO, HTO, and DTO the most seriously resonating levels are (n_3, n_1, n_2) and (n_3, n_1-1, n_2+2). For these

$$\delta_1 = hc[n_1(n_2+1)(n_2+2)]^{\frac{1}{2}}\gamma$$

where $\gamma = \alpha_{21}/\sqrt{2}$.

Table X gives these γ values.

IV. ISOTOPIC EQUILIBRIA BETWEEN THE WATER AND HYDROGEN MOLECULES

The equilibrium constants for the following equilibria can now be evaluated.

(1) $H_2O+HD=HDO+H_2$
(2) $H_2O+HT=HTO+H_2$
(3) $D_2O+DT=DTO+D_2$
(4) $D_2O+HD=HDO+D_2$
(5) $H_2O+D_2O=2HDO$
(6) $T_2O+DT=DTO+T_2$
(7) $T_2O+HT=HTO+T_2$
(8) $H_2O+T_2O=2HTO$
(9) $D_2O+T_2O=2DTO.$

The fundamental frequencies and anharmonicities for the hydrogen molecules are given in Table XI.

TABLE XV. Equilibrium constants.

Equilibrium	20°C	100°C	200°C	300°C	400°C	500°C
(1) $\frac{(HDO)(H_2)}{(H_2O)(HD)}$	3.78	2.65	2.09	1.75	1.54	1.37
(2) $\frac{(HTO)(H_2)}{(H_2O)(HT)}$	6.24	3.83	2.66	2.09	1.77	1.52
(3) $\frac{(DTO)(D_2)}{(D_2O)(DT)}$	1.58	1.37	1.17	1.15	1.12	1.08
(4) $\frac{(HDO)(D_2)}{(D_2O)(HD)}$	1/3.00	1/2.27	1/1.78	1/1.55	1/1.40	1/1.29
(5) $\frac{(HDO)^2}{(H_2O)(D_2O)}$	4.10	4.13	4.16	4.17	4.17	4.18
(6) $\frac{(DTO)(T_2)}{(T_2O)(DT)}$	1/1.77	1/1.45	1/1.36	1/1.24	1/1.19	1/1.18
(7) $\frac{(HTO)(T_2)}{(T_2O)(HT)}$	1/5.00	1/3.10	1/2.27	1/1.84	1/1.62	1/1.52
(8) $\frac{(HTO)^2}{(H_2O)(T_2O)}$	3.18	3.57	3.71	3.77	3.82	3.83
(9) $\frac{(DTO)^2}{(D_2O)(T_2O)}$	3.32	3.66	3.74	3.78	3.78	3.79

[16] E. Fermi, Zeits. f. Physik **71**, 250 (1931).

TABLE XVI.

Temp. (°C)	K_{Theor}	$K_{1\text{Exp}}$	Reference
20	3.78	2.67	(1)
		3.2	(2*a*, *b*)
			Corrected from value of 3.8 for liquid water
527	1.37	1.28	(3)

[1] A. Farkas and L. Farkas, Trans. Faraday Soc. **30**, 1076 (1934).
[2a] Bonhoeffer and Rummel, Naturwiss. **22**, 45 (1934).
[2b] K. F. Bonhoeffer, Zeits. f. Elektrochemie **40**, 469 (1934).
[3] See reference 4 in text.

The values for D_2 and HD are those given by Teal and MacWood.[17] The other values were calculated from the H_2 values by use of the ratios of the reduced masses of the molecules.

Table XII contains the H_0^0 values for the water and hydrogen molecules calculated from the fundamental frequencies and anharmonicities contained in Tables I, VII, and XI.

Table XIII contains $(F-H_0^0)/T$ values for the water and hydrogen molecules, nuclear spin entropies being omitted.

The masses and moments of inertia used are listed in Table XIV.

The equilibrium constants are given in Table XV. K_1 and K_2 are plotted in Figs. 2 and 3. They should be accurate to about two percent.

V. DISCUSSION

The experimental values for $(HDO)(H_2)/(H_2O)(HD)$ reported in the literature are given in Table XVI.

[17] G. K. Teal and G. E. MacWood, J. Chem. Phys. **3**, 760 (1935).

TABLE XVII. Experimental values for $(HTO)(H_2)/(H_2O)(HT)$.

Temp. (°C)	$K_{\text{Theor.}}$	$K_{\text{Exp.}}$	Source
20	6.24	6.3±0.08	Taylor and Black Private communication
28	5.80	5.3±0.5	Author
280	2.00	1.9±0.1	Author

The analogous tritium constant $(HTO)(H_2)/(H_2O)(HT)$ can be measured by equilibration with Pt of a H_2O, H_2 system containing tritium in both the H_2O and H_2 species as HTO or HT. The concentration of tritium will be so low ($\sim 10^{-10} M$) that no precautions need be taken about other equilibria. After equilibration the hydrogen and water vapor are introduced into the gas of a Geiger-Müller counter or electroscope and the relative specific radioactivities determined. The author has made a few measurements of this constant and a more extensive study is being made by Mr. James F. Black and Professor H. S. Taylor of Princeton University. Table XVII gives the results to date.

In view of the agreement for the tritium case and the difficulties of the determination in the deuterium case due to other equilibria, the author believes that the fundamental assumption of the essential identity of the potential functions of isotopic molecules is correct.

The author is much indebted to Professor H. S. Taylor and Mr. James F. Black for permission to quote their data. He wishes to thank the John Simon Guggenheim Memorial Foundation also for the Fellowship during which this work was completed.

APPENDIX I. EXPRESSIONS FOR THE ANHARMONICITIES IN TERMS OF THE POTENTIAL CONSTANTS

$$X_{11}=\tfrac{3}{2}\beta_1-\frac{15}{4}\frac{\alpha_1^2}{\omega_1}-\frac{\overset{2}{\alpha}_{12}}{2\omega_2}-\frac{\overset{2}{\alpha}_{13}}{2\omega_3}-\frac{\overset{2}{\alpha}_{12}}{8(2\omega_1-\omega_2)}+\frac{\overset{2}{\alpha}_{12}}{8(2\omega_1-\omega_2)}-\frac{\overset{2}{\alpha}_{13}}{8(2\omega_1+\omega_3)}+\frac{\overset{2}{\alpha}_{13}}{8(2\omega_1-\omega_3)},\tag{5}$$

$$X_{22}=\tfrac{3}{2}\beta_2-\frac{15}{4}\frac{\alpha_2^2}{\omega_2}-\frac{\overset{2}{\alpha}_{23}}{2\omega_3}-\frac{\overset{2}{\alpha}_{21}}{2\omega_1}-\frac{\overset{2}{\alpha}_{21}}{8(2\omega_2+\omega_1)}+\frac{\overset{2}{\alpha}_{21}}{8(2\omega_2-\omega_1)}-\frac{\overset{2}{\alpha}_{23}}{8(2\omega_2+\omega_3)}+\frac{\overset{2}{\alpha}_{23}}{8(2\omega_2-\omega_3)},$$

$$X_{33}=\tfrac{3}{2}\beta_3-\frac{15}{4}\frac{\alpha_3^2}{\omega_3}-\frac{\overset{2}{\alpha}_{31}}{2\omega_1}-\frac{\overset{2}{\alpha}_{32}}{2\omega_2}-\frac{\overset{2}{\alpha}_{31}}{8(2\omega_3+\omega_1)}+\frac{\overset{2}{\alpha}_{31}}{8(2\omega_3-\omega_1)}-\frac{\overset{2}{\alpha}_{32}}{8(2\omega_3+\omega_2)}+\frac{\overset{2}{\alpha}_{32}}{8(2\omega_3-\omega_2)},$$

$$X_{12}=\beta_{12}-\frac{3\alpha_1\alpha_{21}}{\omega_1}-\frac{3\alpha_2\alpha_{12}}{\omega_2}-\frac{\overset{2}{\alpha}_{12}}{2(2\omega_1+\omega_2)}-\frac{\overset{2}{\alpha}_{12}}{2(2\omega_1-\omega_2)}-\frac{\overset{2}{\alpha}_{21}}{2(2\omega_2+\omega_1)}-\frac{\overset{2}{\alpha}_{21}}{2(2\omega_2-\omega_1)}$$
$$-\frac{\alpha_{13}\alpha_{23}}{\omega_3}-\frac{\overset{2}{\alpha}_{123}}{8(\omega_1+\omega_2-\omega_3)}-\frac{\overset{2}{\alpha}_{123}}{8(\omega_1+\omega_2+\omega_3)},$$

$$X_{13}=\beta_{13}-\frac{3\alpha_1\alpha_{31}}{\omega_1}-\frac{3\alpha_3\alpha_{13}}{\omega_3}-\frac{\overset{2}{\alpha}_{13}}{2(2\omega_1+\omega_3)}-\frac{\overset{2}{\alpha}_{13}}{2(2\omega_1-\omega_3)}-\frac{\overset{2}{\alpha}_{31}}{2(2\omega_3+\omega_1)}-\frac{\overset{2}{\alpha}_{31}}{2(2\omega_3-\omega_1)}$$
$$-\frac{\alpha_{12}\alpha_{32}}{\omega_2}-\frac{\overset{2}{\alpha}_{123}}{8(\omega_1+\omega_3-\omega_2)}-\frac{\overset{2}{\alpha}_{123}}{8(\omega_1+\omega_2+\omega_3)},$$

$$X_{23}=\beta_{23}-\frac{3\alpha_2\alpha_{32}}{\omega_2}-\frac{3\alpha_3\alpha_{23}}{\omega_3}-\frac{\overset{2}{\alpha}_{23}}{2(2\omega_2+\omega_3)}-\frac{\overset{2}{\alpha}_{23}}{2(2\omega_2-\omega_3)}-\frac{\overset{2}{\alpha}_{32}}{2(2\omega_3+\omega_2)}-\frac{\overset{2}{\alpha}_{32}}{2(2\omega_3-\omega_2)}$$
$$-\frac{\alpha_{21}\alpha_{31}}{\omega_1}-\frac{\overset{2}{\alpha}_{123}}{8(\omega_2+\omega_3-\omega_1)}-\frac{\overset{2}{\alpha}_{123}}{8(\omega_1+\omega_2+\omega_3)},$$

APPENDIX II. EXPRESSIONS FOR THE POTENTIAL CONSTANTS OF ONE ISOTOPIC MOLECULE IN TERMS OF THOSE OF ANOTHER

$$\alpha_i=\alpha_1'\overset{3}{\gamma}_{1i}+\alpha_2'\overset{3}{\gamma}_{2i}+\alpha_{12}'\overset{2}{\gamma}_{1i}\gamma_{2i}+\alpha_{21}'\gamma_{2i}\overset{2}{\gamma}_{1i}+\alpha_{31}'\overset{2}{\gamma}_{3i}\gamma_{1i}+\alpha_{32}'\gamma_{3i}\overset{2}{\gamma}_{2i}, \qquad (i=1,2,3) \quad (6)$$

$$\alpha_{ij}=3\alpha_1'\overset{2}{\gamma}_{1i}\gamma_{1j}+3\alpha_2'\overset{2}{\gamma}_{2i}\gamma_{2j}+\alpha_{12}'(\overset{2}{\gamma}_{1i}\gamma_{2j}+2\gamma_{1i}\gamma_{2i}\gamma_{1j})+\alpha_{21}'(\overset{2}{\gamma}_{2i}\gamma_{1j}+2\gamma_{1i}\gamma_{2i}\gamma_{2j}) \qquad (i,j=1,2,3)$$
$$+\alpha_{31}'(\overset{2}{\gamma}_{3i}\gamma_{1j}+2\gamma_{1i}\gamma_{3i}\gamma_{3j})+\alpha_{32}'(\overset{2}{\gamma}_{3i}\gamma_{2j}+2\gamma_{2i}\gamma_{3i}\gamma_{3j}), \quad (7)$$

$$\alpha_{123}=6\alpha_1'\gamma_{11}\gamma_{12}\gamma_{13}+6\alpha_2'\gamma_{21}\gamma_{22}\gamma_{23}+2\alpha_{12}'(\gamma_{11}\gamma_{12}\gamma_{23}+\gamma_{11}\gamma_{22}\gamma_{13}+\gamma_{21}\gamma_{12}\gamma_{13})$$
$$+2\alpha_{21}'(\gamma_{21}\gamma_{22}\gamma_{13}+\gamma_{21}\gamma_{12}\gamma_{23}+\gamma_{11}\gamma_{22}\gamma_{23})+2\alpha_{31}'(\gamma_{31}\gamma_{32}\gamma_{13}+\gamma_{31}\gamma_{12}\gamma_{33}+\gamma_{11}\gamma_{32}\gamma_{33})$$
$$+2\alpha_{32}'(\gamma_{31}\gamma_{32}\gamma_{23}+\gamma_{31}\gamma_{22}\gamma_{33}+\gamma_{21}\gamma_{32}\gamma_{33}), \quad (8)$$

$$\beta_i=\sum_1^3\beta_j'(\gamma_{ji})^4+\beta_{12}'(\overset{2}{\gamma}_{1i}\overset{2}{\gamma}_{2i})+\beta_{13}'(\overset{2}{\gamma}_{1i}\overset{2}{\gamma}_{3i})+\beta_{23}'(\overset{2}{\gamma}_{2i}\overset{2}{\gamma}_{3i})+\epsilon_1(\gamma_{1i}\overset{3}{\gamma}_{2i})+\epsilon_2(\gamma_{2i}\overset{3}{\gamma}_{1i}), \qquad (i=1,2,3) \quad (9)$$

$$\beta_{jk}=6\sum_1^3\beta_i'\overset{2}{\gamma}_{ij}\overset{2}{\gamma}_{ik}+\beta_{12}'(\overset{2}{\gamma}_{1j}\overset{2}{\gamma}_{2k}+4\gamma_{1j}\gamma_{2j}\gamma_{1k}\gamma_{2k}+\overset{2}{\gamma}_{1k}\overset{2}{\gamma}_{2j})+\beta_{13}'(\overset{2}{\gamma}_{1j}\overset{2}{\gamma}_{3k}+4\gamma_{1j}\gamma_{3j}\gamma_{1k}\gamma_{3k}+\overset{2}{\gamma}_{1k}\overset{2}{\gamma}_{3j}) \qquad (j,k=1,2,3)$$
$$+\beta_{23}'(\overset{2}{\gamma}_{2j}\overset{2}{\gamma}_{3k}+4\gamma_{2j}\gamma_{3j}\gamma_{2k}\gamma_{3k}+\overset{2}{\gamma}_{2k}\overset{2}{\gamma}_{3j})+3\epsilon_1(\gamma_{1j}\gamma_{2j}\overset{2}{\gamma}_{2k}+\gamma_{1k}\gamma_{2k}\overset{2}{\gamma}_{2j})+3\epsilon_2(\gamma_{2j}\gamma_{1j}\overset{2}{\gamma}_{1k}+\gamma_{2k}\gamma_{1k}\overset{2}{\gamma}_{1j}). \quad (10)$$

The Surface Recombination of H Atoms and OH Radicals

W. V. SMITH
*Jefferson Physical Laboratory, Harvard University, Cambridge, Massachusetts**

(Received November 20, 1942)

A diffusion method of investigating surface recombination of atoms by substances of low catalytic power is presented. By this method we have evaluated the coefficient of recombination γ for H and OH on Pyrex for a temperature range of over 500°C. For smaller ranges of temperature we have found the recombination of H on a number of salts, and have found this recombination to be strongly dependent on the dryness of the surface. All salts investigated save KCl strongly recombined H when dry. Salts recombining H could not be investigated for OH recombination. However KCl, which did not recombine H, did recombine OH strongly. A number of strong dehydrogenating and dehydrating agents were tested for differences in H and OH recombination, but no difference was found.

INTRODUCTION

ALTHOUGH the investigation of surface recombinations of many atoms and radicals is still in the qualitative stage, quantitative results have already been obtained for the rate of recombination of H atoms on glass[1] and on certain metals.[2] By a modification in the experimental arrangement of previous investigators involving a change in the theory of the experiment, we have been able to extend these data and especially to find the variation of the coefficient of recombination γ (the fraction of times an atom striking the surface leaves as part of a molecule) with temperature.

1. EXPERIMENTAL PROCEDURE

The experimental procedure consists in allowing atoms that are formed by a low pressure gaseous discharge to diffuse through a side arm part of whose inner surface is coated with the material under investigation. Some of the atoms are lost to the coated walls and the remainder which succeed in passing through the side arm are detected by the heat of recombination they liberate at a small probe coated with some highly catalytic substance (Pt to detect H[2]; KCl to detect OH).[3] A high probe temperature indicates that few atoms are lost to the walls of the side arm, whereas a low probe temperature shows that many atoms are lost to the walls. By varying the probe distance, the decay in atomic concentration with distance from the juncture of discharge tube and side arm can be found, yielding an absolute measure of the coefficient of recombination; and with probe distance fixed, variation of the temperature of the coated section of the side arm yields the temperature dependence of the recombination coefficient.

Figure 1 is a diagram of the apparatus. The hydrogen was evolved electrolytically from a concentrated solution S of NaOH and passed through a water trap T which regulated the

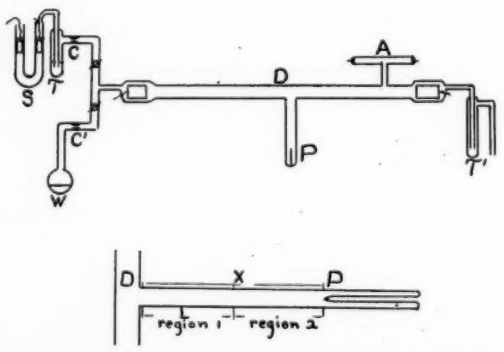

FIG. 1. Diagram of apparatus. S and W are sources of H_2 and H_2O, respectively. T and T' are traps. C and C' are capillary tubes restricting gas flow through discharge tube D. A is auxiliary discharge. P is probe at distance X from discharge. The temperature of region 1 of length L is varied. Region 2 is at room temperature.

* Now at Massachusetts Institute of Technology, Radiation Laboratory.

[1] H. G. Poole, Proc. Roy. Soc. **163**, 404 (1937); W. Steiner, Trans. Faraday Soc. **31**, 962 (1935). These values were obtained by complicated computations under conditions where the surface recombination was only a correction to a predominant volume recombination.

[2] K. F. Bonhoeffer, Zeits. f. physik. Chemie **113**, 199 (1924).

[3] H. S. Taylor and G. I. Lavin, J. Am. Chem. Soc. **52**, 1910 (1930).

percent of water vapor in the gas.[4] It was thence pumped through a capillary tube C and on through the discharge tube D by a Cenco Hyvac pump. A continuous flow of hydrogen through the discharge tube ensured freedom from impurities. The water vapor source was simply a bulb W of distilled water, the vapor of which was pumped through a capillary tube C' into the discharge tube. The trap T', placed in dry ice, kept the water vapor out of the pump. A 100-milliampere current passed through the tube dissociated the gases respectively into H+H and H+OH[5].

The gases were investigated at pressures less than 0.1 mm, the pressure being governed by the capillary restriction and the pumping speed. The dark space of an auxiliary discharge A with plane electrodes was used to measure the pressure. It was calibrated against a McLeod gauge for hydrogen and against the vapor pressure of ice at known temperatures for water vapor. All stopcocks were lubricated with special low vapor pressure grease and were placed out of range of the atomic hydrogen.

The temperature of the probe P was measured by a copper-advance thermocouple with the cold junction 2 or 3 cm from the hot junction, thereby measuring the temperature difference of the gas and the heated probe. The whole thermocouple was separated from the low pressure gas by a glass wall, thin at the tip, so that the thermocouple junction (at atmospheric pressure) assumed the temperature of the platinum coating on the low pressure side of the glass. The probe was glass-blown to the side arm to avoid waxes or greases which might be attacked by atomic hydrogen.

The experimental procedure is based on the following considerations: The surface recombination of atoms must compete with recombination by triple collisions in the gas phase. Simple calculations show that with γ of the order of 10^{-5} (the smallest value found was 2×10^{-5}), in apparatus of the dimensions used a pressure of 0.1 mm is sufficiently low to make volume recombination negligible.[6] However at this low pressure diffusion becomes very rapid. Therefore, one cannot very well observe the recombination by the decay of concentration along a tube through which gas is flowing. A pumping speed high enough to make diffusion negligible is not practicable, particularly for H. Furthermore, the smaller γ, the smaller is the pumping speed required to produce a given concentration gradient of atoms along the side arm. Thus, rather than attempt cumbersome and inaccurate corrections for the influence of diffusion on flow velocity, it is far simpler to rely on diffusion alone to transport the atoms to the probe. It is in this reliance on diffusion rather than pumping that our experiment differs from previous ones.

Adoption of a diffusion scheme however requires that our detecting apparatus influence the atomic concentration as little as possible. Two techniques are available which have less disturbing influence than the one we adopted. They are the spectroscopic method of Steiner[7] and the Wrede slit method.[8] Both techniques are rather complicated however, the Wrede one especially so, and both have difficulties in interpretation, particularly the Steiner spectroscopic method. Simplicity of design was a consideration in our experiment as we investigated numerous different samples, necessitating frequent cleaning of our apparatus. Furthermore, we are able to show that most of our results are unaffected by the recombination at the probe.

---

[4] Addition of about two percent water vapor poisons the glass walls to H recombination. [R. W. Wood, Proc. Roy. Soc. **97**, 455 (1920).] Other poisoning agents such as metaphosphoric acid were avoided as they contain an indeterminate amount of water vapor and also make cleaning of the apparatus more difficult.

[5] Spectroscopic observations have shown H and OH to be the only important decomposition products of an electric discharge through water vapor. [K. F. Bonhoeffer and T. G. Pearson, Zeits. f. physik. Chemie. **B-14**, 1 (1931).]

[6] Steiner (reference 1), reports volume recombination 3 times as effective as surface recombination for a pressure of 0.3 mm and tube diameter of 25 mm. This is not inconsistent with our criterion when due account is taken of his different pressure and diameter. Furthermore, his lower value of γ indicates better poisoned glass than that with which we worked.

[7] Z. Bay and W. Steiner, Zeits. f. physik. Chemie **B3**, 149 (1929). The relative atomic concentration at points along a side arm from the discharge tube is deduced from the spectra of weak localized high frequency discharges induced at these respective points.

[8] This method relies on the different velocities of effusion of molecules and atoms through a small slit. The differences in theoretical slit sizes necessary and the sizes used by experimenters has been criticized by Poole [Proc. Roy. Soc. **163**, 424 (1937)].

Besides simplifying the mathematics, the diffusion method avoids stray discharges as there are no grounded points along the side arm. We wish to emphasize this point as it is particularly important if any significance is to be attached to low probe temperatures, which might otherwise be ascribed to the effect of stray discharges. With a flow through the side arm, which always ends with the pump as a grounded point, it is difficult to be sure stray discharges are avoided, especially when an alternating voltage is applied to the discharge.

2. THEORY OF THE EXPERIMENT

The atomic concentration at various distances from the discharge along a side arm will vary, as different parameters such as pressure, temperature, and degree of dissociation in the discharge are varied. The nature of this variation will differ according to the mechanism responsible for the recombination process. Four types of mechanisms are possible. They are:

1. A first-order wall effect with total recombination directly proportional to atomic concentration. Such an effect results from the assumption that each atom striking the wall has a definite probability of sticking to the wall and, once it sticks, is certain eventually to combine with a second atom and leave the wall as part of a molecule. This might be the mechanism of recombination on poor catalysts. The assumption of the wall being completely covered with a monolayer of atoms, independent of pressure, also results in first order recombination as in this case the number of molecules leaving the wall per second can vary only in direct proportion to the number of atoms striking the wall per second. Good catalysts, such as Pt, probably fall in this class. Whatever the mechanism responsible for such an effect, it can be described by assigning a coefficient of recombination γ to each atom striking the wall signifying the probability that the atom will eventually leave the wall as part of a molecule.

2. A second-order wall effect. Recombination proportional to the square of the pressure results from the assumption that each atom striking the wall adheres to it a short time only and that recombination will occur if, during this time, another atom strikes the wall within a certain (small) distance of the first atom. Any practical case intermediate in pressure dependence between 1 and 2 can be resolved into these two parts.

3. Triple collisions in the gas phase.

4. Preponderant effect of the probe. If there were no wall recombination nor any losses of atoms by triple collisions, but only a large recombination at the probe, there would still be a variation of probe temperature with distance from the discharge as the transport of atoms to the probe is a function of the distance and the coefficient of diffusion. We cannot deduce from the small probe area (5×10^{-3} cm^2) that it is negligible, as the recombination is 10^4 or more times as great on Pt as on glass. (See Table II.)

From our measurements we want to decide between cases 1, 2, 3, and 4. For this purpose, we carry through the theory for each of the four cases and find which checks best with experiment.

Let n = number of atoms/cc
x = distance along side arm from junction with discharge tube
D = coefficient of diffusion
F = drift velocity of atoms along side arm
γ = coefficient of recombination
S = cross-sectional area of side arm
C = circumference of side arm
$\bar{v}$ = average atomic speed
p = pressure.

The subscript 0 in the following derivations indicates the junction of the side arm with the discharge tube (Fig. 1).

We will assume the concentration is constant over the cross section so that $n=n(x)$ only. We assume also $F=F(x)$.[9] Hence for all four cases

[9] For the equation of diffusion to be applicable to our problem, we must have $2r \gg \lambda$. (r is the radius of the side arm; λ, the mean free path.) Also, n will equal $n(x)$ only if the diffusion is rapid enough to wipe out concentration gradients within any cross section which the losses to the walls tend to establish. A typical time for diffusion to wipe out these gradients is given by the relaxation time for diffusive equilibrium in an enclosure of dimensions r: $t=r^2/D \backsimeq 3r^2/\lambda\bar{v}$. This time must be small compared to the time necessary for destruction of all atoms in the volume V, neglecting the effect of diffusion. It is

$$t=\frac{nV}{n\bar{v}S\gamma/4}=\frac{2r}{\bar{v}\gamma}.$$

Therefore our complete condition for validity of our

the equation of diffusion applies in its simplest form:

$$nF = -D\frac{dn}{dx}. \tag{1}$$

A second equation between n, F, and x is obtained by expressing the decay of the concentration n along the length x of the side tube in terms of the mechanism by which the atoms are removed. We may derive the dependence of n on x for cases 1 to 3 simultaneously, assuming constant temperature along the side arm. We first equate the number of atoms lost to the wall per cm per second to the gradient of atomic flow through the tube $[-S(d/dx)(nF)]$. The losses to the walls for the three cases are:

$$\begin{aligned}
&\text{(a)}\quad \frac{n\bar{v}}{4}\gamma C && \text{for first-order wall recombination,}\\
&\text{(b)}\quad aCn^2 && \text{for second-order wall recombination,}\\
&\text{(c)}\quad bpSn^2+cSn^3 && \text{for volume recombination.}
\end{aligned} \tag{2}$$

In (c) the first term is for molecules as third bodies and the second for atoms. As our partial pressure of atoms is in general small compared to the total pressure, we will ignore the second term.[10] We then have

$$-S\frac{d}{dx}(nF) = \begin{cases} \dfrac{n\bar{v}}{4}C\gamma \\ aCn^2 \\ bpSn^2. \end{cases} \tag{3}$$

Combining this equation with (1) and solving subject to the boundary condition that $(dn/dx) = 0$ at $n = 0$ [from Eq. (1), dn/dx is proportional to n and in particular approaches 0 as n approaches 0 since although F is variable, it remains finite] we have

$$n = \begin{cases} A\exp(\bar{v}C\gamma/4SD)^{\frac{1}{2}}x + B\exp-(\bar{v}C\gamma/4SD)^{\frac{1}{2}}x \\ \dfrac{n_0}{[1+(n_0aC/6SD)^{\frac{1}{2}}x]^2} \\ \dfrac{n_0}{[1+(n_0bp/6D)^{\frac{1}{2}}x]^2}. \end{cases} \tag{4}$$

In the expression for first-order wall recombination, with a tube of finite length both A and $B \neq 0$. The negative exponent represents a component decreasing with increasing x. The positive exponent represents a stream of atoms reflected from the end of the tube and therefore increases with increasing x. We may however use the rule of thumb that for values of n/n_0 less than about $\frac{1}{4}$ (a condition satisfied by our experimental results) the atoms reflected from the tube end may be ignored; hence, $A \backsimeq 1$ and $B \backsimeq 0$. With obvious changes of constants, we therefore have

$$\begin{aligned}
&\text{(a)}\quad n = n_0\exp-(\beta\gamma^{\frac{1}{2}}x)\\
&\qquad\text{for first-order wall recombination}\\
&\qquad\text{with } \beta = (\bar{v}C/4SD)^{\frac{1}{2}},\\
&\text{(b)}\quad n = \frac{n_0}{[1+K\,(\text{or } K')n_0^{\frac{1}{2}}x]^2}\\
&\qquad\text{for second-order wall recombination}\\
&\qquad\text{(or for volume recombination).}
\end{aligned} \tag{5}$$

We note that β is proportional to $D^{-\frac{1}{2}}$ and hence to $p^{\frac{1}{2}}$ as the coefficient of diffusion D is inversely proportional to the pressure.

To estimate the maximum influence of the probe alone on the concentration (case 4), we will make the assumption that all the atoms striking the cross section where the probe is located are eventually recombined at the probe. We will first analyze the problem under conditions of constant temperature along the side arm.

At X we have destruction of atoms at a rate $(n\bar{v}/4)S$. These atoms are being supplied by diffusion down the side arm at a rate SnF. Therefore at X

$$F = \bar{v}/4. \tag{6}$$

In the region from $x = 0$ to $x = X$, where there are *assumed* to be no losses of atoms by recom-

---

assumptions is $\lambda/2 \ll r \ll 2\lambda/3\gamma$. In practice we have $\lambda = 0.2$ cm, $r = 0.55$ cm, and $\gamma = 10^{-3}$ to 10^{-5}. We see therefore that our assumptions $n = n(x)$ and $F = F(x)$ are valid.

[10] The main conclusion of this derivation—that n/n_0 is a function of n_0, approaching 1 for small n_0, would still hold if this second term were included, but eliminating it simplifies the mathematics. (Data in the literature are not in agreement on the relative effectiveness of atoms and molecules as third bodies promoting volume recombination.)

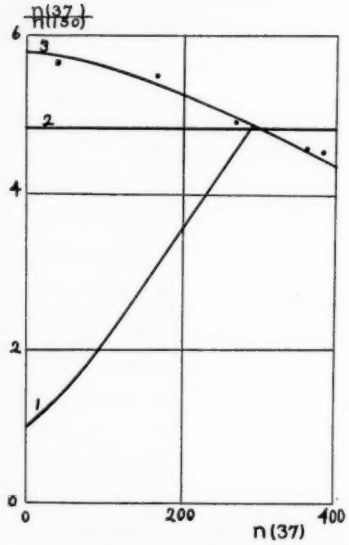

FIG. 2. Variation in the ratio of temperatures of two probes plotted against the temperature of one of these probes. Discharge in H_2; pressure = 78μ. 1 = Theoretical curve for loss of H by three-body collisions. 2 = Theoretical curve for first-order wall recombination of H. 3 = Observed data. (The constants of the theoretical curves were chosen to fit the observed data at the point of intersection.)

bination, we must have conservation of mass transport along the tube, hence

$$\frac{d}{dx}(nF)=0. \tag{7}$$

Combining (7) with the equation of diffusion (1) we get

$$n=n_0-Kx/D, \text{ where } K \text{ is some constant.} \tag{8}$$

This means that there is a linear fall of atomic concentration along the side arm furnishing a gradient to transport atoms to the probe by diffusion. From Eqs. (1), (6), and (8), we therefore derive

$$(F)_X=\frac{K}{n(X)}=\frac{\bar{v}}{4}, \quad \text{whence} \quad K=\frac{n(X)\bar{v}}{4}. \tag{9}$$

Substituting this value of K in (8) and evaluating at $x=X$, we have

$$n(X)=n_0-\frac{n(X)\bar{v}}{4D}X=\frac{n_0}{1+GX} \text{ where } G=\frac{\bar{v}}{4D}. \tag{10}$$

Assuming that not all the atoms crossing X recombine on the probe, but that a large fraction do so (the condition in actual practice) has the effect of making G smaller. We will therefore take the magnitude of G as unknown and examine only the dependence of our equation on X, pressure, and temperature. The latter will prove most useful for correlation with experiment. For this purpose, we will want a solution for the case where the temperature of a portion of the side arm far from the probe is varied (thus changing the density and the coefficient of diffusion). The calculation for this case is straightforward though a bit tedious. The resulting formula is

$$n=\frac{n_0}{1+G\left(X-L+\frac{T_1D_0}{T_0D_1}L\right)}. \tag{11}$$

Here T_1 and D_1 are temperature and coefficient of diffusion in region 1 and T_0 and D_0 are the corresponding values in the discharge tube and in region 2. (See Fig. 1.)

To interpret our results, we must relate probe temperature to atomic concentration. Let us define "probe temperature" $t=T_p-T_0$ where T_p is the actual equilibrium temperature of the probe and T_0 is the temperature of the side arm in which the probe is located. We assume

$$\frac{n\bar{v}}{4}Aq=kt, \tag{12}$$

where A is the probe area, q the heat generated per atom striking the probe, and k the conduction-convection constant. Heat loss of the probe by radiation [which would introduce a term $k'(T_p-T_0)^4$] is neglected.

A complication in our investigation is the necessity of *assuming* this linear relation between probe temperature and atomic concentration, as we cannot divorce the investigation of loss of atoms along the tube from a simultaneous investigation of probe response. Such an assumption is reasonable however, particularly in the case of recombination of H on Pt as it is known that metals are quickly covered with a monolayer of atoms at temperatures ranging from below room temperature to several hundred degree centigrade. If this monolayer is maintained over the partial atomic pressure range investigated, the number of molecules leaving the surface per second must be proportional to the number of atoms striking the surface per second. In any case, a small deviation from linearity in response

would not be serious as most of the concentration variations are exponential in character.

3. RECOMBINATION OF H ON PYREX—DISCHARGE IN H_2

All the samples of Pyrex used were cleaned by scrubbing and rinsing in distilled water, as preliminary investigations showed no difference in results even at high temperatures using other methods of cleaning such as washing in KOH, $KHCrO_4$, H_2SO_4, or HF.

A. Check on Three-Body Collisions and Second-Order Wall Effects

In order to distinguish between Eqs. (5a) and (5b), we note that (5a) predicts n/n_0 independent of n_0, whereas (5b) predicts n/n_0 strongly dependent on n_0, and indeed approaching the value 1 as n_0 approaches 0. The following experiment was therefore performed. Two parallel side arms of equal diameter were attached to the discharge tube, terminating in probes respectively 37 cm and 150 cm from the discharge. The atomic concentration was varied over wide ranges without materially changing the pressure or the coefficient of diffusion by simply varying the current through the discharge tube. The ratio of the two probe readings was then plotted against the temperature of the probe closest to the discharge (Fig. 2). The observed approximate constancy of this ratio, at a value far from 1, is ample evidence that n/n_0 is not dependent on n_0. We conclude therefore that neither three-body collisions nor second-order wall recombination on moist Pyrex walls are important factors in H recombination at the pressure and temperature investigated (78 microns, and 23°C).

B. Check on the Effect of the Probe

If the probe recombination predominates, a change of temperature of region 1, Fig. 1, should have an effect predicted by Eq. (11). This is checked in Fig. 3 where the probe temperature, indicating the number of H atoms arriving per second, is plotted against the temperature of section L of the side arm. For comparison the theoretical curves derived from Eq. (11) (predominant probe recombination) are also plotted. These theoretical curves are adjusted to fit the experimental values at room temperature.

Obviously at temperatures other than room temperature the probe recombination does not predominate. However as the surface recombination is lowest at room temperature (see Fig. 6), this argument does not eliminate the possibility of important disturbance from the probe at room temperature. Values of γ calculated by ignoring the probe effect may however be considered maximum values, and all results for various surfaces at various temperatures yielding a γ considerably larger than the least of these values may be considered reliable. Furthermore, the assumption of negligible probe effect appears justified even at room temperature in view of the agreement between experiment and theory shown below in Figs. 4 and 5. This result is plausible since the pressure is kept so low and the probe area so small that we should expect the first-order wall effect to predominate.

C. Computation of γ at Room Temperature

1. Computation from the Decay in Atomic H *Concentration Along the Side Arm. (Fig. 4)*

From Eqs. (5a) and (12) we have

$$t=\frac{n_0\bar{v}Aq}{4k}\exp-(\beta\gamma^{\frac{1}{2}}x). \tag{13}$$

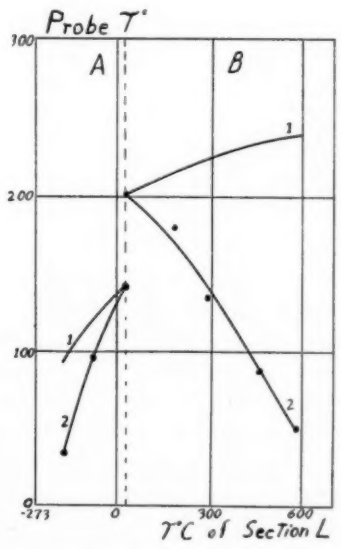

FIG. 3. Variation of probe temperature with temperature of furnace located at region 1 of Fig. 1. H_2 pressure = 80μ. 1 = Theoretical curve for atomic gradient caused by recombination at probe, normalized to observed data at 20°C. 2 = Observed data. A: $L=58$; $X=70$. B: $L=20$; $X=50$.

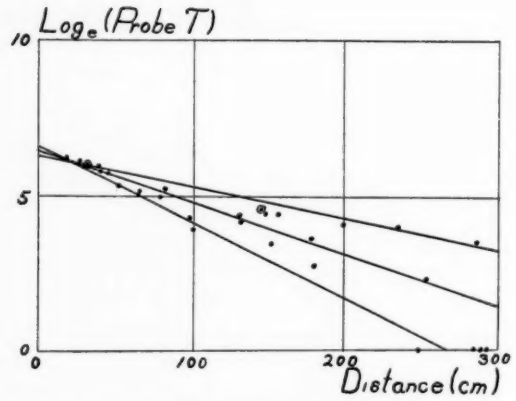

FIG. 4. Variation of probe temperature with distance from a H_2 discharge. Pressure = 75μ. Circled points correspond to circled point of Fig. 5.

Therefore in a series of experiments in which n_0, $\bar{v}$, etc., are kept constant, we derive

$$\log_e t = -\beta_0 \gamma^{\frac{1}{2}} x + C', \tag{14}$$

where C' = some constant.

For $p = 75\mu$, $\beta_0 = 3.73$ (see Section D).

Three lines are drawn through the points in Fig. 4 showing the mean and extreme values of the slope. The corresponding values of γ calculated are

$$\gamma = \left.\begin{matrix} 0.75 \\ 2.01 \\ 4.56 \end{matrix}\right\} \times 10^{-5}. \tag{15}$$

The variations in γ are of the order of 2 or $\frac{1}{2}$ from the mean. As numerous different samples of Pyrex were used the variation in γ is reasonable.

2. Computation from Pressure Variation of n_0/n

Equation (5a) may be written

$$\log_e (n_0/n) = \left(\frac{\beta' x_0 \gamma^{\frac{1}{2}}}{75^{\frac{1}{2}}}\right) p^{\frac{1}{2}} \tag{16}$$

where p is in microns and β' is the value of β at 75μ pressure.

In Fig. 5, $\log_e n(30)/n(145)$ is plotted against $p^{\frac{1}{2}}$. The theoretical curve 16, a straight line through the origin, gives a good fit to the experimental points. Some deviation is observed at pressures below 80 microns. This is possibly caused by a breakdown in the assumption of uniform drift velocity F along the tube cross section since for these pressures the mean free path (1.1 mm at 80μ) is no longer negligible compared to the tube diameter (1.1 cm).

The value of γ calculated from 16 and Fig. 5 is

$$\gamma = 1.05 \times 10^{-5}. \tag{17}$$

The probe temperatures at 30 and 145 cm used in Fig. 5 for a pressure of 75μ are also plotted on Fig. 4 (the circled points). They are seen to represent a value of γ nearer the lowest value than the mean value deduced from Fig. 4. These values (see 15) are 0.75×10^{-5} and 2.01×10^{-5}. The check of 1.05 with 0.75 is excellent.

3. Comparison with Other Values

Steiner[1] reported γ on moist glass varying between 2×10^{-6} and 9×10^{-6}. Poole[1] reported a value of γ of 1.6×10^{-4}. Our values lie between these two extremes. Poole's results are for glass under the actual conditions of the discharge however, for which γ is to be expected comparatively large. The agreement of these values with ours is very good in view of the complicated mathematics used in the work of the other two investigators where the wall recombination was a minor effect. The simplicity of interpretation of our results plus the fact that the wall recombination was the preponderant agent removing the atoms in the pressure region we investigated would seem to give greater confidence to our results.

D. Experiments at Other Temperatures

In these experiments, the pressure, tube current, and distance X are kept constant while the temperature of a section L near the discharge is changed by means of a furnace or low temperature bath (see Fig. 1). In some runs a parallel check side arm and probe was used to see if the atomic H production remained constant during the run. It was found that the probe temperature in this check side arm would vary by a factor of 2 or $\frac{1}{2}$ for the first few hours and then remain constant often to 10 percent for over twelve hours. Occasional larger fluctuations seemed to be caused by local variations in the check side arm or check probe and to have no relation to the H concentration near the main side arm, as this probe did not show fluctuations at the same time. The best check on our temperature variation curves however is their reversibility. In

runs extending even over several days, with furnace temperature raised from 20°C to 580°C, the probe temperature would drop to $\frac{1}{4}$ its original value or less, and on returning the furnace to 20°C, the probe temperature would return to within 20 percent of its original value.

From the known rate of loss of atoms to the walls at room temperature and the observed change in probe temperature with temperature of section L of the side arm, the variation in γ may be found by a simple computation providing we assume we can piece together solutions of the form $n=n_0 \exp -\beta\gamma^{\frac{1}{2}}x$ rather than complete solutions of the form

$$n=A \exp \beta\gamma^{\frac{1}{2}}x+B \exp -\beta\gamma^{\frac{1}{2}}x.$$

This assumption is valid however whenever we are sure that we can neglect the reflection of atoms beyond the length L, and can therefore attribute all changes of n to the change of decay along the heated tube. Actually the length L is long enough so that at room temperature the value of n falls to a small fraction of its original value at the far end of L, and as actually the recombination coefficient was in all cases observed to rise with temperature, this condition is even better fulfilled at higher temperatures, At temperatures below room temperature, γ remains nearly constant, again introducing no appreciable error. We therefore derive

$$t_1=k' \exp(-\beta_1\gamma_1^{\frac{1}{2}}L)\cdot\exp[-\beta_0\gamma_0^{\frac{1}{2}}(x-L)]$$

where k' is some constant

$$t_0=k' \exp(-\beta_0\gamma_0^{\frac{1}{2}}x)$$

whence

$$t_0/t_1=\exp(\beta_1\gamma_1^{\frac{1}{2}}L-\beta_0\gamma_0^{\frac{1}{2}}L),$$

$$\log_e(t_0/t_1)=\beta_1\gamma_1^{\frac{1}{2}}L-\beta_0\gamma_0^{\frac{1}{2}}L,$$

$$\gamma_1=\left(\frac{\beta_0\gamma_0^{\frac{1}{2}}L+\log_e(t_0/t_1)}{\beta_1 L}\right)^2,$$

t_0 = probe T for L at T_0,

t_1 = probe T for L at T_1. (18)

TABLE I. Variation of β with temperature.

T°C	β	T°C	β
−180	7.26	180	2.91
− 80	4.70	300	2.55
15	3.73	450	2.28
		590	2.09

The variation of β with temperature must also be computed. We remember

$$\beta=(\bar{v}C/4SD)^{\frac{1}{2}}. \quad (19)$$

With $p=75\mu$, using Amdur's[11] value for D, we obtain Table I for β.

The experimental runs were taken by varying the furnace temperature in steps of about 120°, allowing from one hour to five hours or more for the furnace to reach equilibrium. A minimum of one hour was found necessary for any approach to equilibrium, and several runs were made leaving the furnace at various temperatures overnight to be sure a close approach to equilibrium was attained. As the variation of probe temperature with furnace temperature was reversible, the values obtained do represent equilibrium values. Several different pressures near 75 microns were used, and since the results for all the different runs showed more random variations than systematic variations, all were averaged and plotted in Fig. 3. The low temperature portion of the experiment was conducted with the section L bent into a U tube and immersed in dry ice or liquid air.

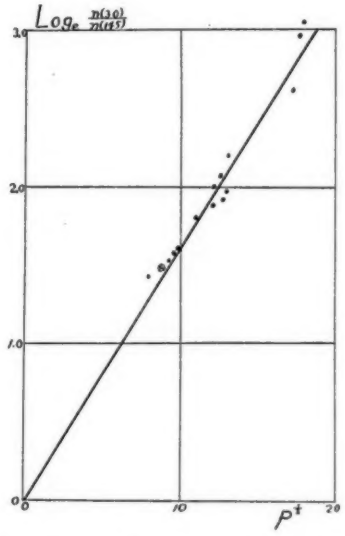

FIG. 5. Variation with pressure (in μ) in the ratio of temperatures of two probes at two different distances from a H_2 discharge. Circled point corresponds to circled points of Fig. 4.

[11] I. Amdur, J. Chem. Phys. **4**, 339 (1936).

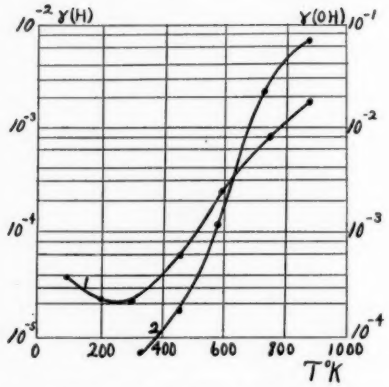

FIG. 6. 1, γ(H) on Pyrex in H_2+2 percent H_2O at 75μ pressure as a function of temperature. 2, γ(OH) on Pyrex in H_2O at 50μ pressure as a function of temperature.

The value of γ may be calculated from Fig. 3, Eq. (18), and Table I. The results are plotted in Fig. 6, together with those for γ (OH) on Pyrex (see Section 5). We may note that the observed variation cannot be simply explained by any mechanism involving some single energy of activation or heat of reaction as the resulting equations will predict log γ inversely proportional to temperature rather than almost directly proportional as observed in the high temperature region of Fig. 6. So simple an explanation could not be expected however as the temperature is sure to modify the properties of the surface, in particular the layer of adsorbed water.

E. Variation of γ with Water Vapor Content

Three runs were made with respectively ½ percent, 2 percent, and 9 percent water vapor added to the hydrogen. It was found that the probe temperature increased with increasing water vapor content for all furnace temperatures, but especially at the higher temperatures. The results are plotted in Fig. 7. A pressure of 60 microns was employed, and at least three hours were allowed for equilibrium at each temperature. The three curves were obtained in one continuous run of over 200 hours; curves 2, 1, and 3 consecutively. In such a long run, the probe is apt to change its sensitivity somewhat and there is reason to believe curve 2 should be more nearly intermediate between 1 and 3 than it is, as a check point taken at room temperature with H_2+2 percent H_2O just before the run 3 gave a probe temperature of 175°. The general nature of the variation with water vapor content is however unmistakable.

Increasing water vapor content in the discharge may mean either better poisoning of the walls or increased OH concentration (see Part 5) or both. In Part 5 it will be shown that the uncertainty in OH decay is such that OH radicals might still reach the Pt probe. However, using the most probable value of OH decay, the OH concentration at the Pt probe may be neglected, and the observed variation may be attributed entirely to better poisoning of the glass walls for H recombination.

4. RECOMBINATION OF H ON OTHER SUBSTANCES

Substances investigated include quartz, combustion tubing, and K_2SiO_3 chosen for their similarity to Pyrex; KCl because of its importance in certain investigations of OH recombination; Al_2O_3 as a typical dehydration catalyst; $ZnO \cdot Cr_2O_3$ as a typical dehydrogenation catalyst; Pt; and also KOH, K_2CO_3, metaphosphoric acid, and Na_3PO_4.

Two arrangements were used in the investigation. The first is the same as was used in Section 1 on Pyrex—an *indirect method*, good for substances of low catalytic power. In this method, the atoms diffuse down a side arm coated in part with substances under investigation, and the atoms passing through this coated section are detected by a Pt coated probe (see Fig. 1). The coated

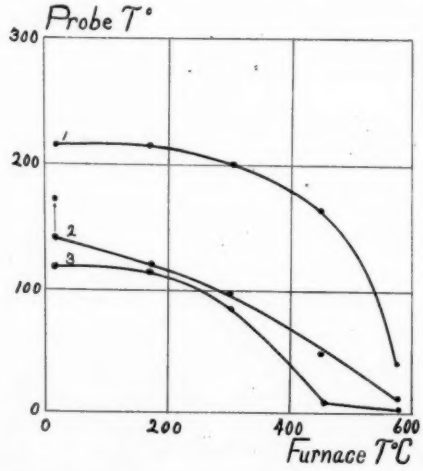

FIG. 7. Variation of Pt probe temperature with water vapor content of discharge. Arrow points to an independent check of first point of curve 2. 1 = H_2+9 percent H_2O. 2 = H_2+2 percent H_2O. 3 = H_2+½ percent H_2O.

TABLE II. H recombination on various substances. We may note from the close check between the values of the last two rows that γ (Pt)200° is nearly equal to 1.

Substance	Sample length L probe dist. x	Condition	Furnace temp.	Pt probe temp. (indirect method)	Probe U temp. (direct method)	Probe U temp. corrected for changing atomic concentration and speed	γ (indirect method)	γ/γ Pt (direct method)
Quartz	$L=20$	erratic	15	45	—	—	$7.0\cdot10^{-4}$	—
	$x=30$	behavior	300	22	—	—	$2.6\cdot10^{-3}$	—
			500	15	—	—	$3.4\cdot10^{-3}$	—
Combustion	20		15	70	—	—	$4.6\cdot10^{-4}$	—
Glass	30		300	50	—	—	$1.8\cdot10^{-3}$	—
			500	30	—	—	$2.8\cdot10^{-3}$	—
K_2SiO_3	6	moist	15	200	0	0	10^{-4}	$1.7\cdot10^{-3}$
	30	dry	15	10°	—	—	$7\cdot10^{-2}$	—
		dry	200	4°	35	47	$7\cdot10^{-2}$	$1.6\cdot10^{-1}$
		dry	500	2°	—	—	$1\cdot10^{-1}$	—
KCl[1]	6		15	350	0	0	$2\cdot10^{-5}$	
	30		400	240	0	0	$2\cdot10^{-4}$	
KOH	6	moist	15	200	0	0	10^{-4}	10^{-3}
	30	dry	15	0	—	—	$\geq \cdot10^{-1}$	—
		dry	200	0	20	27	—	$9\cdot10^{-2}$
		dry	300	0	—	—	$\geq 2\cdot10^{-1}$	—
K_2CO_3	6	moist	15	200	0	0	10^{-4}	10^{-3}
	30	dry	15	0	14	14	$\geq 1\cdot10^{-1}$	$5\cdot10^{-2}$
		dry	200	0	10	13	$\geq 2\cdot10^{-1}$	$4\cdot10^{-2}$
		dry	400	0	—	—	$\geq 2\cdot10^{-1}$	—
Metaphosphoric acid	20	moist	15	350	0	0	$2\cdot10^{-5}$	—
	30							
Sodium	6	moist	15	200	0	0	10^{-4}	$\leq 10^{-3}$
Phosphate	30	moist	300	150	—	—	$5\cdot10^{-4}$	—
		dry	15	0	20	20	$\geq 1\cdot10^{-1}$	$7\cdot10^{-2}$
		dry	200	0	15	20	—	$7\cdot10^{-2}$
		dry	300	0	—	—	$\geq 2\cdot10^{-1}$	—
Al_2O_3	2.5	moist	15	20	20	20	$9\cdot10^{-2}$	$7\cdot10^{-2}$
	30	moist	200	—	10	13	—	$4\cdot10^{-2}$
		dry	15	0	100	100	—	$3.3\cdot10^{-1}$
		dry	200	0	60	80	—	$2.7\cdot10^{-1}$
		dry	400	0	25	67	—	$2.2\cdot10^{-1}$
$ZnO\cdot Cr_2O_3$	2.5	moist	15	0	160	160	—	$5.3\cdot10^{-1}$
	30	or	200	0	120	160	—	$5.3\cdot10^{-1}$
		dry	400	0	65	170	—	$5.6\cdot10^{-1}$
Pt	2.5	moist	15	0	300	300	—	1
	30	or	200	0	250	330	—	1.1
		dry	400	0	120	320	—	1.1

[1] Numerous other runs established that within experimental error the catalytic effect of KCl on H recombination cannot be distinguished from that of Pyrex. As the KCl coating did not completely shield the glass surface from the discharge, it is therefore possible that KCl is even less catalytic to H recombination than Pyrex. This is hard to establish definitely as measuring the recombination coefficient on glass represents about the limit of our experimental technique with the present method of investigation.

sections were 11 mm inside diameter, glass blown to the system save for quartz, combustion tubing, Al_2O_3, $ZnO\cdot Cr_2O_3$ and Pt. (These latter substances were of 8 mm inside diameter tubing slipped inside the main side arm where they fitted snugly.)

The *indirect method* is obviously not good for substances of high catalytic power such as K_2CO_3, KOH, etc., because few atoms would reach the probe, but we have used it as a very rough estimate of γ. Where zero probe readings were observed, we have assumed the probe T to be equal to or less than one-half degree and we have assumed that the probe T at the discharge end of the tube would be at least 500°. These assumptions yield our lower limits of γ listed in

Table II. γ is calculated from the probe temperatures, the data for Pyrex, and the obvious equation[12]

$$\log_e(t) = -(\beta\gamma^{\frac{1}{2}}L)_z - [\beta\gamma^{\frac{1}{2}}(X-L)]_{\text{Pyrex}} + C' \quad (20)$$

where z is the substance under investigation.

The second system of probes, utilizing a *direct method* of comparing different substances, is illustrated in Fig. 8. It is good for substances of high catalyzing power.

The unknown substance is coated on probe "U." Probe "T" is coated with Pt as an indicator of the minimum H concentration near "U." (The actual concentration near "U" is of course in general much greater than that indicated by "T," and the reading of "T" was never interpreted quantitatively. In some runs however, a portion of the active substance coated on probe "U" would become dislodged or would be sublimed onto the surface of the side arm. This coating then would decrease the total H concentration as measured by "T" without increasing the reading of "U." The presence of the check probe "T" was useful in eliminating these runs.)

Probe "U" is inserted in the middle of a 20 cm long furnace whereby the temperature variation in the response of "U" can be measured. To correlate the readings of probe "U" at different furnace temperatures, the change in heat loss of the probe with temperature of the surrounding furnace must be known. Calculations of heat losses, including radiation losses,—necessarily rough because of the comparatively long mean free path (of the same order of magnitude as the probe diameter) and the inaccurately known accommodation coefficient—show that this heat loss does not vary very greatly with temperature over the range from 20°C to 450°C. That is, in Eq. (12), the term A/k may be taken as constant over this temperature range, and q will be proportional to γ. In this equation however, the factor $n\bar{v}$ varies with temperature. We assume n is not different for different coatings on the probe. This assumption is only a first approximation, and as n will actually be somewhat larger in the presence of less catalytic substances, a direct comparison of these with a Pt coating on "U" will make the unknown

[12] Derived analogously to Eq. (14).

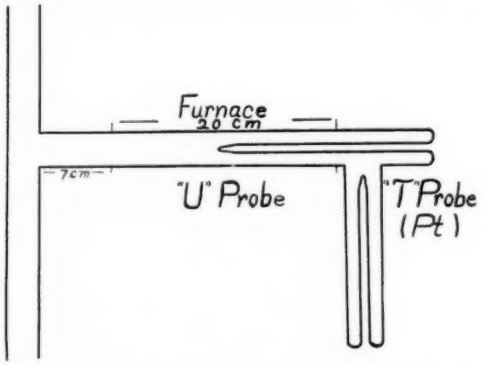

FIG. 8. Direct method of investigating γ. Substance to be investigated is coated on "U" probe.

substance appear more catalytic than it really is. N also varies with temperature however due to losses to the clean glass walls of the side arm. This correction may be computed from Eq. (20), substituting $L=10$, $X=17$ (here z is Pyrex at the furnace temperature), the observed temperature variation of γ (Fig. 6), and the computed values of β (Table I). These changes in n and $\bar{v}$ are corrected for in Table II.

The data in this section are not as accurate as in Section 1. In the first place, the salts at high temperatures (around 500°C) sublimed somewhat to different parts of the side arm, and even a slight invisible layer of salt on the glass completely changes its catalytic effect. In the second place, certain salts such as KCl were reduced in or very near the discharge. Also, some substances lost water of crystallization in violent miniature explosions which spread the coating. Most important of all, however, was the fact that the catalytic effects of almost all these substances depended far more on their moisture content than on their temperature. Moist salts were non-catalytic; dry ones (save KCl) catalytic to H recombination. As a result, the data obtained with these salts with varying temperature are in general non-reversible, low catalytic effect being initially observed, increasing as the increasing furnace temperature dries out the salt, and remaining high when the furnace temperature is again lowered.

5. EXPERIMENTS WITH WATER VAPOR

When a discharge is passed in water vapor, the molecules are dissociated into H atoms and OH

radicals. There is a negligible concentration of O atoms.[5] Three possible two-body surface recombinations can occur.

$$1— \quad H+H+M \rightarrow H_2+M+4.3 \text{ ev},^{13}$$
$$2— \quad H+OH+M \rightarrow H_2O+M+5.5 \text{ ev},$$
$$3— OH+OH+M \rightarrow H_2O_2+M+3.1 \text{ ev}.$$

M is the surface catalyzing the recombination. All three reactions are strongly exothermic. No previous work has been done to distinguish between recombination processes 2 and 3.

The state of knowledge with respect to these three recombinations prior to these experiments may be briefly summarized. All the data were known only at room temperature. At this temperature Pyrex glass was known to catalyze 1 very poorly and 2 and 3 also poorly, although it was thought to be somewhat more catalytic for one or both of the latter reactions than for reaction 1. Numerous substances—such as Pt, $ZnO \cdot Cr_2O_3$, KOH, etc., were known to catalyze 1 strongly, but their effect for 2 or 3 was unknown. Al_2O_3 was known to catalyze 1 strongly and was thought to catalyze 2 also. KCl was known to be quite ineffective in catalyzing 1, and quite effective in catalyzing either 2 or 3 or both. All these conclusions may be drawn from the work of Taylor and Lavin,[3] although they do not try to distinguish the two possible types of OH recombination.

The present investigation has added to the existing data and narrowed down the possible interpretations, but has not succeeded in uniquely distinguishing between recombination processes 2 and 3. We have succeeded in obtaining a rough estimate of the recombination coefficient γ for process 2 or 3 on glass, and have found its change with temperature. We have also investigated the effect of temperature on other substances, especially KCl.

The experimental arrangement is indicated in Fig. 1. Water vapor is pumped through the discharge tube from the water reservoir. The OH concentration is detected by the heating of probes coated with KCl. (Note that Pt probes could not be used as Pt recombines atomic H. KCl does not recombine H and does recombine OH—see below.) The response of these KCl surfaces was quite erratic, and they almost always required activation for 15 minutes at 250°C to manifest their catalytic power. The probe response was fairly reproducible for an average of about 5 runs, after which it would usually become very erratic. The glass walls near the probe were observed to become coated with KCl in patches by fragments exploded from the probe in the course of repeated activation. This coated section robbed the probe of OH and caused part at least of the erratic nature of the probe response. Because of this effect, probe temperatures below 10° were considered unreliable.

To avoid possible reduction of the KCl by the discharge, the probe was always kept at least 10 cm distant from the discharge.

A. Pyrex

1. Investigation of γ (OH) *at Room Temperature*

Figure 9 is a logarithmic plot of KCl probe temperature against distance from the discharge. The scattering in observed points is very large. A greater range of distance could not be investigated as for shorter distances there was danger of reduction of KCl by the discharge and for larger distances the probe temperature was so small as to be unreliable. The scattering here, in contrast to that in Fig. 4, is believed due more to variation in probe response than in surface conditions of the glass. One sequence of points (the circled values) was taken with the same KCl coating on the probe, readings at small and large values of x alternating.

Whether OH disappears by process 2 or 3 is immaterial in the calculation of γ as γ is defined as the fraction of times the OH radical strikes the wall and is recombined there *by any process*. We have therefore the same equation as for γ(H). [Eq. (14)], but in this case $\beta_0=4.63$ (see Section 2). From Fig. 9, we get therefore

$$\gamma=8\times10^{-5}. \tag{21}$$

The small range in probe temperatures (a factor of 10) and distances (a factor of 5) available (compare factors of several hundred and 20 respectively in experiments on H recombination)

[13] Energies of recombination calculated from data of Int. Crit. Tab. V, p. 176, and A. v. Engle and M. Steenbeck, *Electrische Gasentladungen* I, p. 43.

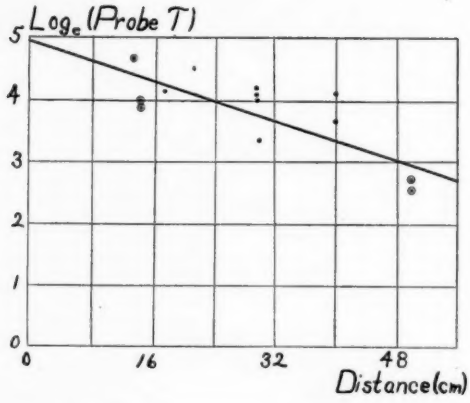

FIG. 9. KCl probe temperature as a function of distance from a water vapor discharge. Pressure = 50μ. Circled points are for one sequence of runs with the same KCl surface on probe.

together with the relative unreliability of the KCl probes rendered attempts to distinguish between surface recombination and losses of OH by three-body collisions useless. However as the pressures are even lower than in the work on H recombination, surface effects probably preponderate. The nature of the temperature variation in probe response (Fig. 10) evidently precludes the possibility of recombination at the probe overshadowing losses of radicals to the Pyrex walls.

2. γ(OH) *at Other Temperatures*

Investigations were made in the temperature range from 15°C to 590°C. The experimental set-up is the same as that in Fig. 1 except that two probes "U_1" and "U_2" in two independent side tubes were used instead of one. The double probe system was used to eliminate random fluctuations. An average of several runs is plotted in Fig. 10. Here the temperature of the 7 cm furnace was varied by jumps of 150° every two hours. Reversibility of probe response with furnace temperature showed that probe readings represented equilibrium values. The short reliable life of the KCl probes made it impossible to vary the furnace temperature more slowly.

Computation of β for OH diffusion is not accurate as no data are available on the coefficient of diffusion of OH. We may get a rough estimate however by assuming that the coefficient of diffusion of OH nearly equals the self-diffusion coefficient of H_2O. This we compute from the viscosity data by means of the equation

$$D = C\eta/\rho \tag{22}$$

where we take $C = 1.36$ as a compromise between the hard sphere and inverse fifth power repulsion values of C (1.200 and 1.543, respectively). The resulting values of β, calculated from equations analogous to those of Part 3, are given in Table III.

The values of γ computed from this table and the data of Fig. 10 are plotted in Fig. 6.

3. γ(H) *on Pyrex in* H_2O

In Part 3 we have measured γ(H) on Pyrex in moist H_2. Here we may do the same for H atoms produced in a water vapor discharge. Different values of coefficient of diffusion, etc., make this determination of γ an interesting check with the previous ones. Furthermore, if the recombination $H+OH \rightarrow H_2O$ is considerably stronger than either $H+H \rightarrow H_2$ or $OH+OH \rightarrow H_2O_2$, a large value of γ should result as the initial dissociation of H_2O yields equal amounts of H and OH.

OH disappears more rapidly with distance from the discharge along the side arm than does H. This is known from the data of Taylor and Lavin,[3] and also from the large value of γ(OH) which we have found. It is not known whether

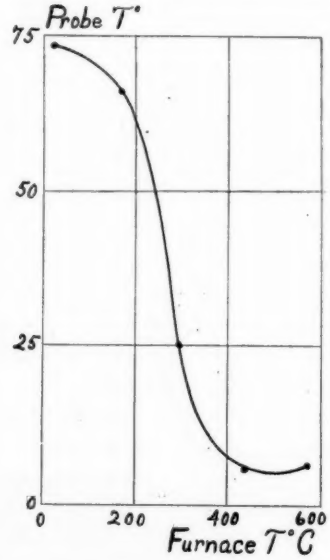

FIG. 10. KCl probe temperature as a function of furnace temperature in a water vapor discharge. Pressure = 40μ.

OH recombines on Pt or not, but presumably it does. Consequently the Pt probe is affected by both H *and* OH. However, for distances sufficiently far from the discharge (around 50 cm), the larger recombination of OH on Pyrex assures small concentrations of OH compared to H, and thus the decay of H alone may be measured.

Pt probe readings in H_2O are therefore plotted logarithmically in Fig. 11 for a pressure of 50μ. The scattering of points is not great. The deviation from a straight line shown by the initial group of points is presumably from the effect of OH on the probe. The final two points near 300 cm are zero probe readings whose logarithms are plotted arbitrarily as zero (equivalent to a temperature of 1°), and their deviation from linearity is not significant.

The following equation[14] holds for the diffusion of *molecular* H_2 into H_2O.

$$D=0.7516(T/273)p/160 \quad (p \text{ in mm of Hg}). \quad (23)$$

As H has nearly the same diameter as H_2 [15] and as for large differences of masses of the interdiffusing molecules, D is proportional to the velocity of the lighter component, we can conclude that for the diffusion of *atomic* H into H_2O,

$$D=2^{\frac{1}{2}}\cdot 0.7516(T/273)p/760. \quad (24)$$

With this value of D, for a pressure of 50μ, at room temperature, we get $\beta=3.72$, whence, using Fig. 11 and Eq. (14), we get

$$\gamma(\mathrm{H})=1.9\times10^{-5}. \quad (25)$$

The agreement with values of γ for moist hydrogen is surprisingly good and indicates that the recombination $H+OH\rightarrow H_2O$ on Pyrex is weaker than $H+H\rightarrow H_2$ or $OH+OH\rightarrow H_2O_2$.

Experiments similar to those in Part 3 showed three-body collisions to be negligible compared to the surface recombination of H.

TABLE III. Values of β for OH diffusion.

T°C	β	T°C	β
20	4.63	450	2.08
180	3.16	590	1.89
300	2.53		

[14] Int. Crit. Tab. V, p. 62.

[15] Calculations from Amdur's viscosity data (reference 11) for atomic H give this result.

B. Other Substances

1. KCl

Numerous experiments with alternating H_2 and H_2O discharges establish definitely that KCl coated probes are heated appreciably—up to around 100°—at 10 cm from a H_2O discharge and are not heated above 1°–2° at the same distance from a discharge in moist H_2. We may therefore conclude that KCl catalyzes OH recombination and does not catalyze H recombination. This is important because it establishes a test for free OH which is not affected by H. Our conclusion agrees with the results of Taylor and Lavin[3] and Frost and Oldenberg.[16]

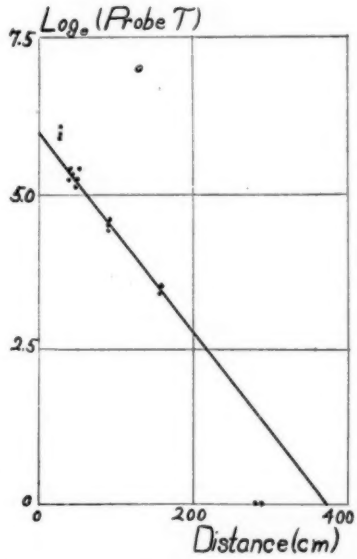

FIG. 11. Pt probe temperature as a function of distance from a water vapor discharge. Pressure = 50. O probe temperatures plotted as 1°.

Similar experiments with a furnace surrounding the probe have been carried out. At a furnace temperature of 180°C, the KCl response decreased by a factor of two. Possibly this was due to some KCl sputtered onto the walls. Insertion of a check probe beyond the furnace proved useless as the OH concentration was too small to be accurately detected.

To estimate the magnitude of γ(OH) on KCl, we observe that a KCl coated probe 20 cm from a H_2O discharge heats up to 65° whereas a Pt

[16] A. A. Frost and O. Oldenberg, J. Chem. Phys. **4**, 642 (1936).

TABLE IV. Comparative probe temperatures with H_2 and H_2O discharges.

Gas	Al_2O_3 (unactivated)	Al_2O_3 (activated)	$ZnO \cdot Cr_2O_3$	Pt
H_2	290	315	290	580
H_2O	80	180	220	415

probe 20 cm from a H_2 discharge heats up to 500°. As γ(OH) on Pyrex is greater than γ(H) on Pyrex, the OH concentration near a H_2O discharge surely does not exceed the H concentration near a H_2 discharge. Furthermore the mean of the heats of recombination by the processes $H+OH \rightarrow H_2O$ and $OH+OH \rightarrow H_2O_2$ is nearly the heat of recombination of atomic H. We may therefore conclude that γ(OH) on KCl is surely greater than 0.1 times γ(H) on Pt.

The temperature variation of OH recombination on KCl could not be followed closely, but since a KCl probe located 10 cm beyond a 6 cm section of the side arm coated with KCl showed no response for any temperature of the 6 cm section up to and including 400°C, evidently KCl remains catalytic to OH recombination at high temperatures.

2. KOH, K_2CO_3, K_2SiO_3, Na_3PO_4

These substances all have the property of recombining atomic H strongly when dry and poorly when wet. Measurements of OH recombination by the *direct method* therefore are useless as the H recombination masks the OH response, and any systematic variations between response in H_2 and in H_2O are as easily ascribed to varying catalytic effect for H (because of the strong dependence of H catalysis on surface dryness) as to some catalytic recombination of OH.

Measurements by the *indirect method* with KCl coated probes are useless if the KCl catalyzed recombination is by the process $H+OH \rightarrow H_2O$, as no H passes the coated section of the side arm. Similarly, measurements with a Pt probe are valid only if the reaction $OH+OH \rightarrow H_2O_2$ proceeds strongly on Pt. The nature of OH recombination on KCl and Pt is not known however. Furthermore, a positive response with a Pt probe can also be interpreted as a change in γ(H) on the coatings on the Pyrex walls with increased H_2O content of the discharge.

We have nonetheless made these measurements, as a positive response of the KCl probe in any case where no H passes the coated section would establish the reaction $OH+OH \rightarrow H_2O_2$ on KCl, and a null response with the Pt probe shows γ(H) is still large on the wall coatings investigated.

The substance under investigation was coated inside the 7 cm length of side arm in the furnace. Probes "U_1" and "U_2" were located 5 cm beyond the furnace, and were coated with KCl. Probe "T" was located 5 cm beyond U_1 and U_2 and was coated with Pt. Alternate runs were taken with a clean glass side arm to check the response of the KCl.

Positive readings on U_1 or U_2 were found only with a Na_3PO_4 coated side arm at temperatures below 400°C—i.e., in an unactivated condition where H recombination was known to be uncatalyzed. This therefore established only the fact that unactivated Na_3PO_4 catalyzes neither H recombination nor OH recombination.

Null readings were found with "T" for activated coatings, except that readings of a few degrees were observed with a K_2SiO_3 coated side arm even at high furnace temperatures. This behavior is the same as with moist hydrogen, showing that for the substances investigated it is a function of *surface* wetness, not H_2O concentration in the gas.

3. Pt, Al_2O_3 *and* $ZnO \cdot Cr_2O_3$

Indirect measurements with these substances (3 cm samples) established zero KCl probe readings which proved little (see previous section). The Pt probe response was the same as with H_2 (part 4) except that with an Al_2O_3 sample, Pt probe readings of 1°–2° were observed at room temperature even after activation of the Al_2O_3 at high temperatures (at which temperatures the Pt probe response was zero). Probable interpretation of this result is that there is greater poisoning of Al_2O_3 for H recombination in H_2O than in moist H_2 at the pressures employed. (See below for confirmation of this interpretation).

Direct measurements at 17 cm from the discharge established the data in Table IV for alternate H_2 and H_2O discharges. (The data are aver-

age values for several runs. H_2 pressure 75μ; H_2O pressure 50μ).

To obtain high readings with an H_2O discharge, it was necessary to heat the Al_2O_3 probe in a furnace to 320°C for 30 minutes. As even after this activation the Al_2O_3 probe temperature slowly decreased over the course of 30 minutes to 125°, it seems probable that the lower ratio of readings with H_2O to readings with H_2 for Al_2O_3 compared with $ZnO \cdot Cr_2O_3$ and Pt is caused by increased poisoning of the Al_2O_3 surface by water vapor.

Our observation that Al_2O_3 does not heat up more with a H_2O discharge than with a H_2 discharge disagrees with that of Taylor and Lavin. However if the ratio of their Al_2O_3 probe readings to their silver probe readings is examined, it is seen not to change appreciably with changing H_2O concentration in the discharge. Their data, together with ours, therefore show no significant difference in relative heating of Al_2O_3, $ZnO \cdot Cr_2O_3$, Pt, and Ag with H_2O and H_2 discharges—and therefore no measurable difference in the *relative* catalytic effect of the dehydration catalyst Al_2O_3 and the dehydrogenation catalyst $ZnO \cdot Cr_2O_3$ for H and OH recombination.

The author wishes to express his appreciation to Professor O. Oldenberg for suggesting this problem and for his continued interest and help in its development. He is also indebted to Professor W. H. Furry for clarification of many aspects of the diffusion problems considered.

MARCH, 1943 JOURNAL OF CHEMICAL PHYSICS VOLUME 11

Mechanical Properties of Polymeric Materials

ARTHUR TOBOLSKY AND HENRY EYRING
Princeton University, Princeton, New Jersey
(Received November 12, 1942)

A molecular model in terms of which the elastic viscous properties of rubber-like substances can be interpreted is presented. Experiments on stress relaxation at constant extension, creep under constant load, extrusion, vibration, and breaking are discussed in terms of a mathematical formulation of this molecular model.

A VERY large class of substances composed of large molecules, such as nylon and other fibers, natural and synthetic rubbers, muscle tissue, and so on, exhibit elastic-viscous properties that are qualitatively similar, which fact reflects an over-all similarity in molecular structure.

These substances are composed of long chain molecules linked together at some points by primary cross bonds and at other points by bonds of a secondary nature such as strong Van der Waals' bonds (as in regions of local crystallinity) dipole-dipole bonds, etc. The cross linking bonds give these polymers an effective network structure. Between the cross bonds there is a rather long length of coiling, twisting molecular chain, the segments of which are rotating more or less freely. This amorphous liquid-like structure comprises the bulk of the polymer, when the latter is in the temperature range of the rubbery state of aggregation.

Because of statistical considerations, the molecular chains spend most of their time in very coiled configurations when no external stresses are acting. When the polymeric network is rapidly stretched, the molecular chains are stretched and thereby have fewer conformations that are consonant with this extended state. The probability of a unit cell of the network having dimensions x, y, z is[1,2]

$$P_{(xyz)} = A \exp\left[-\beta(x^2+y^2+z^2)\right]. \qquad (1)$$

The entropy is related to the probability by

[1] E. Guth and H. M. James, Ind. Chem. **33**, 624 (1941). See also earlier work of Meyer, Mark, Kuhn, and Guth referred to in this paper.

[2] Tobolsky, Powell, and Eyring, Chapter on "Elastic Viscous Properties of Matter" in *Frontiers of Chemistry*, Interscience Publishers (in press).

Boltzmann's relation $S=klnP$, and the tension X to the entropy by the relation $L=-T(\partial S/\partial x)_T$. It is assumed that the volume of the unit cell of the network $xyz=v$ does not change during stretching because of the interpenetrating character of the network structure. On this basis it had been shown by Guth and James[1] that the tension X is given by

$$X=\frac{2\beta v^{\frac{1}{3}}ZkT}{L_0}\left\{\frac{L}{L_0}-\left\{\frac{L_0}{L}\right\}^2\right\}. \tag{2}$$

Choosing suitable values of Z, the number of unit cells in the network, one can explain the values of the modulus of rubber which is about 10^7 dynes/cm^2 instead of 10^{11} dynes/cm^2 characteristic of short chain crystalline substances.

Many of the interesting phenomena regarding the elastic behavior of rubber are described by such terms as creep, creep recovery, relaxation, hysteresis, etc. We shall treat these phenomena in terms of molecular rate and flow processes.

In any given cross section of the polymer perpendicular to the stress there are a number of deformation mechanisms in which relaxation processes can occur independently, and over which the stress distributes itself. In all these unit processes of deformation, the effect of stress on the rate of strain is twofold, there being first an elastic component for which the rate of strain is in phase with the rate of stress, and a contribution to the rate of strain of relaxation processes such as slipping, tearing, etc.[2] It is convenient to classify the various unit processes of deformation into categories which group together similar processes. Let us suppose that there are in a square cm of cross section N_i such parallel processes of type i, so that if the total stress f_i distributes itself on this type of unit process of deformation, the average force acting on each is f_i/N_i. Suppose, too, that per unit length, there are n_i such processes of deformation in series, then the total rate of strain is given by

$$\frac{ds}{dt}=\frac{1}{G_i}\frac{df_i}{dt}+n_i\lambda_i\frac{kT}{h}\times\exp\left(-\Delta F^{\mp}/kT\right)2\sinh\frac{f_i\lambda_i}{2N_ikT}, \tag{3}$$

where λ_i is the average distance projected in the direction of stress between equilibrium positions in the relaxation process and $\Delta F^{\mp}$ the free energy of activation for the process.[3] G_i is the appropriate partial modulus to be associated with the deformation process, and the first term on the right represents the elastic contribution. The contribution to rate of strain due to relaxation (slipping, flow, etc.) is given in the second term, and this term is derived in similar fashion to the treatment of viscous flow. The force f_i/N_i acts on each unit of type i and tends to favor motion from one equilibrium position to another in the direction of stress. The sum of all the partial stresses on the various deformation mechanisms is equal to the total stress and the stress is distributed in such a way that the rate of strain is the same for each.

Equation (3) can be written in a more condensed form:

$$\frac{ds}{dt}=\frac{1}{G_i}\frac{df_i}{dt}+A_i\sinh B_if_i. \tag{4}$$

In case $B_if_i\ll 1$ then

$$\frac{ds}{dt}=\frac{1}{G_i}\frac{df_i}{dt}+A_iB_if_i=\frac{1}{G_i}\frac{df_i}{dt}+\frac{1}{\eta_i}f_i. \tag{5}$$

Equation (5) is of the form that was postulated by Maxwell to explain elasto-viscous behavior.

The deformation mechanisms found in polymers in the rubbery state of aggregation are of the following types. There are first the structural elements of the network, which support most of the stress. Some of these elements are composed of primary cross-linking bonds, and so behave purely elastically for small loads. Other units of the network structure are partly joined together by secondary cross bonds, which can slip on the application of a stress. Some of the total stress is also distributed on the mobile segments of the long molecules which form an amorphous liquid-like structure pervading the network. The equations of motion for the polymeric material

[3] The flow term in (3) will be seen to be the same as (8) in a previous paper [H. Eyring, J. Chem. Phys. **4**, 283 (1936)] if one writes $n=\lambda_1^{-1}$, $N_i=(\lambda_2\lambda_3)^{-1}$, and $\lambda_i=\lambda$.

are:

$$\text{(a)}\quad \frac{ds}{dt}=\frac{1}{G_1}\frac{df_1}{dt}+A_1\sinh B_1 f_1 \qquad \text{primary network units,}$$

$$\text{(b)}\quad \frac{ds}{dt}=\frac{1}{G_2}\frac{df_2}{dt}+A_2\sinh B_2 f_2 \qquad \text{secondary network units,} \qquad (6)$$

$$\text{(c)}\quad \frac{ds}{dt}=\frac{1}{G_3}\frac{df_3}{dt}+\frac{1}{\eta_3}f_3 \qquad \text{segment motion.}$$

The constants A and B are to be interpreted in terms of Eq. (3). A_i is small, and in some cases the breaking of primary cross bonds is to be neglected. G_1 and G_2 are moduli of the "entropy elasticity" type discussed previously, and of the order of 10^6-10^8 dynes/cm^2. G_1 and G_2 are related to n_1, N_1, n_2, and N_2.‡ G_3 is the same kind of modulus as is associated with short chain crystalline hydrocarbons, namely, of the order of 10^{11} dynes/cm^2. The viscosity associated with the motion of segments is much smaller than that associated with slipping at secondary network cross bonds, and since the stress distributed on this deformation mechanism is small, the equation is of the Maxwell type.

A scheme mathematically similar to the above had been introduced by Kuhn[4] and extended by Simha.[5] However, these authors use Maxwell type equations throughout. A non-mathematical discussion of the properties of hard rubber has recently appeared which uses a qualitative picture and terminology similar to that used above.[6] A somewhat similar qualitative picture has been presented by other workers for various polymeric materials.[7,8]

Equations (6), when applied to experimental results, present the possibility of analyzing data in terms of molecular properties. For example, B_2 depends on N_2, the number of secondary bonds per unit area. This will be seen to be a function of temperature and of initial deformation. In the subsequent paragraphs we shall discuss some typical experiments which can be interpreted in the light of Eqs. (6). It is to be realized that very strong secondary bonds can play the role of primary bonds in certain experiments.

STRESS RELAXATION OF CONSTANT ELONGATION

If a substance is rapidly stretched to a given elongation and held fixed, the stress necessary to maintain that elongation decreases with time. For slightly vulcanized rubber Meyer and Ferri[9] concluded that the tension decays to a certain value below which the decrease is very slow. The same thing was observed by Misch and Picken[10] for polyvinyl acetate. As a result of their studies of stress relaxation and decay of birefringence of polyvinyl acetate held at constant elongation these authors conclude that the polymer is composed of a netted system of chains through which interpenetrates a system of relatively free chains.

For this type of experiment $ds/dt=0$, the stress due to the segment motion [Eq. (6c)] decays so rapidly that it is not observable. The stress on the primary network units decays very slowly, and if a limiting stress is really reached it must be due to the primary network. We shall assume, therefore, that the primary bonds are not broken during the course of the experiment.

The observed decay of stress is, therefore, due to the relaxation of secondary network bonds. If Maxwell's equation held, the decay of f_2 would be given by $f_2=f_2{}^0e^{-t/\tau}$, where τ is the relaxation time ($\tau=\eta_2/G_2$). The decay of stress does not follow such a law. Of course one can by using the Laplace transform find a suitable distribution of relaxation times, but it will be shown that integration of Eq. (6b), which has a natural

‡ n_2 is the reciprocal of l, the mean distance between secondary network bonds projected in the direction of stress. N_2 is the number of secondary bonds per unit area in a slab whose height is l. The number of secondary bonds ν_2 per unit volume is equal to n_2N_2. Similar considerations hold for primary bonds.

[4] W. Kuhn, Zeits. f. physik. Chemie **B42**, 1 (1939; also K. Bennewitz and H. Rotger, Physik. Zeits. **40**, 416 (1939).

[5] R. Simha, J. App. Phys, **12**, 680 (1941). This paper gives a large list of references to early work in this field. See also J. D. Ferry, J. Am. Chem. Soc. **64**, 1330 (1942).

[6] J. R. Scott, Trans. Faraday Soc. **38**, 284 (1942).

[7] T. Alfrey and H. Mark, J. Phys. Chem. **46**, 112 (1942); H. Mark, Ind. Eng. Chem. **34**, 449 (1942); Mark, Cold Spring Harbor Symposia on Quantitative Biology **9**, 204 (1942).

[8] H. Leaderman, Lecture presented at A.C.S. meeting in Buffalo, New York, September, 1942.

[9] K. H. Meyer and C. Ferri, Helv. Chem. Acta **18**, 574 (1935).

[10] L. Misch and L. Picken, Zeits. f. physik. Chemie **B36**, 400 (1937).

basis in terms of molecular behavior, can also explain the observed data. The result of such an integration is

$$\tanh (B_2 f_2/2) = \tanh (B_2 f_2^0/2) \exp (-A_2 B_2 G_2 t), \quad (7)$$

where f_2^0 is the initial stress. If $B_2 f_2/2$ is larger than unity and $f_2^0 > f > 1/2B_2$, one gets the approximate result that

$$f_2 = -(1/B_2) \log_e (c_2/2) - (1/B_2) \log_e t, \quad (8)$$

where $A_2 B_2 G_2$ is put equal to c_2. The total stress is, of course, $f_1 + f_2$ and the decay of f_1 is very slow.

It had been observed by Phillips[11] that the decay of tension at constant extension for rubber can be represented by a formula of the type

$$f = a - b \log t \quad (9)$$

in agreement with (6).

In Fig. 1 is shown a plot of f_2 against $\log_{10} ct$ according to (5) for various values of the parameter $B_2 f_2^0$. Some of the subsequent figures show data for some of the stress relaxation measurements found in the literature plotted against logarithmic time. See, for example, Figs. 2 and 3.[12, 13]

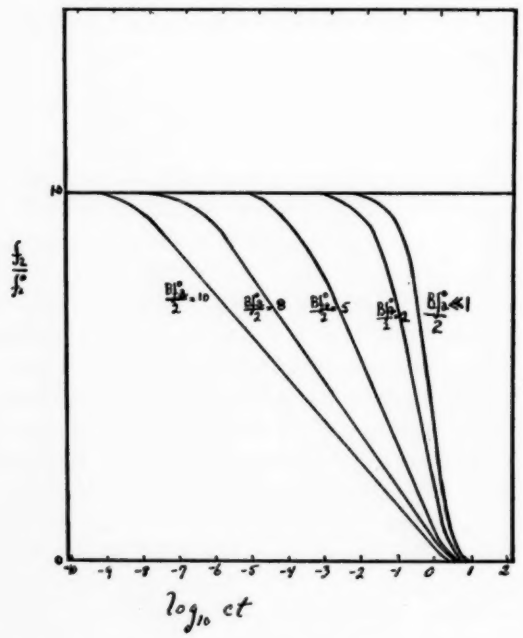

FIG. 1. Relaxation of stress.

By measuring the slope of the stress plotted against log time curves one can find values for N_2, the number of secondary bonds per unit area: this number is found to increase with decreasing temperature and also appears to be roughly proportional to the initial deformation or initial stress.

The equation for stress relaxation

$$\tanh (Bf/2) = \tanh (Bf^0/2) e^{-ct} \quad (10)$$

appears to hold more generally than for polymers. In Fig. 3 is plotted data from Trumpler[13] on relaxation of steel. The solid curves are calculated curves based on Eq. (10). The parameters B and c for various values of the initial stress were very simply related. Bf_0 is found to be a constant ($=6.32$), and $\log c$ is a linear function of f_0, which means that $\Delta F^{\mp}$ is a linearly decreasing function of f_0. Thus it appears that the number of relaxing mechanisms per unit area increases with increasing initial stress (or deformation) and the free energy of activation for flow decreases linearly.*

Creep under Constant Stress

Several experiments in the literature deal with the creep of fibers or rubbers under constant load.[14] See Fig. 4. If the amount of creep is not too large, so that the change of cross-sectional area is not very great, we can suppose the experiments carried out under conditions of constant stress. For small loads many of these substances show a delayed elasticity. There is an instantaneous deflection, then a recoverable creep till a limiting deflection is reached. Of course even for small loads, the primary network bonds will eventually break and flow. For nylon and other fibers for small loads and ordinary experimental times, a definite limiting deflection is reached. (See Fig. 5.) For natural and synthetic

[11] P. Phillips, Proc. Phys. Soc. London **19**, 491 (1905).

[12] L. R. G. Treloar, Trans. Faraday Soc. **36**, 538 (1940).

[13] W. E. Trumpler, Jr., J. App. Phys. **12**, 248 (1941).

* This fact indicates that when the initial deformation is increased the units of flow become smaller (hence more numerous per unit area), and the free energy of activation decreases with the decrease in size in a manner to be expected.

[14] P. Kobeko, E. Kuvshinskij, and G. Gurevitch, Tech. Phys. U.S.S.R. **4**, 622 (1937).

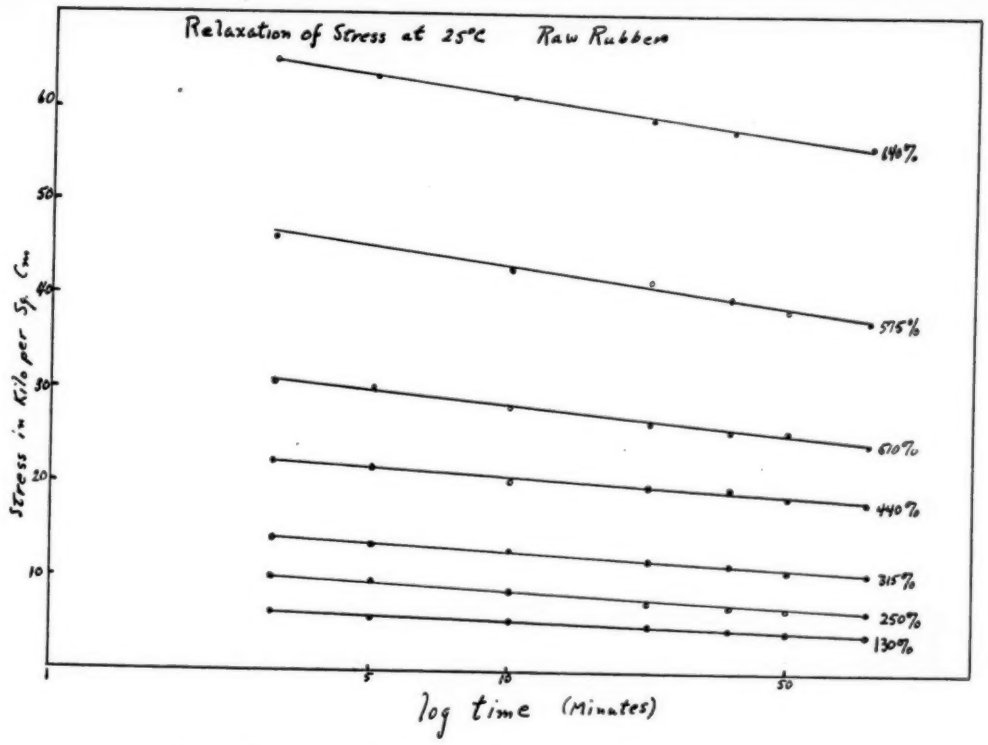

FIG. 2. Relaxation of stress at 25° for raw rubber (after Treloar).

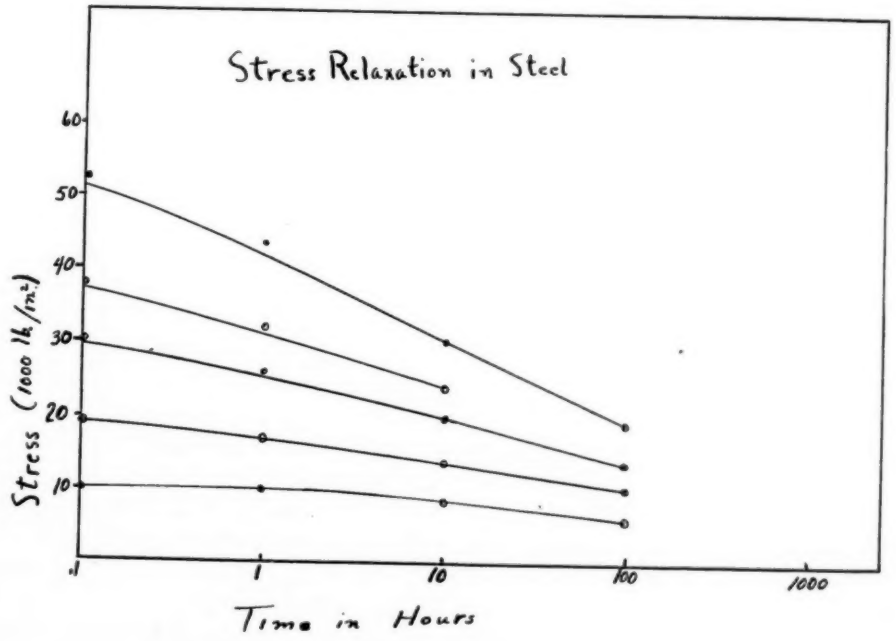

FIG. 3.

rubbers the literature contains mainly experiments using large loads, and the long time effects are further complicated by aging due to oxygen, light, and crystallization. We can, however, assume that while the secondary network bonds can relax and slip, the primary cross bonds

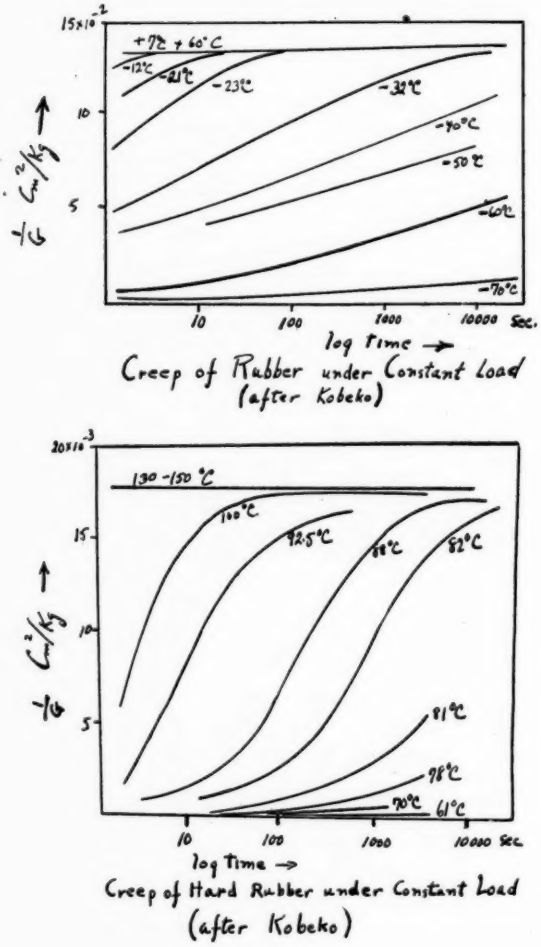

FIG. 4.

remain rigid, and carry through our calculations on that basis. After a fairly long time the primary network units will also start breaking.

For this case, too, the equation describing segment motion can be neglected. For a constant stress the immediate extension is seen to be $f/(G_1+G_2)$. The limiting extension is f/G_1, if breaking of the primary network is disregarded. We have to integrate the equations

$$\text{(a)} \qquad \frac{ds}{dt}=\frac{1}{G_1}\frac{df_1}{dt},$$

$$\text{(b)} \qquad \frac{ds}{dt}=\frac{1}{G_2}\frac{df_2}{dt}+A_2 \sinh B_2 f_2, \tag{6^1}$$

under the condition that $f_1+f_2=f$, where f is constant so that

$$df_1/dt=-df_2/dt.$$

Hence

$$\frac{df_2}{dt}\left(\frac{1}{G_1}+\frac{1}{G_2}\right)=-A_2 \sinh B_2 f_2.$$

Let

$$\frac{1}{G_\mu}=\frac{1}{G_1}+\frac{1}{G_2}.$$

Integrating we get

$$\tanh\frac{B_2 f_2}{2}=\tanh\frac{B_2 f_2^0}{2}\exp\left(-G_\mu A_2 B_2 t\right), \tag{11}$$

where

$$f_2^0=\frac{G_2}{G_1+G_2}f.$$

From (6^{1}a)

$$S=(f-f_2)/G_1. \tag{12}$$

The similarity of Eq. (11) to Eq. (7) is to be noted.

For

$$f_0>f>\frac{1}{2B_2}$$

$$f_2=-\frac{1}{B_2}\log_e A_2 B_2 G_\mu-\frac{1}{B_2}\log_e t, \tag{13}$$

so that

$$S=\frac{f}{G_1}+\frac{1}{B_2 G_1}\log A_2 B_2 G_\mu+\frac{1}{BG_1}\log t. \tag{14}$$

It has been observed that the creep under constant load can be expressed in the form $S=a^1+b^1 \log t$. Once again we see that B_2 is inversely proportional to initial stress, because b^1 above is found to be proportional to the stress.

Figure 5 shows the creep under constant load on the basis of this theory for several values of the parameter Bf_2^0. It is to be noted that these values are closely related to those in Fig. 1 by reflection about the x axis. Since $G_\mu<G_2$ the time scale for these types of experiments will be somewhat different.

Data on natural and synthetic rubbers creeping under fairly heavy load often appear to be best fitted by a sequence of straight lines when plotted against log time. This indicates that the bonds which have been assumed not to break

are also breaking after sufficiently long times. As before stated, there is probably a wide distribution of bond strengths, and the use of only two types of bonds is an idealization.

The phenomena of creep recovery are best explained by the Boltzmann memory principle,[15] which is a consequence of these equations of motion.

Extrusion Experiments

The non-Newtonian character of the flow in rubber-like materials is best shown by their behavior in being forced through a tube.[2] If the flow were Newtonian, Poiseuille's equation would apply and the rate of efflux through the tube would be proportional to the pressure head. This is definitely not the case for plastic and rubber-like polymers.

Suppose that we had a tube of length l, radius R, and were forcing material through it under a pressure head p. At any point whose distance from the axis of the tube is r, the shear force f is given by

$$f=pr/2l, \tag{15}$$

the shearing velocity du/dr we shall assume to be given by

$$du/dr=A \sinh Bf=A \sinh (Bpr/2l). \tag{16}$$

By integration we can find the velocity in the axial direction as a function of r. We make use of the condition that the velocity is zero when $r=R$. This gives

$$u=\frac{2Al}{Bp}\left[\cosh\frac{BpR}{2l}-\cosh\frac{Bpr}{2l}\right]. \tag{17}$$

The volume of matter delivered per second is

$$\frac{dV}{dt}=\int_0^R u2\pi r dr \tag{18}$$

and substituting for u from Eq. (17)

$$\frac{dV}{dt}=\frac{2\pi lR^2A}{Bp}\left[\cosh\frac{BpR}{2l}-\frac{4l}{BpR}\sinh\frac{BpR}{2l}+\frac{16l^2}{(BpR)^2}\sinh^2\frac{BpR}{4l}\right]. \tag{19}$$

[15] H. Leaderman, Textile Research **11**, 171 (1941).

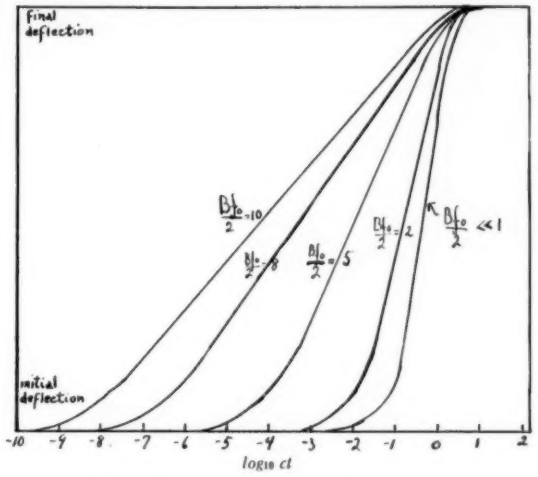

FIG. 5. Creep under constant stress.

For sufficiently large pressures

$$\frac{dV}{dt}\cong\frac{\pi lR^2A}{Bp}\exp(BpR/2l). \tag{20}$$

Once again it must be remarked that whereas some of the data on extrusion indicate that Eq. (19) is essentially correct (see Fig. 6), other data for materials with a high percent of primary cross bonds or with large amounts of filler indicate that more than one type of flow mechanism has to be accounted for. The data in reference 16 appear to be fitted by $N\cong10^{12}$ and $\Delta F^{\mp}\cong15$ kcals.

Vibration Experiments

If a rubber sample is subjected to a periodic stress, heat is generated because of the internal viscosities. Whereas the "viscosities" that one calculates for experiments of the type described in the above paragraphs is about 10^9 poises, the viscosity calculated in vibration experiments is from 10^3–10^5 poises. Most experiments on the effect of an alternating stress on rubber are carried out by a resonance method.[17,18] A mass is attached to the rubber sample, and either the applied frequency or the mass is changed until the amplitude is a maximum, at which point the natural frequency of the system is equal to the

[16] J. H. Dillon and N. Johnston, J. App. Phys. **4**, 225 (1933).
[17] S. D. Gehman, J. App. Phys. **13**, 402 (1942).
[18] R. B. Stambaugh, Ind. Eng. Chem. **34**, 1362 (1942).

externally applied frequency. From the height and breadth of the resonance curves one can calculate the "dynamic" viscosity and "dynamic" modulus of the rubber sample used.

For these experiments the amplitude of deformation is quite small. The frequency is usually of the order of 60 cycle/sec. It is reasonable to suppose that large scale breaking of primary or secondary bonds is not involved, but that the viscous dissipation in these experiments is in large part due to a motion of chain segments.

Another method of studying the relaxation mechanisms in polymers is by dielectric constant measurements of absorption and dispersion. Many rubber-like polymers show a broad distribution of relaxation times of the order of 10^{-6} second. It seems unreasonable to attribute these to motions of entire molecules, and so these rapid relaxations must be due to motions of chain segments.[19]

Let us for simplicity assume that Kuhn's formulation is adequate for these low stresses.

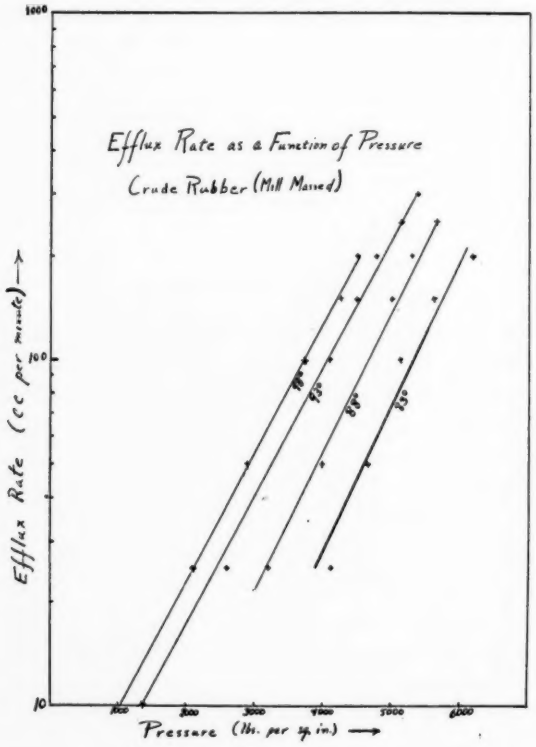

FIG. 6.

[19] W. Kauzmann and H. Eyring, J. Am. Chem. Soc. **62**, 3113 (1940).

Then in terms of the relaxation mechanisms the measured modulus and viscosity would be:

$$G \text{ dynamically measured} = \sum_i \frac{G_i \omega^2 \tau_i^2}{1+\omega^2 \tau_i^2}, \quad (21)$$

$$\eta \text{ dynamically measured} = \sum_i \frac{\eta_i}{1+\omega^2 \tau_i^2}, \quad (22)$$

where ω is the angular frequency and the subscript i refers to the ith relaxation mechanism. We see from the above that η is a decreasing function of ω and G is an increasing function of ω, so that the fact that the "static" modulus is lower than the dynamic modulus measured by these experiments is not surprising. Also at very high frequencies we might expect that the moduli of rubber approach the values encountered in crystalline hydrocarbons.

If segment motion causes the heat dissipation in rubber subjected to rapidly varying periodic forces, we might then expect some kind of correlation between the effect of side chains on the internal viscosity of polymers and of the viscosity corresponding short chain compounds. Figure 7 shows the effect of adding various groups to a hydrocarbon skeleton six atoms long.

Side groups alone do not determine the internal viscosity of polymeric materials. Intermolecular forces play an important role, and if the polymeric chains, for stereochemical reasons, pack very well the internal friction is high.

The exact dependence of G and η on frequency has not as yet been determined over a sufficiently wide frequency range to determine an appropriate distribution of relaxation times for the segment motion. The indications are that the distribution is quite broad.

If one makes the approximation that there are three relaxing mechanisms of the Kuhn type corresponding to the motion of primary network units, secondary network units, and segments, with relaxation times τ_1, τ_2, and τ_3, respectively, then Eqs. (21) and (22) can be simplified. Since τ_1 is very large, τ_2 is of the order of seconds and τ_3 is of the order of 10^{-6} second, and remembering the values of the G's and η's discussed previously, it can be seen from Eqs. (21) and (22) that for frequencies of the order of 60 cycles per second,

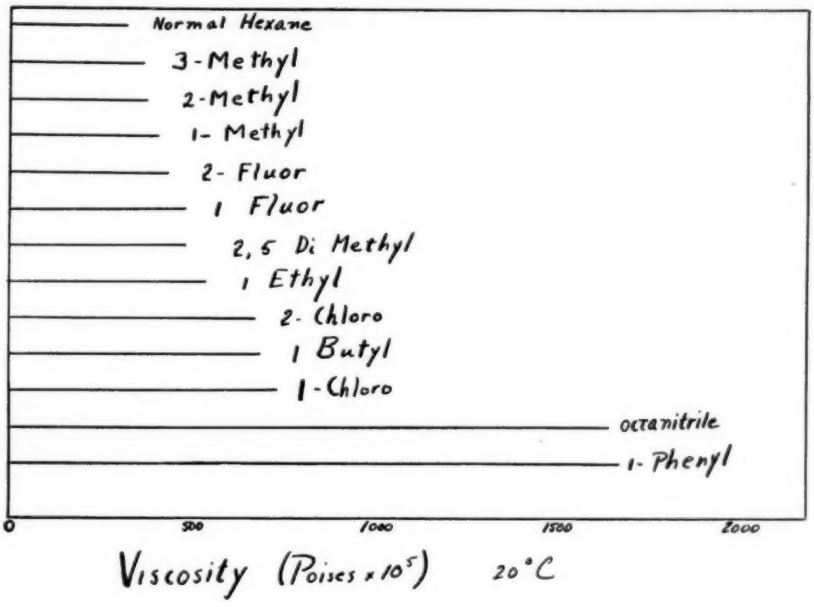

FIG. 7.

G and η are approximately given by

$$G=G_1+G_2=G \text{ dynamically measured,} \quad (23)$$

$$\eta=\frac{\eta_2}{1+\omega^2\tau_2^2}+\eta_3=\eta \text{ dynamically measured.} \quad (24)$$

In other words in a suitable frequency (perhaps from 20 to 200 cycles per second) the modulus should be independent of frequency and the viscosity plotted against $1/\omega^2$ should be approximately linear. Such appears to be the case for the data of Stambaugh.[18] (See Fig. 8.) From the graphs discussed above one can find G_1+G_2, which is the "dynamic modulus." η_3 can be obtained as the intercept of the η *vs.* $1/\omega^2$ plots, and G_2/τ_2 is the slope of these plots.

From Stambaugh's data one obtains Table I. Since G_1 is approximately the "static modulus" as measured in non-alternating experiments, which is of the same order of magnitude as the "dynamic modulus" (often one-third to one-half as large), G_2 can presumably be found. τ_2 will therefore turn out to be of the order of seconds.

It is to be noted that both segment viscosity and viscosity due to relaxation of secondary bonds contribute to the dynamic viscosity at 60 cycles per second. This may be the reason why plots of log η *vs.* $1/T$ show anomalous behavior which Stambaugh interpreted as due to crystallization phenomena.

Breaking of Polymeric Threads Under Load

In certain recent experiments on cotton and rayon threads,[20] the life of these threads at various temperatures was measured as a function of the load.

Suppose that the breaking is due to the slipping of bonds (which act as "primary" bonds for small loads, but which may be micellar bonds). If the number of such bonds per unit area is N, the rate of breaking of such bonds under stress f_0 if repair is possible is

$$-\frac{1}{N}\frac{dN}{dt}=\frac{kT}{h}\times\exp(-\Delta F^{\mp}/RT)2\sinh\frac{f_0\lambda}{2NkT}. \quad (25)$$

For large values of the stress, or when repair of the bonds does not take place, the equation is

$$-\frac{1}{N}\frac{dN}{dt}=\frac{kT}{h}\times\exp(-\Delta F^{\mp}/RT)\exp(f_0\lambda/2NkT). \quad (26)$$

[20] Busse, Lessig, Loughborough, and Larrick, J. App. Phys. **12**, 715 (1942).

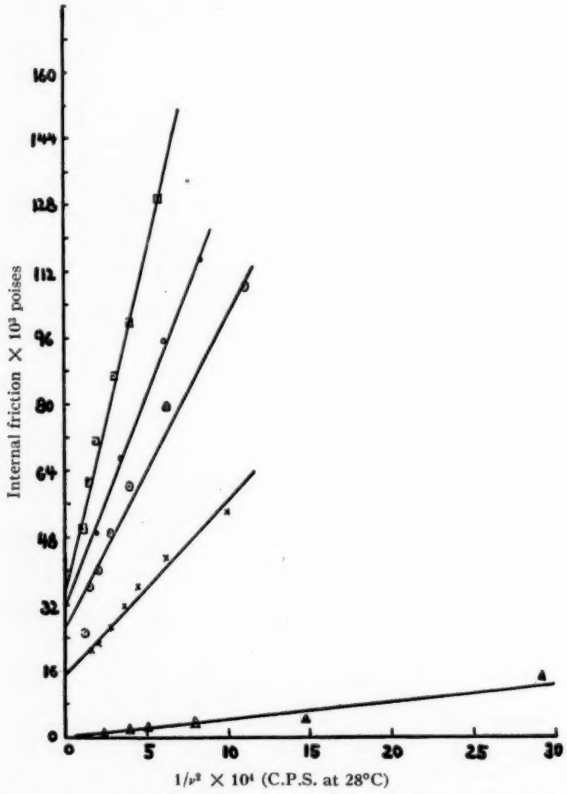

FIG. 8. △, rubber gum stock; X, rubber; ⊡, synthetic *D*; *o*, thiokol; ⊙, neoprene *E* and *GN*.

By the substitution $y=f_0\lambda/2NkT$ we obtain the following:

$$\int_{f_0\lambda/2N_0kT}^{\infty}\frac{e^{-y}}{y}dy=\frac{kT}{h}\exp(-\Delta F^{\mp}/kT)\tau, \quad (27)$$

where τ is the lifetime of the thread and N_0 the initial number of bonds per cross section. The upper limit of the integral is infinite because when the thread breaks the number of remaining bonds is zero.

The integral is the well-known and tabulated logarithmic integral $-Ei(-x)$. For sufficiently large values of x

$$-Ei(-x)\cong\frac{e^{-x}}{x}. \quad (28)$$

Equation (27) therefore becomes approximately

$$\frac{e^{-f_0\lambda/2N_0kT}}{f_0\lambda/2N_0kT}=\frac{kT}{h}\exp(-\Delta F^{\mp}/kT)\tau. \quad (29)$$

Or rewriting

$$\log\tau=\frac{-f_0\lambda}{2N_0kT}-\log\frac{f_0\lambda}{2N_0kT}-\log\frac{kT}{h}+\frac{\Delta F^{\mp}}{RT}. \quad (30)$$

This equation is in essential agreement with the experimentally observed equation of Busse, Lessig, Loughborough, and Larrick. It is to be noted that:

$$R\frac{d\log\tau}{d\frac{1}{T}}=\Delta H^{\mp}-\frac{f_0\lambda N_{\text{avogadro}}}{2N_0}. \quad (31)$$

It is to be noted that $[Rd\log\tau/d(1/T)]$ is only the apparent heat of activation. To obtain the true heat of activation one must either extrapolate the apparent heat to zero load or add $(f_0\lambda N_{\text{avogadro}})/2N_0$.

From the data of the above paper it appears that N, the number of bonds per unit area, is about 7×10^{12}, and $\Delta F^{\mp}$, the free energy of activation, is about 27 kcals.

TABLE I.

Polymer	η_3 poises	G_1+G_2 $\frac{\text{dynes}}{\text{cm}^2}$	G_2/τ_2
Natural gum	3×10^3	2.8×10^7	3.67×10^6
Natural rubber	1.4×10^4	9.6×10^7	4.2×10^7
Synthetic *D*	3.5×10^4	1.7×10^8	1.63×10^8
Thiokol	3.2×10^4	1.4×10^8	1.0×10^8
Neoprene *GN*	2.6×10^4	1.4×10^8	7.5×10^7

The Diffusion of Air Through Monel Metal

H. S. COLEMAN AND H. L. YEAGLEY
Department of Physics, The Pennsylvania State College, State College, Pennsylvania
(Received December 9, 1942)

The rate at which gases from the atmosphere diffuse through monel metal at various temperatures has been observed. An evacuated heavy-walled metal tube, a section of which was machined to a thin wall, was heated in a furnace. The rate at which the pressure inside the tube increased as a result of the diffusion of gases from the atmosphere was noted. The log R *vs.* $1/T$ curves, which are usually linear, show breaks about 900°C indicating some unusual physical change occurring in the alloy at this temperature. Dilatometric measurements on the same alloy were used to check the location of this break.

PREVIOUS studies of the diffusion of gases through metals have been largely confined to hydrogen-pure metal systems. A few studies of the diffusion of oxygen and nitrogen through certain metals have been made. These studies have been carefully summarized by McBain,[1] Smithells,[2] and Barrer[3] and, therefore, will not be reviewed here.

It is the purpose of this paper to present data relative to the diffusion of gases from the atmosphere through a common alloy of nickel, copper, and iron. This alloy is of great importance because of its wise usage in research apparatus, its non-corrosive properties, and the ease with which it may be machined at high speeds.

Briefly the experiment to be described is:

A metal tube closed at one end, the other end being connected to a vacuum system was heated in a furnace. The diffusion of gases from the atmosphere was observed by noting rate at which the pressure increased on the inside of the tube. The diffusion rate was observed at various temperatures.

THE APPARATUS

The apparatus essentially consists of the diffusion tube, the furnace, a vacuum system, and a temperature control. These parts are shown in Fig. 1.

The Diffusion Tube

The diffusion tube was made from heavy-walled tubing (4.5 mm), a section of which was machined to a wall thickness of 1.15 mm. The inside diameter of the tube was 1.74 cm. The length of this section of tube was 10 cm. One end of the tube was closed by welding a nickel disk on to the tube. Atomic hydrogen welding equipment was used. The tube was obtained from The International Nickel Company, and was found to be of the following chemical composition: 69.70 percent nickel, 28.00 percent copper, and 2.57 percent iron.

In addition, carbon was found to be present and estimated to be 0.1 percent.

The Furnace

A Nichrome resistance furnace was used to heat the diffusion tube. This furnace was provided with special booster coils near its open ends to reduce temperature gradients. This is shown in Fig. 2.

The Vacuum System

The open end of the diffusion tube was connected to a vacuum system by means of a glass to metal joint using DeKhotinsky cement. This joint was kept cold by means of a water cooler as indicated in Fig. 2.

The vacuum system was arranged with suitable stopcocks such that the diffusion tube and McLeod gauge could be isolated. A mercury diffusion pump and a Cenco Hi-Vacuum pump were used to exhaust the system. See Fig. 3. The fore pump was arranged with a special exhaust which made it possible to collect the diffusing gas by the displacement of water.

[1] J. W. McBain, *The Sorption of Gases by Solids* (Routledge, 1932).
[2] C. J. Smithells, *Gases and Metals* (Wiley, 1937).
[3] R. M. Barrer, *Diffusion in and Through Solids* (Macmillan, 1941).

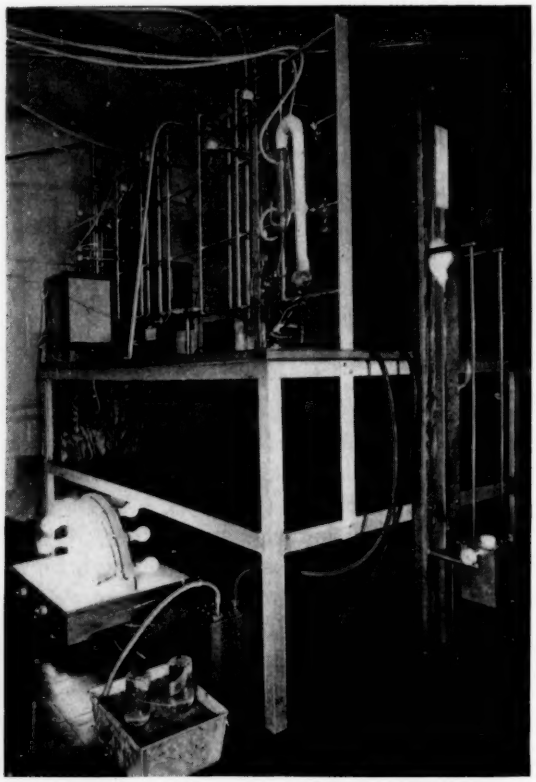

FIG. 1.

The Temperature Control

The temperature was measured by means of two Chromel-Alumel thermocouples fastened to the outside of the diffusion tube. One thermocouple was placed near the center of the thin section of the tube, the other at the edge as indicated by Fig. 2. The relative currents in the main heating coil and the booster coils were adjusted to reduce the temperature gradient along the length of the thin section of the diffusion tube to a minimum. The temperature was controlled both manually and automatically using a capacitrol in conjunction with a Leeds and Northrup portable potentiometer. See Fig. 4. The temperatures did not deviate from the mean by more than 2°C.

PROCEDURE

After the diffusion tube was evacuated and known to be vacuum tight, it was heated to 1250°C and degassed for one hour. Then a series of isothermal runs were made by closing the stopcock leading to the pumps and noting the rate at which the pressure built up inside the diffusion tube as a result of the diffusion of gases from the atmosphere through the thin section of the diffusion tube. The stopcock leading to the pumps was opened between each run to remove the diffused gas at which time the temperature was changed for the subsequent run. This technique of observing diffusion is known as the "trapping method" and is described in detail by Ham and Post[4] in their report on hydrogen diffusion through nickel and iron. Also the "steady state" method of observing diffusion developed by Ham[5] was used to check the trapping rates. The "steady state" method involves the partial closing of the cock leading from the diffusor to the pumps. The cock is adjusted by partly closing it until a desired pressure builds up in the diffusion tube. This pressure is permitted to come to equilibrium so

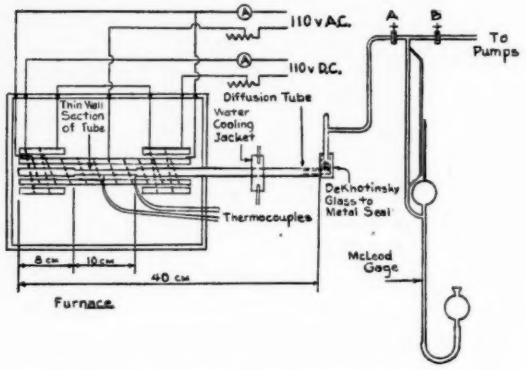

FIG. 2. Apparatus for diffusion of air through metals.

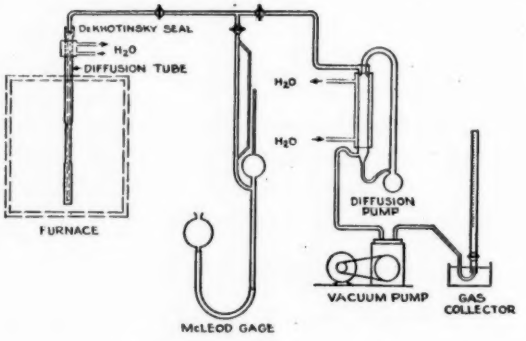

FIG. 3. Diffusion apparatus.

[4] C. B. Post and W. R. Ham, J. Chem. Phys. **6**, 598 (1938).
[5] W. R. Ham, Trans. A. S. M. E. (June, 1937).

that the pumps are removing the gas at the same rate at which it enters. The magnitude of this build-up pressure depends upon the temperature and has been shown to be proportional to the actual diffusion rate by Ham and Post.[4] The results of this experiment tend to confirm their claims for the "steady state" method.

THE DATA

The data are presented in graphic form using the usual coordinates of $\log_{10} R$ *vs.* $1/T$, where R is the diffusion rate and T is the absolute temperature at which the diffusion rate is determined.

(1) Figure 5 shows the degassing rate of the tube using the "steady state" method during a temperature range from 20°C to 1250°C and from 1250°C to 400°C.

(2) Figure 6 shows the diffusion rate as a function of temperature. The temperature was varied in a cycle from 450°C to 1250°C and from 1250°C to 450°C. The "steady state" method was used in this run.

(3) Figure 7 shows the trapping curves for a temperature range of 672°C to 1150°C. The pressure is expressed in microns of mercury and the time in minutes.

(4) Figure 8 shows the relation of the pressure, built up during the first minute after the gas was trapped, as a function of temperature.

(5) Figure 9 shows the steady state data which were obtained as a by-product in obtaining the trapping data. Each time the temperature was increased for the next run, the cock which isolated the diffusor from the pumps had to be opened in order to remove the diffused gas. Even with the stopcock wide open, there is a slight pressure built up in the system. This "steady state" pressure is a function of temperature and is referred to as the zero sensitivity steady state rate.

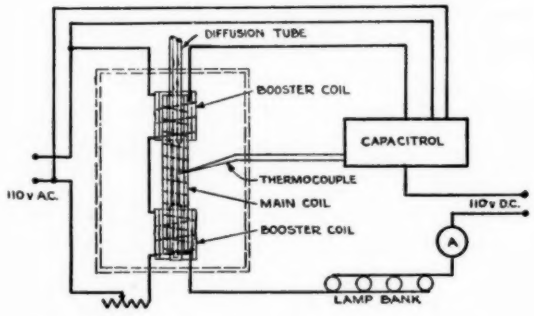

FIG. 4. Wiring diagram for diffusion apparatus.

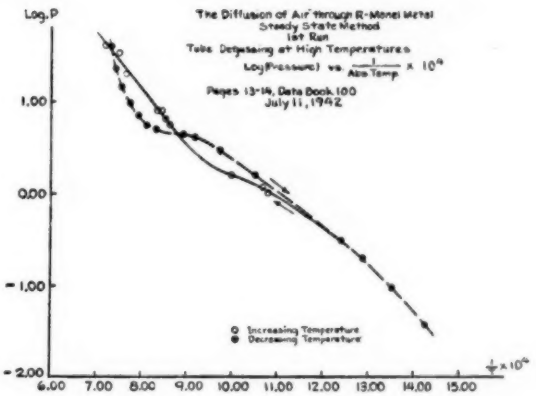

FIG. 5.

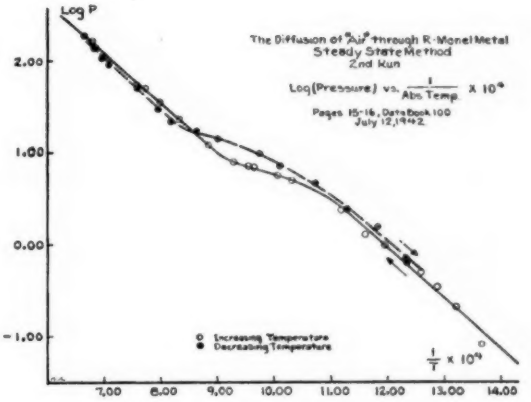

FIG. 6.

(6) Figure 10 shows the functional relation between the pressure and time for the trapping data. The plots are made using the coordinates P^2 *vs.* t. The pressure P is expressed in microns, and the time t in minutes. This method of plotting is used to rectify the $P-t$ curves and make possible the determination of the velocity constants at various temperatures.

(7) Figure 11 shows a logarithmic plot of the slopes of the rectified pressure-time curves as a function of the reciprocal of the absolute temperature.

(8) Figure 12 shows "steady state" data for an entirely new diffusor and completely rebuilt apparatus used to check the results indicated in Figs. 5–11 inclusive.

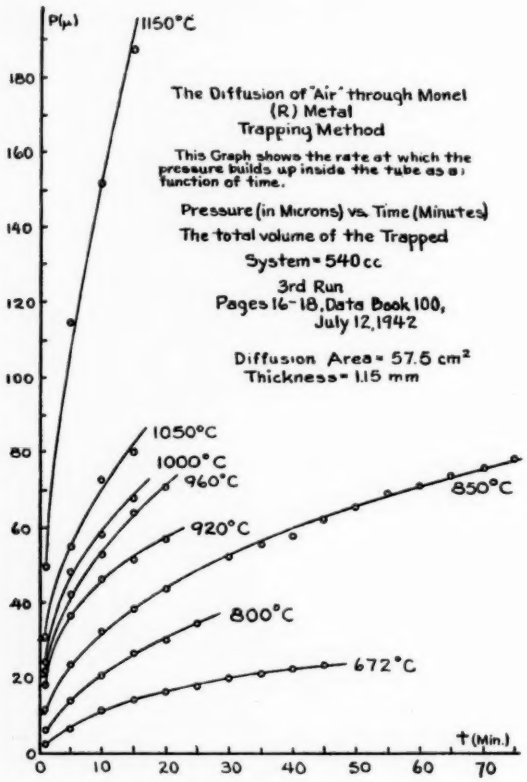
P(μ)
1150°C
The Diffusion of "Air" through Monel (R) Metal Trapping Method
This Graph shows the rate at which the pressure builds up inside the tube as a function of time.
Pressure (in Microns) vs. Time (Minutes)
The total volume of the Trapped System = 540 cc
3rd Run
Pages 16-18, Data Book 100, July 12, 1942
Diffusion Area = 57.5 cm²
Thickness = 1.15 mm
1050°C
1000°C
960°C
920°C
850°C
800°C
672°C
t (Min.)

FIG. 7.

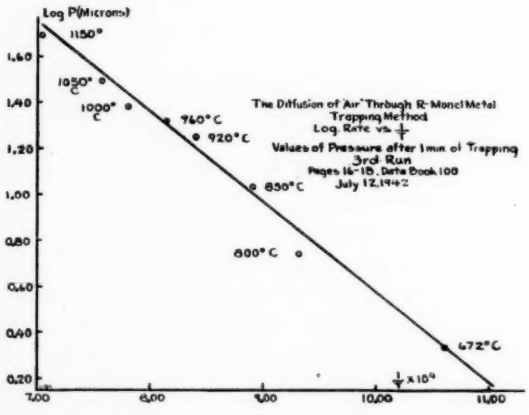

FIG. 8.

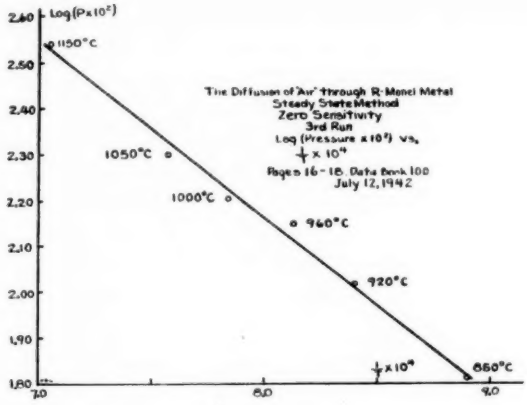

FIG. 9.

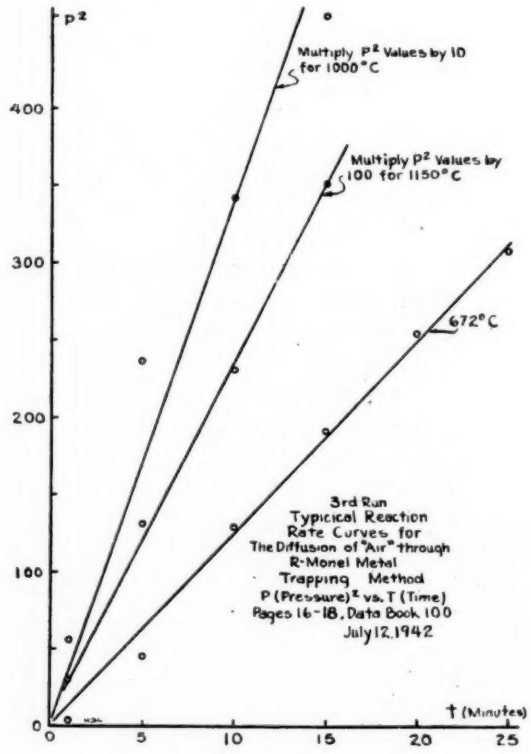
P²
Multiply P² Values by 10 for 1000°C
Multiply P² Values by 100 for 1150°C
672°C
3rd Run
Typical Reaction Rate Curves for The Diffusion of "Air" through R-Monel Metal
Trapping Method
P (Pressure)² vs. T (Time)
Pages 16-18, Data Book 100
July 12, 1942
t (Minutes)

FIG. 10.

DISCUSSION OF RESULTS

(1) It is evident that gases from the atmosphere diffuse through an alloy of nickel, copper, iron, and carbon.

(2) The slopes of the log R *vs.* $1/T$ curves obtained by the "steady state" and by the "trapping methods" are substantially the same.

(3) The slopes of the log R *vs.* $1/T$ are variable in certain regions. These regions are referred to as "breaks."

(4) The breaks in the log R *vs.* $1/T$ curves for the various runs occur in the same temperature region.

(5) The exact cause of the breaks in the log R *vs.* $1/T$ curves is not known. It is possible

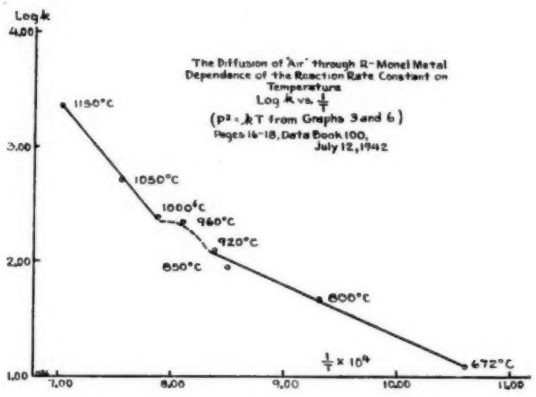

FIG. 11.

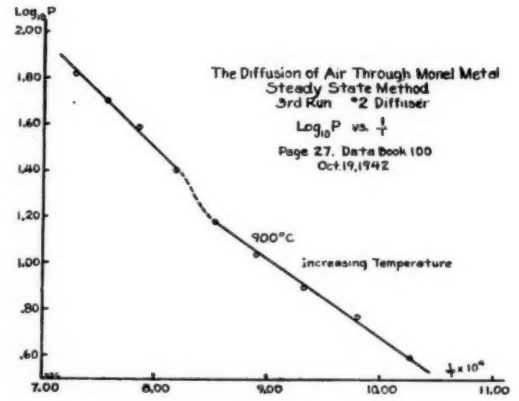

FIG. 12.

that it is a result of either the formation of a solid solution of NiO and Ni or an order-disorder occurring among the constituents.

(6) The breaks in the log R *vs.* $1/T$ curves are reproducible and do not appear to be greatly influenced by the heat treatment received during the experiment.

(7) The break in the log R *vs.* $1/T$ curves shows a hysteresis very similar to that obtained by Ham and Post[4] in their study of hydrogen diffusion through nickel and iron in the Cure regions for these metals.

(8) The material of diffusion tube was tested magnetically and was found to be non-magnetic above 50°C. Therefore the break occurring at

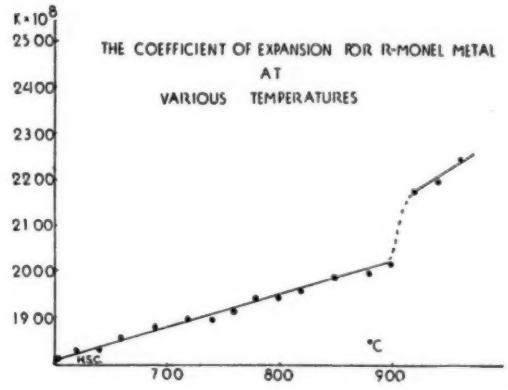

FIG. 13.

900°C in the log R *vs.* $1/T$ curves could not have been a magnetic change.

(9) The functional relation between the pressure and time of the reaction rate curves indicates that the diffusing gas leaves the inside surface of the tube as a diatomic molecule.

(10) The mechanism by which gases from the atmosphere diffuse through the tube is not known except that the gas is an atomic form as indicated by the reaction rate curves.

(11) The break in the log R *vs.* $1/T$ curves is an indication that there is some physical change occurring in the alloy at about 900°C. This results in a change in resistance of the alloy to the passage of the ironized atmospheric gas (or gases), much like an electrical resistance change to an ordinary electric current. This being the case, one would expect to find deviations in other physical properties at 900°C, such as thermal expansion, density, etc. Thermal expansion data were obtained by dilatometric methods using a section of the actual diffusor as a sample. These data are shown on Fig. 13 and indicate that there is a sharp change in the coefficient of expansion at about 925°C. This is an excellent check on the break obtained by diffusion methods. We are indebted to Dr. Carl H. Samans of The American Optical Company for the dilatometer curves.

A Note Concerning *l*-Type Doubling in Linear Polyatomic Molecules

HARALD H. NIELSEN AND WAVE H. SHAFFER
Mendenhall Laboratory of Physics, Ohio State University, Columbus, Ohio

(Received January 4, 1943)

It is shown that certain Coriolis interaction terms in the rotation-vibration Hamiltonian of a linear polyatomic molecule give second-order contributions to the energy which remove the degeneracy of levels associated with the quantum number l of internal angular momentum arising from a doubly degenerate perpendicular mode of oscillation. This type of splitting is called "*l*-type doubling" because it is exactly like "Λ-type doubling" in the electronic energy levels of diatomic molecules.

A TYPE of oscillation occurring in linear polyatomic molecules is one in which the constituent atomic nuclei are displaced perpendicularly to the internuclear axis of the molecule. Such oscillations are isotropic in two dimensions and are known as perpendicular modes. The quantum states of such oscillations are defined by two quantum numbers v_k and l_k; the first of these is the total vibration number which may assume positive integral values and the second is a measure, in units of $h/2\pi$, of the internal angular momentum directed along the internuclear axis which is associated with the doubly degenerate mode of oscillation. For a given value of v_k the quantum number l_k may assume the values $\pm v_k$, $\pm(v_k-2)$, $\pm(v_k-4)$, $\cdots\pm 1$ or 0. In zero order of approximation the vibration energy $E_v^0=hc\omega_k(v_k+1)$ is independent of l_k; hence such a state is (v_k+1)-fold degenerate in l_k. The rotation energy depends on l_k^2 and in second order of approximation the anharmonic terms in the potential function of the molecule also contribute to the energy terms which depend on l_k^2. The degeneracy in l_k is, therefore, partially removed up to second order of approximation and the zero-order vibration energy level splits up into $(v_k+1)/2$ components for odd values of v_k and into $1+(v_k/2)$ components for even values of v_k. The energy remains independent, however, of the algebraic sign of l_k and each sub-level remains twofold degenerate.

In a recent paper Herzberg[1] has suggested that there must be terms of interaction between the rotational and vibrational motion present in the Hamiltonian for a linear molecule which will further remove this degeneracy. In an attempt to clarify the character of these perturbations he has presented certain arguments of a semi-classical nature. In particular he has pointed out that certain terms in the Hamiltonian for the linear X_2Y_2 type molecule developed by Shaffer and Nielsen[2] (SN) have matrix elements diagonal in the quantum number v_k but non-diagonal in l_k. These terms lead to a splitting of the levels and Herzberg has computed the magnitude of this splitting for Π-vibration states (i.e., where $l_k=1$). Herzberg has, moreover, recognized the similarity of this type of splitting to that known as Λ-type splitting in diatomic molecules and he has accordingly termed it "*l*-type doubling." He has, moreover, demonstrated that such an *l*-type doubling is consistent with the existing data on the spectra of CO_2 and C_2H_2.

While we cannot subscribe to the classical arguments of Herzberg except in a very rough way, it is indeed true that there exist interaction terms in the Hamiltonian for a linear polyatomic molecule which further remove the degeneracy in l_k. The purpose of this note is essentially to point out that the Hamiltonian for the X_2Y_2 linear molecule developed by SN, although entirely adequate to give the elements of the energy matrix diagonal in v and l to second order of approximation, is not suitable for computing the correct value of the *l*-type splitting. This is not due to an error in computation, but as the authors indicate, certain terms which did not contribute to the diagonal elements of the energy matrix in this approximation were omitted to save space. We simply state here the correct form of the Hamiltonian for this type of

[1] Gerhard K. Herzberg, Rev. Mod. Phys. **14**, 219 (1942).

[2] W. H. Shaffer and A. H. Nielsen, J. Chem. Phys. **9**, 847 (1941).

molecule and then compute the value of the l-type splitting. The calculations could be carried out readily for the general linear polyatomic molecule; we have chosen the linear X_2Y_2 model because of its relative simplicity and especially since it is one of the models considered by Herzberg in his recent paper.

After the usual contact transformation has been performed the Hamiltonian for the linear X_2Y_2 molecule has the following form complete to second order of approximation and suitable for calculation of the l-type splitting:

$$H^0=(hc/2)\{\sum_{i=1}^{3}\omega_i(p_i^2/h^2+q_i^2)+\sum_{k=4}^{5}\omega_k[(p_{k1}^2+p_{k2}^2)/h^2+(q_{k1}^2+q_{k2}^2)]\}+(1/2I_e)(P_x^2+P_y^2). \quad (1a)$$

$$\begin{aligned}H^{(2)}=&(h^2/2I_e)-(ih/I_e)[\delta^2q_1p_1+\gamma^2q_2p_2-\gamma\delta(q_2p_1+q_1p_2)]+(1/2I_e)(p_x^2+p_y^2)+U_2\\
&-(1/2)(I_e)^{-3}[(\delta^2/\lambda_1)+(\gamma^2/\lambda_2)](P_x^2+P_y^2)^2+(1/2I_e)\{a_{11}q_1^2+a_{11}'p_1^2/h^2+a_{22}q_2^2\\
&+a_{22}'p_2^2/h^2+a_{33}q_3^2+a_{33}'p_3^2/h^2+a_{44}(q_{41}^2+q_{42}^2)+a_{44}'(p_{41}^2+p_{42}^2)/h^2+a_{55}(q_{51}^2+q_{52}^2)\\
&+a_{55}'(p_{51}^2+p_{52}^2)/h^2\}(P_x^2+P_y^2)+(1/I_e)\{b_{44}(q_{42}^2P_x^2+q_{41}^2P_y^2)+b_{44}'(p_{42}^2P_x^2+p_{41}^2P_y^2)/h^2\\
&+b_{55}(q_{52}^2P_x^2+q_{51}^2P_y^2)+b_{55}'(p_{52}^2P_x^2+p_{51}^2P_y^2)/h^2\}-(1/I_e)\{b_{44}q_{41}q_{42}+b_{44}'p_{41}p_{42}/h^2\\
&+b_{55}q_{51}q_{52}+b_{55}'p_{51}p_{52}/h^2\}(P_xP_y+P_yP_x)-hc\{\sum_{i=1}^{2}(\beta_{iii}^2/\omega_i)[1+(3q_i^4/2)+(3p_i^2q_i^2/h^2)]\\
&+\sum_{i=1}^{2}\sum_{i\neq j=1}^{3}(\beta_{ijj}^2/2\omega_i)(4\omega_j^2-\omega_i^2)^{-1}[(2\omega_j^2-\omega_i^2)q_j^4+4\omega_i\omega_jq_i^2q_j^2+2\omega_j^2q_j^2p_j^2/h^2]\\
&+\sum_{i=1}^{2}\sum_{k=4}^{5}(\beta_{ikk}^2/2\omega_i)(4\omega_k^2-\omega_i^2)^{-1}[(2\omega_k^2-\omega_i^2)(q_{k1}^2+q_{k2}^2)^2+4\omega_i\omega_kq_i^2(q_{k1}^2+q_{k2}^2)\\
&+2\omega_k^2(q_{k1}^2p_{k1}^2+q_{k2}^2p_{k2}^2)/h^2]+3\sum_{i=1}^{2}\sum_{j=1\neq i}^{3}(\beta_{iii}\beta_{ijj}/\omega_i)q_i^2q_j^2+3\sum_{i=1}^{2}\sum_{k=4}^{5}(\beta_{iii}\beta_{ikk}/\omega_i)q_i^2\\
&\times(q_{k1}^2+q_{k2}^2)+(\beta_{122}\beta_{133}/\omega_1)q_2^2q_3^2+(\beta_{211}\beta_{233}/\omega_2)q_1^2q_3^2+\sum_{i=1}^{2}\sum_{i\neq j=1}^{3}\sum_{k=4}^{5}(\beta_{ijj}\beta_{ikk}/\omega_i)q_j^2\\
&\times(q_{k1}^2+q_{k2}^2)+\sum_{i=1}^{2}(\beta_{i44}\beta_{i55}/\omega_i)(q_{41}^2+q_{42}^2)(q_{51}^2+q_{52}^2)\}. \quad (1b)\end{aligned}$$

The notation used here is that of SN except for the substitution of q_{k1} for r_k and q_{k2} for s_k. The following constants are defined differently from the corresponding ones in the paper of SN:

$$\begin{aligned}a_{11}&=(h/I_e\lambda_1^{\frac{1}{2}})\{3-2\gamma^2(\lambda_1-2\lambda_5)/(\lambda_1-\lambda_5)\}\\
&\quad+4\pi c(h/I_e)^{\frac{1}{2}}\{(2\beta_{111}\delta/\lambda_1^{\frac{3}{2}})-\beta_{112}\gamma(3\lambda_1-\lambda_2)/[\lambda_2^{\frac{3}{2}}(4\lambda_1-\lambda_2)]\},\\
a_{11}'&=2(h/I_e\lambda_1^{\frac{1}{2}})\gamma^2\lambda_1/(\lambda_1-\lambda_5)+4\pi c(h/I_e)^{\frac{1}{2}}\{(\beta_{111}\delta/\lambda_1^{\frac{3}{2}})-(\beta_{112}\gamma\lambda_1/[\lambda_2^{\frac{3}{2}}(4\lambda_1-\lambda_2)]\},\\
a_{22}&=(h/I_e\lambda_2^{\frac{1}{2}})\{3-2\delta^2(\lambda_2-2\lambda_5)/(\lambda_2-\lambda_5)\}\\
&\quad+4\pi c(h/I_e)^{\frac{1}{2}}\{(-2\beta_{222}\gamma/\lambda_2^{\frac{3}{2}})+\beta_{122}\delta(3\lambda_2-\lambda_1)/[\lambda_1^{\frac{3}{2}}(4\lambda_2-\lambda_1)]\},\\
a_{22}'&=2(h/I_e\lambda_2^{\frac{1}{2}})\delta^2\lambda_2/(\lambda_2-\lambda_5)+4\pi c(h/I_e)^{\frac{1}{2}}\{(-\beta_{222}\gamma/\lambda_2^{\frac{3}{2}})+\beta_{122}\delta\lambda_2/[\lambda_1^{\frac{3}{2}}(4\lambda_2-\lambda_1)]\},\\
a_{33}&=(h/I_e\lambda_3^{\frac{1}{2}})(\lambda_3+\lambda_4)/(\lambda_3-\lambda_4)\\
&\quad+4\pi c(h/I_e)^{\frac{1}{2}}\{\delta\lambda_1^{-\frac{1}{2}}\beta_{331}(3\lambda_3-\lambda_1)/(4\lambda_3-\lambda_1)-\gamma\lambda_2^{-\frac{1}{2}}\beta_{332}(3\lambda_3-\lambda_2)/(4\lambda_3-\lambda_2)\},\\
a_{33}'&=2(h/I_e\lambda_3^{\frac{1}{2}})\lambda_3/(\lambda_3-\lambda_4)+4\pi c(h/I_e)^{\frac{1}{2}}\{\delta\lambda_1^{-\frac{1}{2}}\beta_{331}\lambda_3/(4\lambda_3-\lambda_1)-\gamma\lambda_2^{-\frac{1}{2}}\beta_{332}\lambda_3/(4\lambda_3-\lambda_2)\}, \quad (2)\\
a_{44}&=4\pi c(h/I_e)^{\frac{1}{2}}\{\delta\beta_{441}\lambda_1^{-\frac{1}{2}}(3\lambda_4-\lambda_1)/(4\lambda_4-\lambda_1)-\gamma\beta_{442}\lambda_2^{-\frac{1}{2}}(3\lambda_4-\lambda_2)/(4\lambda_4-\lambda_2)\},\end{aligned}$$

$$a_{44}'=4\pi c(h/I_e)^{\frac{1}{2}}\{\delta\beta_{441}\lambda_1^{-\frac{1}{2}}\lambda_4/(4\lambda_4-\lambda_1)-\gamma\beta_{442}\lambda_2^{-\frac{1}{2}}\lambda_4/(4\lambda_4-\lambda_2)\},$$

$$a_{55}=4\pi c(h/I_e)^{\frac{1}{2}}\{\delta\beta_{551}\lambda_1^{-\frac{1}{2}}(3\lambda_5-\lambda_1)/(4\lambda_5-\lambda_1)-\gamma\beta_{552}\lambda_2^{-\frac{1}{2}}(3\lambda_5-\lambda_2)/(4\lambda_5-\lambda_2)\},$$

$$a_{55}'=4\pi c(h/I_e)^{\frac{1}{2}}\{\delta\beta_{551}\lambda_1^{-\frac{1}{2}}\lambda_5/(4\lambda_5-\lambda_1)-\gamma\beta_{552}\lambda_2^{-\frac{1}{2}}\lambda_5/(4\lambda_5-\lambda_2)\},$$

$$b_{44}=(h/2I_e)\lambda_4^{-\frac{1}{2}}(\lambda_4+\lambda_3)/(\lambda_4-\lambda_3),$$

$$b_{44}'=(h/I_e)\lambda_4^{-\frac{1}{2}}\lambda_4/(\lambda_4-\lambda_3),$$

$$b_{55}=(h/2I_e)\lambda_5^{-\frac{1}{2}}\{[(\lambda_5+\lambda_2)/(\lambda_5-\lambda_2)]\delta^2+[(\lambda_5+\lambda_1)/(\lambda_5-\lambda_2)]\gamma^2\},$$

$$b_{55}'=(h/2I_e)\lambda_5^{-\frac{1}{2}}\{[\lambda_5/(\lambda_5-\lambda_2)\delta^2]+[\lambda_5/(\lambda_5-\lambda_1)]\gamma^2\}.$$

As Herzberg has pointed out, it is just the terms containing a_{44}, a_{44}', b_{44}, b_{44}', a_{55}, a_{55}', etc., which will give rise to the l-type splitting. These terms originate entirely with the Coriolis forces and are not, as Herzberg suggests,[3] in part due to the harmonic deformation of the molecule. When one replaces q_{k1} by $\rho_k\cos\phi_k$, q_{k2} by $\rho_k\sin\phi_k$, ip_{k1}/h by

$$\left(\cos\phi_k\frac{\partial}{\partial\rho_k}-\frac{\sin\phi_k}{\rho_k}\frac{\partial}{\partial\phi_k}\right),$$

and ip_{k2}/h by

$$\left(\sin\phi_k\frac{\partial}{\partial\rho_k}+\frac{\cos\phi_k}{\rho_k}\frac{\partial}{\partial\phi_k}\right),$$

the term in question reduces to

$$\begin{aligned}(1/2I_e)\sum_{k=4}^{5}&\left\{b_{kk}\rho_k^2-b_{kk}'\left[\frac{\partial^2}{\partial\rho_k^2}+\frac{1}{\rho_k}\frac{\partial}{\partial\rho_k}+\frac{1}{\rho_k^2}\frac{\partial^2}{\partial\phi_k^2}\right]\right\}(P_x^2+P_y^2)\\
&-(1/4I_e)\sum_{k=4}^{5}e^{2i\phi_k}\left\{b_{kk}\rho_k^2-b_{kk}'\left[\frac{\partial^2}{\partial\rho_k^2}+\frac{1}{\rho_k}\frac{\partial}{\partial\rho_k}+\frac{1}{\rho_k^2}\frac{\partial^2}{\partial\phi_k^2}\right]\right.\\
&\left.-2ib_{kk}'\left[\frac{1}{\rho_k}\frac{\partial^2}{\partial\rho_k\partial\phi_k}-\frac{1}{\rho_k^2}\frac{\partial}{\partial\phi_k}+\frac{i}{\rho_k}\frac{\partial}{\partial\rho_k}+\frac{i}{\rho_k^2}\frac{\partial^2}{\partial\phi_k^2}\right]\right\}[(P_x^2-P_y^2)-i(P_xP_y+P_yP_x)]\\
&-(1/4I_e)\sum_{k=4}^{5}e^{-2i\phi_k}\left\{b_{kk}\rho_k^2-b_{kk}'\left[\frac{\partial^2}{\partial\rho_k^2}+\frac{1}{\rho_k}\frac{\partial}{\partial\rho_k}+\frac{1}{\rho_k^2}\frac{\partial^2}{\partial\phi_k^2}\right]\right.\\
&\left.+2ib_{kk}'\left[\frac{1}{\rho_k}\frac{\partial^2}{\partial\rho_k\partial\phi_k}-\frac{1}{\rho_k^2}\frac{\partial}{\partial\phi_k}-\frac{i}{\rho_k}\frac{\partial}{\partial\rho_k}-\frac{i}{\rho_k^2}\frac{\partial^2}{\partial\phi_k^2}\right]\right\}[(P_x^2-P_y^2)+i(P_xP_y+P_yP_x)]. \quad (3)\end{aligned}$$

The matrix elements of H diagonal in all the quantum numbers, including the first term in (3), have been calculated in the work of SN and will not be repeated here. The additional matrix elements which we shall investigate are the following:

$$(v_4l_4v_5l_5|H^{(2)}|v_4'l_4'v_5'l_5')=\int\psi^*_{v_4l_4}\psi^*_{v_5l_5}R^*_{Jl}H^{(2)}\psi_{v_4l_4}\psi_{v_5l_5}R_{J'l'}d\tau, \quad (4)$$

where $v_k\neq v_k'$ and $l_k\neq l_k'$ and where

$$\psi_{v_kl_k}=N_{v_kl_k}\exp((-\rho_k^2/2)+il_k\phi_k)F^{l_k}{}_{\frac{1}{2}(v_k+l_k)}(\rho_k^2)$$

if

$$N_{v_kl_k}=2^{\frac{1}{2}}\{[(v_k-l_k)/2]!\}^{\frac{1}{2}}/\{[(v_k+l_k)/2]!\}^{\frac{1}{2}},$$

[3] That these terms originate entirely with the Coriolis forces may be seen from an inspection of a problem suggested to us by Herzberg in a private communication. The quantum mechanical Hamiltonian for the linear XY_2 molecule is derived from a classical kinetic energy expression where the classical Coriolis terms have been set equal to zero. The eigenvalues are readily obtained and one sees that the l-type doubling is identically zero.

and $F^{|l_k|}{}_{\frac{1}{2}(v_k+u)}$ is an associated Laguerre polynomial, and R_{J1} is the rotator wave function in which $l=\sum_k l_k$.

To calculate the energies arising from l-type doubling it is necessary to evaluate only those matrix elements for which $v_k=v_k'$ and $l_k\neq l_k'$ because any element not diagonal in v_k can contribute to the energy only in a still higher order of approximation. The second and third parts of (3) are the only terms in $H^{(2)}$ which have non-vanishing matrix elements when $v_k=v_k'$ and $l_k\neq l_k'$, and only for $l_k'=l_k\pm 2$, because the only non-vanishing elements of P_x^2, P_y^2, P_xP_y, or P_yP_x are those for which either $l_k=l_k'$ or $l_k'=l_k\pm 2$. It can be shown that

$$(v_k l_k|\rho_k^2|v_k l_k\pm 2)=[(v_k\mp l_k)(v_k\pm l_k+2)]^{\frac{1}{2}}$$

and that the corresponding matrix elements of

$$\left(\frac{\partial^2}{\partial\rho_k^2}+\frac{1}{\rho_k}\frac{\partial}{\partial\rho_k}+\frac{1}{\rho_k^2}\frac{\partial^2}{\partial\phi_k^2}\right)$$

have the same values as those of ρ_k^2. It can be shown that

$$\left(\frac{1}{\rho_k}\frac{\partial^2}{\partial\rho_k\partial\phi_k}-\frac{1}{\rho_k^2}\frac{\partial}{\partial\phi_k}\pm\frac{i}{\rho_k}\frac{\partial}{\partial\rho_k}\pm\frac{i}{\rho_k^2}\frac{\partial^2}{\partial\phi_k^2}\right)$$

has no non-vanishing matrix elements diagonal in v_k. Integration over the rotational wave functions gives

$$\begin{aligned}(Jl|P_x^2|Jl\pm 2)&=-(Jl|P_y^2|Jl\pm 2),\\&=\pm\frac{i}{2}(Jl|P_xP_y+P_yP_x|Jl\pm 2),\\&=(\hbar^2/4)[f-l(l\pm 1)]^{\frac{1}{2}}[f-(l\pm 1)(l\pm 2)]^{\frac{1}{2}},\end{aligned}$$

where

$$f=J(J+1)\quad\text{and}\quad l=\sum_k l_k.$$

The non-diagonal matrix elements of $H^{(2)}$ which contribute to the l-type doubling have the value

$$\begin{aligned}&(v_k l_k|H^{(2)}|v_k l_k\pm 2)\\&\quad=(hcB_e^2/\omega_k)[(v_k\mp l_k)(v_k\pm l_k+2)]^{\frac{1}{2}}\\&\quad\times[f-l(l\pm 1)]^{\frac{1}{2}}[f-(l\pm 1)(l\pm 2)]^{\frac{1}{2}},\end{aligned}\tag{5}$$

where $B_e=(h/8\pi^2cI_e)$. The values of the energy associated with the l-type doubling can be determined from the secular determinant

$$|(v_k l_k|H^{(2)}|v_k l_k')-E\delta_{kk'}|=0.$$

The twofold degeneracy in l_k associated with the independence of energy of algebraic sign of l_k is thus removed not only for $l_k=l$, as Herzberg indicates, but for all values of l_k. A few examples of l-type doubling are considered below.

For $v_k=1$ the quantum number l_k takes the values $+1$ and -1 and if the quantum number $l_{k'}=0$ we have what may be termed a Π-vibration state. In this case the only non-vanishing off-diagonal matrix elements are

$$(1,\pm 1|H^{(2)}|1,\mp 1)=2hc(B_e^2/\omega_k)J(J+1).\tag{6}$$

The two roots of the secular determinant are

$$E=\bar{E}\pm 2hc(B_e^2/\omega_k)J(J+1),\tag{7}$$

where $\bar{E}$ denotes the energy value given by SN.

When $v_k=2$ the quantum number l_k may take the values ± 2 and 0, and if $l_{k'}=0$ we have what may be termed a Δ-vibration state and a Σ-state. The non-vanishing off-diagonal matrix elements are

$$\begin{aligned}(2,\pm 2|H^{(2)}|2,0)&=(2,0|H^{(2)}|2,\pm 2)\\&=2^{\frac{1}{2}}hc(B_e^2/\omega_k)[f(f-2)]^{\frac{1}{2}}=A.\end{aligned}$$

If $\bar{E}_2$ and $\bar{E}_0$ denote for $l_k=\pm 2$ and $l_k=0$, respectively, the values of the energies given by SN, the secular determinant for the l-type splitting for this case is

$$\begin{vmatrix}\bar{E}_2-E & A & 0\\ A & \bar{E}_0-E & A\\ 0 & A & \bar{E}_2-E\end{vmatrix}=0.\tag{8}$$

The roots are $E=\bar{E}_2$ and

$$E=(1/2)\{(\bar{E}_0+\bar{E}_2)\pm[(\bar{E}_2-\bar{E}_0)^2+8A^2]^{\frac{1}{2}}\}.\tag{9}$$

By referring to the paper by SN the reader may readily verify that $(\bar{E}_2-\bar{E}_0)=4(X_{kk}-B_e)$. The magnitude of $(\bar{E}_2-\bar{E}_0)$ is, in general, large compared with $(B_e^2/\omega_k)^2$ and the latter two roots in Eq. (9) may be expanded and expressed approximately as

$$E=\bar{E}_2+f(f-2)(4h^2c^2B_e^4/\omega_k^2)/(X_{kk}-B_e),\tag{10a}$$

$$E=\bar{E}_0-f(f-2)(4h^2c^2B_e^4/\omega_k^2)/(X_{kk}-B_e).\tag{10b}$$

The l-type doubling thus produces a splitting of the Δ-state of magnitude $(4hcB_e^4/\omega_k^2)f(f-2)/(X_{kk}-B_e)$ cm^{-1}, that is, the splitting is proportional to $(B_e^2/\omega_k)^2/(X_{kk}-B_e)$. In a similar manner it may be shown the l-type splitting for any vibration state is proportional to $(B_e^2/\omega_k)^{l_k} \times (X_{kk}-B_e)^{-l_k+1}$. It may be verified by reference to the works of Hill and Van Vleck[4] and Kronig[5] that the l-type splitting in the case of fundamental and harmonic vibration states is entirely analogous to Λ-type splitting for singlet electronic states in the case of diatomic molecules.

An interesting case of l-type doubling may be found in the example of the combination state $\omega_4+\omega_5$. In this case $v_4=v_5=1$ and l_4 and l_5 may each take the values ± 1. If $a=2hc(B_e^2/\omega_4)f$, $b=2hc(B_e^2/\omega_5)f$ and $f=J(J+1)$ the secular determinant for this case is:

	$l_4=l_5=1$	$-l_4=l_5=1$	$-l_5=l_4=1$	$l_4=l_5=-1$
$l_4=l_5=1$	$\bar{E}_2-E$	a	b	0
$-l_4=l_5=1$	a	$\bar{E}_0-E$	0	b
$-l_5=l_4=1$	b	0	$\bar{E}_0-E$	a
$l_4=l_5=-1$	0	b	a	$\bar{E}_2-E$

$=0,$ (11)

where $\bar{E}_2$ and $\bar{E}_0$ are obtained from the energy expressions of SN by setting $l_4=l_5=\pm 1$ and $l_4=-l_5=\pm 1$, respectively. The four roots of Eq. (11) can readily be shown to be, since $\bar{E}_2-\bar{E}_0=4B_e$,

$$E=\bar{E}_2+h^2c^2B_e^3f^2(\omega_4^{-1}\pm\omega_5^{-1})^2, \quad (12a)$$

$$E=\bar{E}_0+h^2c^2B_e^3f^2(\omega_4^{-1}\pm\omega_5^{-1})^2. \quad (12b)$$

The l-type splitting for this case thus becomes $4hc(B_e^3/\omega_4\omega_5)f^2$ cm^{-1}. This case resembles the Λ-type doubling of doublet states in Hund's case a.

The preceding considerations may as readily be applied to the general linear polyatomic molecule discussed by Nielsen.[6] In addition to the matrix elements diagonal in all the quantum numbers given in that work it is necessary to consider the off-diagonal elements corresponding to those given in Eq. (6) for the linear X_2Y_2 model:

$$(v_1l_1\cdots v_kl_k\cdots v_nl_n|H^{(2)}|v_1l_1\cdots v_kl_k\pm 2\cdots v_nl_n)$$
$$=\sum_s\xi_{ks}^2hc(B_e^2/\omega_k)(v_k\mp l_k)^{\frac{1}{2}}(v_k\pm l_k+2)^{\frac{1}{2}}$$
$$\times[f-l(l\pm 1)]^{\frac{1}{2}}[f-(l\pm 1)(l\pm 2)]^{\frac{1}{2}}, \quad (13)$$

where $l=\sum_k l_k$. The expression (13) differs from (5) only in the presence of the coefficient $\sum_s\xi_{ks}^2$ where ξ_{ks} is one of the Coriolis parameters and depends upon the masses of the nuclei, the dimensions of the molecule and the harmonic force constants. In all the linear cases where we have evaluated the sum $\sum_s \xi_{ks}^2$ it has been equal to unity. This is probably true for the general linear molecule but we have no general proof of it.

While the l-type doubling exists for all states having a quantum number $l_k\neq 0$, it is likely that only in Π-vibration states is the effect large enough to be of importance in the interpretation of spectra.

It may be of interest to remark that l-type splitting must also occur in the perpendicular vibration states of axially symmetric molecules. This problem is very complicated and not worth considering since bands of this type are in general so complex that the effect could not be observed. Since the linear molecule is a special case of the axially symmetric molecule, the problem of l-type splitting in axially symmetric molecules could be handled by a procedure similar to that given in this paper.

[4] E. Hill and J. H. Van Vleck, Phys. Rev. **32**, 250 (1928).
[5] R. de L. Kronig, Zeits. f. Physik **50**, 347 (1928).
[6] H. H. Nielsen, Phys. Rev. **60**, 794 (1941).

Crystal Structure of Gadolinium Formate, $Gd(OOCH)_3$

A. PABST
University of California, Berkeley, California

(Received December 8, 1942)

The crystal structure of gadolinium formate has been studied by means of Laue, rotation, and powder x-ray patterns. It has a rhombohedral lattice. The unit cell, $a_0=6.17$A, $a=115°\ 30'$, contains one molecule, $Gd(OOCH)_3$. Density—(calculated) 3.85, (Berman balance) 3.77. By taking into consideration the symmetry of special positions all space groups except D_3^7-R32 and C_{3v}^5-R3m can be excluded. A structure has been found in the latter group which yields excellent agreement of calculated and observed intensities.

INTRODUCTION AND ACKNOWLEDGMENTS

NEARLY ten years ago the writer reported observations on crystals of gadolinium formate.[1] Sometime later more crystals of this substance were kindly prepared by Dr. George C. Nutting, then of the College of Chemistry at the University of California, and these have been used for the determination of the crystal structure. Most of the x-ray diffraction patterns used in this work were obtained while the writer held a fellowship of the John Simon Guggenheim Memorial Foundation in the Department of Mineralogy, British Museum of Natural History. The kindness of Dr. W. Campbell Smith and of Mr. F. A. Bannister in making available the facilities of that department is gratefully acknowledged.

DIMENSIONS, DENSITY, AND CELL CONTENT

From a powder pattern with Mo radiation in an 8-inch cassette, later checked by numerous other patterns, the dimensions of the smallest possible hexagonal cell were found to be $a_h=10.44$A, $c_h=3.98$A, $c_h/a_h=0.381$. The axial ratio previously reported,[2] 0.375, is probably less accurate. It was based on the angle ρ of the unit form, $\{10\bar{1}1\}$. The axial ratio corresponding to the observed angle ρ of the $\{02\bar{2}1\}$ form is 0.381, just checking the x-ray value.

The density of gadolinium formate crystals was determined by Berman torsion microbalance to be 3.77 ± 0.04. This agrees satisfactorily with the value 3.85, which would correspond to a content of three formular units in the smallest hexagonal cell.

[1] A. Pabst, Am. J. Sci. **36**, 72–79 (1933).
[2] Reference 1, p. 73.

TRANSLATION LATTICE

Powder patterns showed only lines for which $h-l-k=3n$, indicating a rhombohedral lattice. The rhombohedral unit cell, containing just one $Gd(OOCH)_3$, has the dimensions $a_r=6.17$A, $\angle a=115°\ 30'$.

The morphology of the crystals[3] is clearly indicative of the lattice character. The following table shows the agreement with the theoretical order of forms.[4]

Forms		Order	
$\{hkil\}$	$\{h_rk_rl_r\}$	Observed	Donnay-Harker law
$\{11\bar{2}0\}$	$\{10\bar{1}\}$	1	1
$\{10\bar{1}1\}$	$\{100\}$	2	2
$\{10\bar{1}0\}$	$\{11\bar{2}\}$	—	3
$\{02\bar{2}1\}$	$\{11\bar{1}\}$	3	4

SYMMETRY AND SPACE GROUP

A Laue pattern with the beam normal to the $(10\bar{1})$ face shows that the crystal belongs in the Laue group $D_{3d}-\bar{3}m$. The only extinctions are those required by a rhombohedral lattice. Rotation patterns with Cu and with Cr radiation show every line, even including all beta-lines, permitted by a simple rhombohedral lattice. This indicates the space groups $D_{3d}^5-R\bar{3}m$, D_3^7-R32 or C_{3v}^5-R3m.

The choice of space groups can be further limited by considering the symmetry of special positions. The rhombohedral unit cell contains three C atoms. From the known configuration of the formate group these C atoms cannot lie at centers of symmetry. In the space group $R\bar{3}m$ there are two sets of threefold positions, both at

[3] Reference 1, p. 72.
[4] J. D. H. Donnay and David Harker, Am. Mineral. **22**, 446–467 (Palache number) (1937).

centers of symmetry. This leaves no suitable position for C and eliminates the group. In the groups $R32$ and $R3m$ the threefold positions are on twofold axes and planes of symmetry, respectively, and either kind of position is compatible with the configuration of the formate group.

Auxiliary observations sometimes help in the choice of space groups which lie in different symmetry classes:

Morphology in this case[5] suggests the class $\bar{3}m$, just eliminated, so that the crystals are certainly pseudosymmetrical. A statistical study of recorded faces on eleven crystals gives no indication of a tendency to hemimorphism which might be expected in class $3m$.

Pyroelectricity is a symmetry criterion in this case only if the distribution of charges on the surface can be observed with exactness, since both possible classes, 32 and $3m$, would permit the effect. The small size of the crystals, diameter less than one millimeter, precluded the possibility of satisfactory observations.

Optical Activity would indicate the class 32. It was not detected, but this does not eliminate the class since the effect generally is very slight and not easily observed.

Etch Figures developed on $\{11\bar{2}0\}\{10\bar{1}\}$ indicate no symmetry normal to that form. This, taken together with the morphology, was previously interpreted[5] as indicating the class $C_{3i}-\bar{3}$, but that class is incompatible with the Laue symmetry or the requirements of the carbon positions. In class 32 these figures should show twofold axes. Since they do not they might be considered to eliminate it. Because the etch figures are not very good it seems safer to say that they merely yield a presumption in favor of class $3m$.

DETERMINATION OF THE STRUCTURE

The positions in space group $R32$ are:

1: (a) 000 (b) $\frac{1}{2}\frac{1}{2}\frac{1}{2}$
2: (c) xxx; $\bar{x}\bar{x}\bar{x}$
3: (d) $0x\bar{x}$; $\bar{x}0x$; $x\bar{x}0$ (e) $\frac{1}{2}x\bar{x}$; $\bar{x}\frac{1}{2}x$; $x\bar{x}\frac{1}{2}$
6: (f) xyz; zxy; yzx; $\bar{y}\bar{x}\bar{z}$; $\bar{z}\bar{y}\bar{x}$; $\bar{x}\bar{z}\bar{y}$.

The choice between positions (a) and (b) corresponds merely to the selection of an origin. It is required to assign coordinates to: one gadolinium, three carbon, three hydrogen, and six oxygen atoms. Assigning Gd to position (a), the carbons may be placed on the twofold axes in (d) or in (e). It will, of course, be impossible to determine parameters for hydrogen from intensities, but the hydrogens will lie on the same axes as the carbons. All the oxygens may then be placed in a sixfold "general" position. This allows the placing of six oxygens about each gadolinium in a slightly deformed octahedral arrangement, each formate group being tied to two gadoliniums. Several variants of this structure may be found which conform to the known configuration of the formate group[6] and the radius of gadolinium. A certain variation of the parameters is possible, sliding the formate groups and rotating them on the twofold axes, within the limits allowed by atomic radii. Intensity calculations were carried out for numerous combinations of parameters within these allowable limits. None of them showed satisfactory agreement with observed intensities and any structure in this space group must be considered eliminated.

The positions in space group $R3m$ are:

1: (a) xxx
3: (b) xxz; xzx; zxx
6: (c) xyz; zxy; yzx; yxz; zyx; xzy.

The choice of a parameter for gadolinium in the (a) position corresponds to selection of an origin and it is best placed at 000. The carbon atoms necessarily go into (b) positions which lie in the planes of symmetry. If all the oxygen atoms are equivalent they must lie in (c) positions, flanking the symmetry planes and forming ditrigonal rings, which might be practically hexagonal, about the threefold axes on which lie the gadoliniums. Such an arrangement does not permit the tying together of the structure by formate bridges between gadoliniums because the two oxygens of each formate group would both be closest to the same gadolinium, as may be seen from an inspection of the symmetry diagram for this space-group.[7] Such a structure would be molecular and possibly even sheetlike. From the

[5] Reference 1, p. 72.

[6] L. Pauling and L. O. Brockway, Proc. Nat. Acad. Sci. **20**, 336–340 (1934), and W. H. Zachariasen, J. Am. Chem. Soc. **62**, 1011–1013 (1940).

[7] *International Tables for the Determination of Crystal Structures* (New York, 1935), vol. I, p. 243.

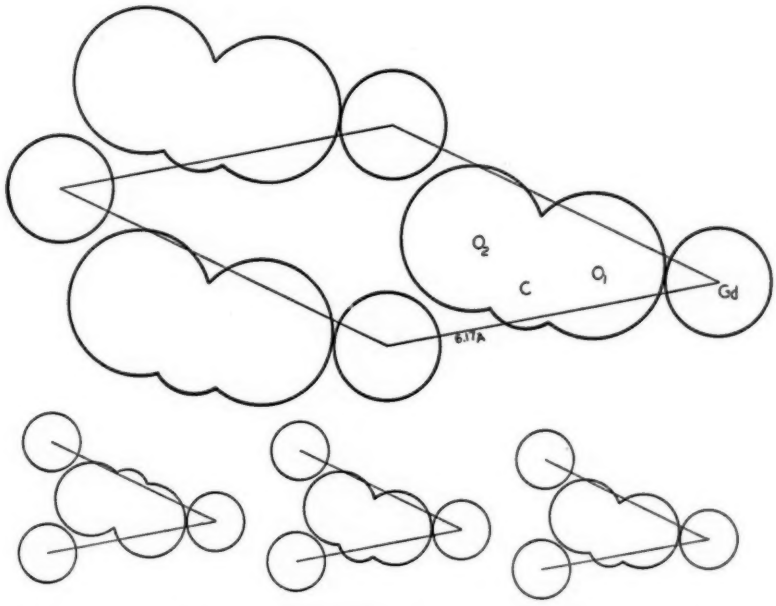

FIG. 1. Top: Section through rhombohedral cell of gadolinium formate in the $1\bar{2}10$ or $0\bar{1}1$ plane, which is a plane of symmetry. The Gd atoms lie on vertical threefold axes which are the intersections of three such planes. Scale is given by length of rhombohedral axis indicated in diagram. Parameters as at head of column 5, Table I. Bottom: Sections through half cells, one-half scale of top diagram. Showing, from left to right, the orientation of formate groups corresponding to parameters in columns 3, 4, and 5 of Table I.

properties of the crystals, hardness, brittleness, prismatic habit, and absence of cleavage, this is clearly not the case.

The final alternative is to place the formate groups in the planes of symmetry, the oxygen atoms going into two non-equivalent sets of threefold positions. The range of positions compatible with atomic radii and the structure of the formate group can be easily determined with the aid of a model or sketch corresponding to Fig. 1. After several trials and intensity calculations it was found that the best agreement is obtained with an arrangement wherein three oxygens, marked 0_1 in Fig. 1, form a ring about each gadolinium whereas three other oxygens, marked 0_2 in Fig. 1, form a somewhat closer ring around each threefold axis equidistant between two gadoliniums.

Table I shows the results of the final intensity calculations leading to a choice of parameters. The calculations were made by the usual formula,

$$I \sim F^2 \cdot j \cdot \frac{1+\cos^2 2\theta}{\sin^2 \theta \cos \theta}.$$

In order to be consistent f values for Gd, C, and O atoms,[8] not ions, were used throughout, though it is not to be supposed that the constituents are wholly in the atomic state. In any event, no great change in the calculated intensities would result if ionic f values were used wholly or in part.

All visual estimates of intensities given in Tables I and II were checked by photometer curves.

For each set of values for the oxygen parameters there are two alternative sets of values for the carbon atoms, corresponding to a rotation of the formate group through 180° on the line connecting its two oxygens and bringing the whole group back into the plane of symmetry. Columns 3 and 4 of Table I show intensities for a structure with three oxygen atoms forming an equatorial ring about gadolinium, the carbon lying above (column 3) or below (column 4) the level of the oxygens as drawn. The general agreement is good in both cases, but calculated intensity of $30\bar{3}$

[8] R. W. James and G. W. Brindley, Phil. Mag. 12, 81 (1932).

TABLE I. Calculated and observed intensities in a powder pattern of gadolinium formate. Cr$-K\alpha$ radiation.

1 Indices Hexagonal	2 Indices Rhombohedral	3 Intensities Calculated		4 Intensities Calculated		5 Intensities Calculated		6 Intensities Observed*	7 Intensities Due to gadolinium alone
		z	x	z	x	z	x		
		C 0.12	0.59	0.45	0.86	0.43	0.85		
		O_1 .25	.87	.25	.87	.19	.81		
		O_2 .33	.58	.33	.58	.33	.58		
$11\bar{2}0$	$10\bar{1}$	406		426		418		S	415
$10\bar{1}1$	100	117		147		139		M	167
$30\bar{3}0$	$11\bar{2}$	44	159	43	110	43	127	M-S	98 196
$02\bar{2}1$	$11\bar{1}$	115		67		84			98
$22\bar{4}0$	$20\bar{2}$	90	210	81	225	83	213	VS	65 195
$21\bar{3}1$	$20\bar{1}$	120		144		130			130
$13\bar{4}1$	$21\bar{2}$	87		91		97		S	70
$41\bar{5}0$	$31\bar{2}$	42	69	45	70	46	74	M-S	56 84
$40\bar{4}1$	$31\bar{1}$	27		25		28			28
$01\bar{1}2$	110	47		44		44		M	26
$32\bar{5}1$	$30\bar{2}$	65		73		72		M-S	45
$20\bar{2}2$	200	22		22		16		VW	22
$33\bar{6}0$	$30\bar{3}$	30		35		35		W	19
$12\bar{3}2$	$21\bar{1}$	26		32		40		M	37
$05\bar{5}1$	$22\bar{3}$	16		22		19		VW	17
$24\bar{6}1$	$31\bar{3}$	41		34		30		W-M	32
$31\bar{4}2$	$30\bar{1}$					22		W	32
$60\bar{6}0$	$42\bar{2}$					12			15
$51\bar{6}1$	$41\bar{2}$					30	53	M	30 60
$04\bar{4}2$	$22\bar{3}$					11			15
$52\bar{7}0$	$31\bar{4}$					25		W	29
$23\bar{5}2$	$31\bar{2}$					30		W-M	29
$43\bar{7}1$	$40\bar{3}$					22		VW	30
$50\bar{5}2$	$41\bar{1}$					22		VVW	16
0003	111					5		—	5
$44\bar{8}0$	$40\bar{4}$					23			17
$16\bar{7}1$	$32\bar{4}$					32	55	M	34 51
$42\bar{6}2$	$40\bar{2}$					39		W-M	34
$11\bar{2}3$	210					27		W	35
$15\bar{6}2$	$32\bar{3}$					29		W	37

* Scale of observed intensities: VS very strong, S strong, M medium, W weak, VW very weak.

exceeds that of $21\bar{1}$, contrary to observation. This discrepancy is only slight when the carbons are below (column 4). It is removed and good general agreement extended to all lines by slightly tilting the formate groups from the positions first considered so that the ring of oxygens closest to gadolinium lies at a slightly higher level (column 5). (Compare lower part of Fig. 1.)

In all cases the observed intensity for the first two or three lines is considerably lower than calculation indicates. This is undoubtedly due to the high absorption of gadolinium for x-rays. On this account intensity observations with Cu radiation were disregarded since the absorption of gadolinium for that radiation is much greater than for Cr radiation. Mo radiation would be absorbed less, but the intensities of lines of low glancing angle cannot be closely estimated on the Mo patterns. Since any correction would have to be largely arbitrary none was attempted. In all other respects the final agreement, columns 5 and 6, is satisfactory.

A further check can be obtained from the calculated and observed intensities for the zero layer line of a [111] axis rotation pattern with Cr radiation, Table II. The habit of the crystals, uniform slender hexagonal prisms, closely approaches the cylindrical shape which is ideal for intensity estimation in this case. Though the observed intensity of $10\bar{1}$ again is lower than indicated by calculation the remaining agreement is most satisfactory. This corroborates the parameters chosen from the powder intensity calculations, namely:

Gd in 000

	z	x
3 C in xxz; xzx; zxx	0.43	0.85
3 O_1 in xxz; xzx; zxx	0.19	0.81
3 O_2 in xxz; xzx; zxx	0.33	0.58

Nearly one-half of the total scattering powder of the crystals belongs to Gd at low glancing angles and at higher angles the scattering powder of Gd greatly exceeds that of the formate groups. As a consequence the intensities are largely determined by the Gd. Column 7, Table I, shows the powder intensities due to Gd alone. It is seen that they show a rough correspondence to the observed intensities, but good agreement is obtained only upon taking into account the formate groups. Nevertheless, small shifts in parameters of the formate group have but a

TABLE II. Calculated and observed intensities in the zero layer line of a [111] axis rotation pattern of gadolinium formate. Cr$-K\alpha$ radiation.

Indices Hexagonal	Indices Rhombohedral	Intensity Observed*	Intensity Calculated	Intensity due to Gd alone
$11\bar{2}0$	$10\bar{1}$	S	45.3	45.2
$30\bar{3}0$	$11\bar{2}$	W	8.3	19.0
$22\bar{4}0$	$20\bar{2}$	VS	18.5	14.3
$41\bar{5}0$	$31\bar{2}$	M-S	13.5	16.2
$33\bar{6}0$	$30\bar{3}$	M	11.6	6.5
$60\bar{6}0$	$42\bar{2}$	W	4.5	5.7
$52\bar{7}0$	$31\bar{4}$	M	10.0	11.7
$44\bar{8}0$	$40\bar{4}$	M	9.8	7.3
7180	$32\bar{5}$	VS	31.4	26.0

* Conventions for observed intensities as in Table I.

slight effect on calculated intensities due to the predominant influence of the heavy Gd so that no great accuracy can be claimed for the chosen parameters.

DISCUSSION OF THE STRUCTURE

The dimensions of the formate group corresponding to the chosen parameters may be compared to those found by electron diffraction in gaseous formic acid[9] and in crystalline sodium formate[10] as follows:

	Formic acid	Sodium formate	Gadolinium formate
Bond angle	125°	124°	121°
C–O	1.29A	1.27A	C–O_1 1.27A C–O_2 1.33A

In view of the different position of O_1 and O_2 in Gd formate it seems improbable that there can here be "complete resonance" of the two C–O bonds as previously found in other structures.

Other interatomic distances are:

O_1 to O_2 in same group	2.26A	O_1 to O_1 in ring 3.96A	O_1 to Gd 2.30A
O_1 to O_2 (upward) in next group (downward)	2.67A 3.01A	O_2 to O_2 in ring 2.63A	O_2 to Gd 2.50A

From this it is possible to make an estimate of the radius of the Gd ion, since it has been shown by crystal structure determinations of numerous other compounds that the nearest approach of carboxyl oxygens to adjacent metal ions closely approximates the sum of the ionic radii. Assigning to carboxyl oxygen the radius 1.32A, this leaves a radius of 0.98A for Gd in Gd formate. This value is close to previous estimates of the Gd ionic radius.[11]

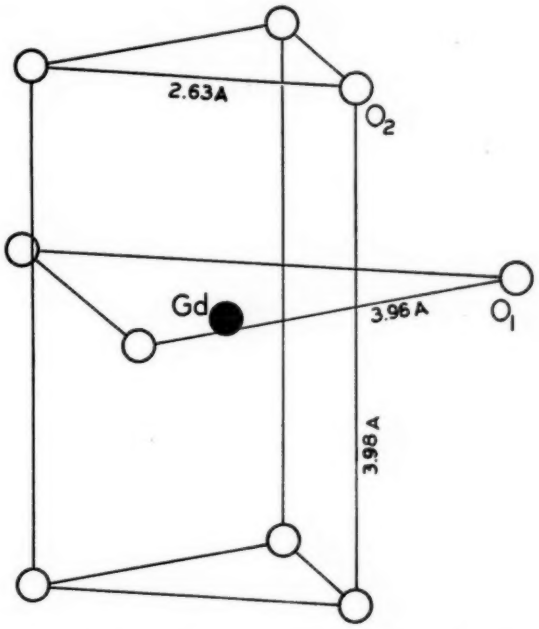

FIG. 2. Clinographic projection to show the ninefold coordination of carboxyl oxygens about gadolinium in gadolinium formate.

The ninefold coordination of oxygen about gadolinium is shown in Fig. 2. This is nearly the same coordination that has been proposed by Ketelaar[12] for Gd and other rare earths in the ethyl sulphates, $R(C_2H_5SO_4)_3 \cdot 9H_2O$. In that case nine water molecules are coordinated about the rare earth atom.

[9] Pauling and Brockway, reference 6.
[10] Zachariasen, reference 6.
[11] L. Pauling and M. D. Shappell, Zeits f. Krist. **75**, 128–142 (1930).
[12] J. A. A. Ketelaar, Physica **4**, 619–630 (1937).

The Electrostatic Influence of Substituents on Reaction Rates. IV.

DONNA PRICE[1,2] AND F. H. WESTHEIMER
Department of Chemistry, University of Chicago, Chicago, Illinois

(Received January 6, 1943)

The rates of saponification of ethyl benzoate, ethyl toluate, ethyl anisate, ethyl *p*-chlorobenzoate, and ethyl *p*-nitrobenzoate have been measured in several alcohol-water mixtures. The relative rates of saponification of the substituted benzoic esters have been compared with those computed by the Kirkwood-Westheimer theory.

IN a recent investigation,[3] the saponification rates of the esters of some aliphatic dibasic acids were measured. It was found that the effect of solvents on the relative saponification rates was roughly in accord with the predictions of electrostatic theory.[4] The present paper deals with the effect of solvent on the relative saponification rates of some aromatic esters. In these cases, the theory is only qualitatively correct, and the work further limits the application of the theory to the aromatic series.[5]

EXPERIMENTAL

Materials

The esters were prepared in the usual manner. The liquids were purified by vacuum distillation; the *p*-nitro derivative by recrystallization from 70 percent alcohol. The constants were:

Ethyl benzoate	b.p. 99°/10 mm,
Ethyl toluate	b.p. 115°/9 mm,
Ethyl anisate	b.p. 144–145°/10 mm,
Ethyl *p*-chlorobenzoate	b.p. 123.2–123.9°/10 mm,
Ethyl *p*-nitrobenzoate	m.p. 57°.

Saponification equivalents for the esters were, in every case, within 0.2 percent of the theoretical value.

The absolute alcohol was dried with magnesium; the alcohol-water mixtures were prepared by measuring the calculated volume of water into a volumetric flask and filling to the mark with alcohol. The alcoholic alkali solutions were prepared by adding stick potassium hydroxide, which had been thoroughly washed with water and then with alcohol mixture, to the appropriate solvent. The solutions were standardized against potassium acid phthalate every three or four days; there was little or no change in the titer. The alcoholic alkali remained satisfactorily colorless when kept in a glass-stoppered bottle.

Method

The saponification rates were determined by titrating from time to time the amount of unreacted alkali present in the reaction mixture. The experimental method was the same as that used in a previous investigation.[3] The thermostat temperature was 50°±0.02. A measured volume of solvent was allowed to come to temperature, and a weighed sample of ester, in an open capsule, was added to the solvent. The reaction was started by adding the potassium hydroxide to this solution. The potassium hydroxide, of the desired strength, was brought to 50° in a stoppered weighing bottle. The bottle was then dropped into the reaction flask and the calibrated sampling pipet inserted. Except for the saponification of the nitro ester, the sampling pipet was filled and allowed to stand for thirty seconds with rinse solution in order to minimize the error due to change in volume with temperature while the sample was being withdrawn. In the case of the nitro derivative, each sample served as a rinsing for the following sample.

The solvent and the potassium hydroxide solution were measured at room temperature by means of a calibrated pipet. The concentrations of ester and potassium hydroxide in the reaction

[1] Samuel S. Fels Fellow in 1942.
[2] Present address: Hercules Powder Company, Wilmington, Delaware.
[3] F. H. Westheimer, W. A. Jones, and R. Lad, J. Chem. Phys. **10**, 478 (1942).
[4] J. G. Kirkwood and F. H. Westheimer, J. Chem. Phys. **6**, 506, 513 (1938); **7**, 437 (1939).
[5] See F. H. Westheimer, J. Am. Chem. Soc. **61**, 1977 (1939); **62**, 1892 (1940).

TABLE I. Saponification rates at 50°.

Compound	Conc. KOH	Conc. ester	Conc. KCl	μ	k in min.$^{-1}$ $(m/1)^{-1}$
		In 30 percent alcohol			
Ethyl benzoate	0.01015	0.01012	—	0.0102	1.64
	.01015	.01016	—	.0102	1.62
	.01015	.01016	0.00757	.0177	1.64
					Average 1.63
Ethyl toluate	.01015	.01014	—	.0102	0.740
	.01015	.01015	—	.0102	0.775
	.01015	.01016	.00924	.0194	0.752
					Average 0.756
Ethyl anisate	.01015	.01015	—	.0102	0.499
	.01015	.01015	—	.0102	0.483
	.01015	.01017	.01017	.0203	0.493
					Average 0.492
Ethyl *p*-chlorobenzoate	.004149	.004161	—	.0041	4.57
	.004149	.004146	—	.0041	4.52
	.004149	.004152	.01148	.0156	4.30
					Average 4.46
Ethyl *p*-nitrobenzoate	.003327	.003322	—	.0033	57.7
	.004149	.004142	—	.0041	66.5
	.004149	.004142	.004114	.0083	63.2
					Average 62.5
		In 60 percent alcohol			
Ethyl benzoate	.01007	.01032	—	.0101	0.641
	.01030	.01032	—	.0103	0.657
	.01530	.01523	—	.0153	0.636
	.02019	.02019	—	.0202	0.641
	.01031	.01031	.05147	.0618	0.684
					Average 0.652
Ethyl toluate	.00980	.01005	—	.0098	0.326
	.01030	.01032	—	.0103	0.312
	.01530	.01524	—	.0153	0.299
	.02019	.02019	—	.0202	0.301
	.01530	.01530	.0470	.0623	0.304
					Average 0.308
Ethyl anisate	.00980	.01005	—	.0098	0.175
	.01030	.01032	—	.0103	0.186
	.01530	.01530	—	.0153	0.184
	.02019	.02019	—	.0202	0.179
	.01085	.01086	.0530	.0639	0.180
					Average 0.181
Ethyl *p*-chlorobenzoate	.00980	.01006	—	.0098	2.20
	.01030	.01029	—	.0103	2.28
	.01530	.01523	—	.0153	2.27
	.02019	.02019	—	.0202	2.29
	.01031	.01031	.01012	.0204	2.52
	.01033	.01033	.01005	.0203	2.19
	.01031	.01031	.03021	.0405	2.38
	.01031	.01030	.04982	.0601	2.38
					Average 2.31
Ethyl *p*-nitrobenzoate	.00980	.01005	—	.0098	40.7
	.01030	.01030	—	.0103	44.8
	.01523	.01524	—	.0152	43.9
	.02019	.02021	—	.0202	40.3
	.01031	.01031	.04699	.0573	43.4
	.01031	.01031	.05058	.0609	41.6
					Average 43.0
		In 90 percent alcohol			
Ethyl benzoate	.01083	.01082	—	.0108	0.270
	.01072	.01071	—	.0107	0.270
	.02091	.02091	—	.0209	0.265
					Average 0.268
Ethyl anisate	.06051	.06077	—	.0605	0.0729
	.06051	.06051	—	.0605	0.0716
	.03099	.03102	—	.0310	0.0715
					Average 0.0717
Ethyl *p*-nitrobenzoate	.01083	.01086	—	.0108	20.6
	.01072	.01072	—	.0107	20.6
	.02091	.02091	—	.0209	21.2
					Average 20.8

TABLE II. Relative saponification rates of substituted esters.

Compound	Δ log k								
	30% alcohol			60% alcohol			90% alcohol		
	Obs.	Calc. $R=5.2$	Calc. $R=5.9$	Obs.	Calc. $R=5.2$	Calc. $R=5.9$	Obs.	Calc. $R=5.2$	Calc. $R=5.9$
Ethyl *p*-nitrobenzoate	1.58	1.55	0.85	1.82	1.60	0.90	1.89	1.70	1.00
Ethyl *p*-chlorobenzoate	0.44	0.65	0.35	0.55	0.65	0.35	0.64[a]	0.70[b]	0.40[b]
Ethyl toluate	−0.33	−0.15	−0.05	−0.33	−0.15	−0.10	−0.33[a]	−0.15[b]	−0.10[b]
Ethyl anisate	−0.52			−0.56			−0.57		

[a] Kindler's data for 87.83 percent alcohol at 35°.
[b] Computed for 87.83 percent alcohol at 35°; see reference (5).

flask were calculated, however, on the basis of the volume at 50°.

The authors wish to thank Mr. L. Frazier for his assistance with the analyses.

RESULTS

The rate constants were determined graphically and were accurate to about 3 percent. Several experiments were tried with varying salt concentrations; as might be expected in the case of a reaction involving uncharged molecules, the salt effects were small. The data are summarized in Table I.

For the esters of monobasic aromatic acids, Δ log k has been defined as the logarithm of the ratio of the saponification constant of the substituted ester to that of ethyl benzoate at the same temperature and in the same solvent. The values of Δ log k have been assembled in Table II. The relative saponification rates at 50° in 90 percent alcohol are comparable to those obtained by Kindler[6] in 87.83 percent alcohol at 35°. The calculated values of Δ log k, given to the nearest 0.05 logarithmic units, have been obtained using the equations and tables previously published.[3,4] The values of the dielectric constant of the alcohol-water mixtures were found by extrapolating Wyman's[7] data from 40° to 50°. The values used were 24.0, 37.1, and 53.8 for 90, 60, and 30 percent alcohol, respectively.

The computation involves as a parameter the value of R, the distance between the dipole of a substituted benzoic ester, and the negative charge contributed to the activated complex by the hydroxide ion. The computations were made using two different values of R. The first value, 5.2A, is the one which most closely reproduces the data obtained by Kindler[5,6] for a large number of esters. When this value of R is used, the theory roughly accounts for the solvent effect in the saponification of the nitro and chloro ester. The observed solvent effect is somewhat greater than that calculated; this result had been foreshadowed by the work of Kilpatrick and Mears[8] on the effect of solvent on the ionization constants of substituted benzoic acids. On the other hand, the value of 5.9A for R, is clearly inadequate, and this is the value which best fits the data for the ionization constants of the substituted benzoic acids. It had previously been noted[5] that in the aromatic as opposed to the aliphatic series, the values of Δ log k for saponification are considerably larger than the values of Δ log K for ionization. No explanation for this fact is at present available.

It should be noted further that the change in solvent does not have a large effect on the Δ log k for the saponification of ethyl anisate. This fact is quite reasonable. The slow rate of saponification of the ethyl ester of dimethylaminobenzoic acid has been shown to be due to a resonance effect,[9] and it is to be expected that the same would be true for ethyl anisate. The stabilization of ethyl anisate can result from resonance involving an ionic structure as well as the usual one; the change of solvent from one rich in water to one rich in alcohol would tend to make the ionic structure less stable with

[6] K. Kindler, Ann. **450**, 1 (1926).
[7] J. Wyman, J. Am. Chem. Soc. **53**, 3292 (1931).
[8] M. Kilpatrick and W. H. Mears, J. Am. Chem. Soc. **62**, 3047 (1940).
[9] F. H. Westheimer and R. P. Metcalf, J. Am. Chem. Soc. **63**, 1339 (1941).

respect to the neutral molecule. This change could only decrease the resonance energy. While this effect would probably be very small, it would be anticipated that the resonance effect would be magnified in solvents of high dielectric constant, whereas the electrostatic effect is minimized

The constancy of the relative saponification rate of ethyl toluate, as well as the comparatively large effect of the methyl group, again suggests the type of conjugation between methyl and phenyl groups postulated by Baker and Nathan.[10]

ACKNOWLEDGMENT

The authors wish to thank the Samuel S. Fels Fund for the financial support which made this work possible.

[10] J. W. Baker and W. S. Nathan, J. Chem. Soc. 1844 (1935); E. D. Hughes, C. K. Ingold, and N. A. Taher, J. Chem. Soc. 949 (1940); R. S. Mulliken, C. A. Rieke, and W. G. Brown, J. Am. Chem. Soc. **63**, 41 (1941).

MARCH, 1943 JOURNAL OF CHEMICAL PHYSICS VOLUME 11

Statistical Mechanics of Binary Mixtures

F. KOTTLER
Research Laboratories, Eastman Kodak Company, Rochester, New York
(Received November 25, 1942)

I

IN the *Journal of Chemical Physics* for May, 1942, there was published a paper by T. Alfrey and H. Mark[1] on a problem in the statistical mechanics of binary mixtures which had been treated previously by R. H. Fowler[2] and his collaborators by an indirect method. The aforementioned authors have attempted a direct derivation of Fowler's results; their attempt, however, seems to me to lack mathematical consistency.

The problem is as follows: Given a lattice of N sites, each being surrounded by z nearest neighbors. N_A molecules of type A and N_B molecules of type B are placed on these sites. There result three different types of pairs of nearest neighbors, AA, BB, and AB. Let N_{AA}, N_{BB}, N_{AB} be their respective total numbers. Obviously, $2N_{AA}+N_{AB}=zN_A$ and $2N_{BB}+N_{AB}=zN_B$ so that the three numbers reduce to a single independent quantity, (say) N_{AB}. Now, the configurational energy depends chiefly on these numbers. For the calculation of the configurational partition function one must know in how many distinguishable arrangements of the molecules over the sites the same value of the configurational energy can be found or, what amounts to the same thing, the same value of N_{AB}. The number of these arrangements is called by Fowler and Guggenheim[2] a "combinatory factor" and denoted by $g(N_{AB})$. If g were known, the configurational partition function would be given by:

$$f_{\text{config}}=\sum_{N_{AB}} g(N_{AB}) \exp(-N_{AB}w/kT). \quad (1)$$

Here, $N_{AB}w$ is the value of the configurational energy referred to a special zero. Since the direct determination of g is difficult, Fowler and Guggenheim treated (1) in several cases indirectly (by means of the "grand partition function"). The value of g is given by them merely as a "guess" and can be written as follows:

$$g\sim(N_{AA}+N_{AB}+N_{BB})!\Big/ N_{AA}!\left(\frac{N_{AB}}{2}!\right)^2 N_{BB}!. \quad (2)$$

Here, a factor independent of N_{AB} remains arbitrary. (Note that the numerator is independent of N_{AB}.)

The form of (2) suggests that g is the solution of a simple combinatory problem where a given

[1] T. Alfrey and H. Mark, J. Chem. Physics **10**, 303–4 (1942).
[2] R. H. Fowler and E. A. Guggenheim, *Statistical Thermodynamics* (Cambridge, 1939), pp. 244–253 (general); pp. 358–366 (liquids); pp. 576–581 (alloys).

number of elements is to be distributed over four groups of N_{AA}, $N_{AB}/2$, $N_{AB}/2$, N_{BB} members, respectively. The pairs cannot be treated as elements, however; they are not independent entities, owing to the overlapping of adjacent pairs. Fowler and Guggenheim knew this perfectly well. They wrote: "This formula . . . cannot be accurate because we cannot treat the pairs as independent entities. Obviously, as soon as we fix the nature of a certain pair of sites this limits the possible manners of occupation of other pairs which share a site with the first pair."

Alfrey and Mark propose to prove (2), and to avoid the difficulty just mentioned. They group the N sites in $N/2$ pairs of nearest neighbors so that each site belongs to one and only one pair. This they call a "reference set of pairs." It should be noted that this is only a fraction of the total numbers of pairs, $Nz/2$, which may be formed between the sites. If the lattice is filled with molecules, three different types of pairs will result among the $N/2$ selected pairs; their respective numbers I shall denote by n_{AA}, n_{BB}, n_{AB}. To find the number of distinguishable configurations, these authors apply the rules of combinatorics to the selected set of pairs, treating them as independent elements. Accordingly, they find a number

$$g' = \left(\frac{N}{2}! \Big/ n_{AA}!n_{AB}!n_{BB}!\right)2^{n_{AB}}. \qquad (3)$$

Is this really the total number of distinguishable configurations of the molecules over the sites which belong to a fixed value of the *total* number of pairs, *viz.*, N_{AB}? Here, the authors adopt a hypothesis, namely:

$$N_{AB} = zn_{AB}. \qquad (4)$$

That is to say, the total number of AB pairs should always be proportional to the number of AB pairs found in the selected set. The authors do not justify (4); they merely say: "This will be true in the overwhelming majority of configurations."

I fail to see that this hypothesis is true. It is impossible to deduce from the *selected* set of pairs anything about the *total* set of pairs. The selection is arbitrary. In one case it may have been made so as to include more pairs of the type AB than in another; the ratio of the number of the selected pairs AB to the total number of such pairs will therefore differ from case to case. Nor is it possible to assume that the hypothesis is true for the probable average of the selections since ordinary statistics are not applicable here because the pairs overlap and are therefore interdependent.

If the hypothesis (4) were correct, it would be possible to prove the formula (2) quite generally: Note that from (4) it follows that $N_{AA} = zn_{AA}$, $N_{BB} = zn_{BB}$ and if Stirling's theorem is applied to (3), this equation reduces to the form (2). However, the hypothesis (4) is incorrect, and therefore so is the proof given by these authors.

The rest of Alfrey and Mark's paper reproduces an argument of Fowler and his collaborators concerning the evaluation of the partition function (1) which is incomplete and requires additional justification (see Part II), although this concerns a point which is usually taken for granted.

II

In a paper[3] presented to this journal on October 14, 1941, I treated the same subject (among other items). I pointed out a special type of mixture for which it is possible to prove Fowler and Guggenheim's formula (2). As far as I can see, this is the only case where this can be done. In view of what has gone before it will be useful to repeat my argument.

The type of mixture adopted whose physical meaning will be discussed later has the following structure: Let the molecules be gathered in clusters and let each cluster be widely separated from the others. Let each cluster consist of a central molecule and a single layer of surrounding outer molecules. The latter's number, z_0, is taken to be so small that the mutual distances of the outer molecules exceed their distances from the center. Under these circumstances the only pairs of closest neighbors are those formed between the centers and the outer molecules. It is obvious that these pairs can be treated as independent entities and hence a proof of (2) becomes possible.

[3] F. Kottler, unpublished paper.

The proof is as follows: Let us consider the sites of the molecules and fill them with molecules A and B. This must be done in such a manner that no ordered structure results, that is to say, there should be no preference of either type of molecules for central or outer sites.

We begin with filling the central sites. There shall be, say, N_A' molecules A and N_B' molecules B on them. Consequently, there remain z_0N_A' molecules A and z_0N_B' molecules B for the outer sites. We may treat separately those clusters with A's at their centers and those with B's at their centers. There are z_0N_A' outer sites in the first clusters altogether. Let X_1 be the number of B's placed among them; the remaining number $z_0N_A'-X_1$, must, therefore, be filled with A's. The number of distinguishable ways in which that can be done is:

$$g_A=(z_0N_A')!/X_1!(z_0N_A'-X_1)!.$$

In a similar manner we obtain for the number of different ways to fill the outer sites of the clusters with B's at their centers:

$$g_B=(z_0N_B')!/X_2!(z_0N_B'-X_2)!,$$

where X_2 is the number of A molecules placed on these outer sites. The total number of different ways to fill the assumed structure with a mixture AB is therefore,

$$g=g_Ag_B=(z_0N_A')!(z_0N_B')!/ X_1!(z_0N_A'-X_1)!X_2!(z_0N_B'-X_2)!. \quad (5)$$

Now, we must have $X_1=X_2$, since there cannot be preference as to the kind of site for any member of a pair AB. Obviously,

$$X_1=X_2=N_{AB}/2, \quad z_0N_A'-X_1=N_{AA}, \quad z_0N_B'-X_2=N_{BB},$$

and hence (5) reduces to the form of (2).

Having thus proved Fowler and Guggenheim's formula for this special mixture it is easy to supply the required justification for their evaluation of the partition function (1) briefly mentioned in Part I. They simply replace the sum in (1) by the greatest term to be found in this sum and remark merely: ". . . the error can as usual be shown to be negligible." The justification is as follows: With the form (5) for g, the series (1) becomes a finite hypergeometric series. The sum can therefore be expressed by a complex integral.[4] This integral, in turn, can be evaluated asymptotically by the method of the saddle point.[5] The result so obtained coincides with the greatest term in series (1).

It remains to discuss briefly the physical meaning of the structure adopted for the mixture. It has certainly nothing to do with a crystalline lattice. Therefore, the above reasoning cannot be applied to the *crystalline* state.* But it seems to me that a limiting stage of the *liquid* state may exist where it applies. As a matter of fact, a dense gas in the transition to liquefaction may consist of the clusters as described. If the density of the liquid increases, these clusters will acquire more than one outer layer and their distances will decrease. Moreover, the coordination number will increase from the low value z_0 to the value for closest packing. There is no experimental evidence, so far as I can see, against the assumption of such a limiting stage. For liquid mixtures, formula (2) may, therefore, be regarded as a useful approximation which is accurate for the assumed limiting stage of the liquid. Unfortunately, our knowledge of the liquid mixtures is not sufficiently advanced to permit an examination of the refined theory based on formula (2).

---

[4] E. T. Whittaker and G. N. Watson, *A Course of Modern Analysis* (Cambridge University Press, Cambridge, 1940), p. 292.

[5] R. Courant and D. Hilbert, *Methoden der Mathematischen Physik* I (J. Springer, Berlin, 1924), pp. 430 *et seq.*

* Formula (2) for a crystalline mixture appears to be incapable of direct proof and is probably not true. Some indication of this may be deduced from the numerical failure of the deductions based on the formula (2) or its analogue, in the explanation of certain anomalies of the specific heats of alloys (reference 2).

Letter to the Editor

PROMPT publication of brief reports of important discoveries in physics may be secured by addressing them to this department. The closing date for this department is the third of the month. Because of the late closing date for the section no proof can be shown to authors. The Board of Editors does not hold itself responsible for the opinions expressed by the correspondents. Communications should not in general exceed 600 words in length.

The Electrical Capacity of the Double Layer

W. G. EVERSOLE AND CHARLES R. ESTEE
Division of Physical Chemistry, State University of Iowa, Iowa City, Iowa
January 21, 1943

IN a recent article,[1] J. J. Bikerman has extended the theory of the diffuse double layer to high potentials and high concentrations by taking into account, (1) the "saturation" effect which relates the maximum possible concentration of ions in the double layer to the size of the ions and the space which is available, and (2) the electrical energy resulting from the polarization of hydrated ions and polar solvent molecules. It becomes desirable, therefore, to define the range of "low" potentials and "low" concentrations in which the equations of a recent paper[2] of the present authors are reasonably valid. This can be done only in a very approximate fashion since the evaluation of the factors (1) and (2) requires a knowledge of the volume of the hydrated ion and its effective moment. However, at least the order of magnitude of this range can be estimated.*

(1) The saturation effect should not be the limiting factor as long as the total ion concentration is less than 12 moles per liter. This is less than the ion concentration in a saturated solution of sodium chloride and corresponds to the condition, $2C^0 \cosh 2\bar{\psi} \leqq 12$, which gives $\psi \leqq 60$ millivolts if C^0 is 1 mole per liter and $\psi \leqq 290$ mv at 10^{-4} molar.

(2) The polarization effect is more difficult to estimate since it involves the difference between the polarization of a hydrated ion and that of an equal volume of solvent molecules. However, the ion should displace approximately one water molecule and exert an undetermined influence on a few others distributed spherically with respect to the ion. This effect should not be important if the electrical energy of an ion ($\epsilon\psi$) is much greater than the electrical energy of a water dipole ($\bar{m}(d\psi/dx)$) where $\bar{m}$ is the average moment of the dipole in the direction of the field. For a water molecule (assumed rigid, with a moment of 1.84×10^{-18} and with free rotation) the value of the ratio $r\,(=\bar{m}(d\psi/dx)/\epsilon\psi)$ in 1 molar solution is 0.014 at $\psi=50$ mv and 0.064 at $\psi=100$ mv. In 10^{-4} molar solution $r=3\times10^{-5}$ at $\psi=150$ mv and $r=3\times10^{-3}$ at $\psi=260$ mv.

Therefore, the neglect of these factors should not greatly reduce the accuracy of the equations derived in the previous paper[2] in the experimentally determined range of ζ-potential values. ζ-potentials greater than 100 mv have rarely been observed and such values have been found only in very dilute solutions where ζ and ψ^0 are not very different (Eq. (3)).

Bikerman's equation for low potentials, on the other hand, involves the assumption that $\sinh 2\bar{\psi} = 2\bar{\psi}$, and, therefore, (allowing a 10 percent error) use of this equation should be limited to the range of potentials where $\sinh 2\bar{\psi} \leqq 1.10(2\bar{\psi})$. This corresponds to the condition $\psi \leqq 20$ mv at all concentrations. At such low potentials (1) and (2) are negligible and, therefore, his equation for the capacity of the double layer is the classical one, $C' = D\kappa/4\pi$, values of which are given in Table II.[2] This gives a "thickness" of the ion atmosphere ($1/\kappa$) which is independent of the electrical condition of the surface. Actually this thickness decreases rapidly with increasing values of the surface potential (Eq. (12)).

Bikerman's equation for high potentials may be applied to the conditions existing near the surface where higher field strengths lead to "saturation" of the surface volume and deformation of ions and molecules. It should not be extended to low potentials (or to greater distances from the surface) since it assumes that one of the ion species is excluded from the outer double layer. From the standpoint of the present equations[2] for "low" potentials its importance lies in the region between the surface of the solid and the ψ^0 plane. For "high" potentials this may be greater than a single molecular thickness. It has long been recognized that such a region is frequently required to account for a large difference between the total potential difference across a phase boundary and the ζ-potential. For example, if the ζ-potential of mercury were equal to the total potential difference between mercury and a normal solution, a mercury droplet detached from a calomel electrode should be expected to have a cataphoretic mobility corresponding to a ζ-potential of over 500 mv. Such high cataphoretic mobilities have not been observed even in dilute solutions.

[1] J. J. Bikerman, Phil. Mag. **33**, 384 (1942).
[2] W. G. Eversole, and C. R. Estee, J. Chem. Phys. **11**, 63 (1943).
* The symbols and equation numbers of this note are those of reference 2.

THE AMERICAN INSTITUTE OF PHYSICS

INCORPORATED

ADMINISTRATIVE STAFF

HENRY A. BARTON, *Director*

MADELINE M. MITCHELL, *Publications Manager*

JOHN T. TATE, *Adviser on Publications*

Office: 175 Fifth Avenue, New York, New York

JOURNALS

THE PHYSICAL REVIEW

REVIEWS OF MODERN PHYSICS
JOHN T. TATE, *Editor (on leave)*
J. W. BUCHTA, *Acting Editor*

JOURNAL OF THE OPTICAL SOCIETY OF AMERICA
GEORGE R. HARRISON, *Editor*

THE JOURNAL OF THE ACOUSTICAL SOCIETY OF AMERICA
FLOYD A. FIRESTONE, *Editor*

AMERICAN JOURNAL OF PHYSICS
DUANE ROLLER, *Editor*

THE REVIEW OF SCIENTIFIC INSTRUMENTS
GAYLORD P. HARNWELL, *Editor*

THE JOURNAL OF CHEMICAL PHYSICS
JOSEPH E. MAYER, *Editor*

JOURNAL OF APPLIED PHYSICS
ELMER HUTCHISSON, *Editor*

GOVERNING BOARD

PAUL E. KLOPSTEG, *Chairman*
Central Scientific Company

GEORGE B. PEGRAM, *Secretary*
Columbia University

For the American Physical Society:

L. A. DUBRIDGE
University of Rochester

GEORGE B. PEGRAM
Columbia University

JOHN T. TATE
University of Minnesota

For the Optical Society:

R. C. GIBBS
Cornell University

A. C. HARDY
Massachusetts Institute of Technology

K. S. GIBSON
National Bureau of Standards

For the Acoustical Society of America:

FLOYD A. FIRESTONE
University of Michigan

HARVEY FLETCHER
Bell Telephone Laboratories

WALLACE WATERFALL
The Celotex Corporation

For the Society of Rheology:

R. B. DOW
Aberdeen Proving Ground

HERMANN MARK
Brooklyn Polytechnic Institute

N. W. TAYLOR
The Pennsylvania State College

For the American Association of Physics Teachers:

GEORGE R. HARRISON
Massachusetts Institute of Technology

PAUL E. KLOPSTEG
Central Scientific Company

A. G. WORTHING
University of Pittsburgh

The American Institute of Physics is a membership corporation of which five societies are the founding members. These five societies are the principal national societies devoted to pure and applied physics in America. Their names, and those of their representatives who form the Governing Board of the Institute, are given above. The principal work of the Institute is the publication of journals sponsored by the societies or by itself. The names and the editors of the journals are also listed above.

The broad purpose of the Institute is to represent, in all matters of wide or common interest, the five thousand or more members and subscribers associated with the Founder Societies and the journals. It aims to advance the science and profession of physics, and to promote cooperation between pure research, the applied sciences and the industries. To achieve these aims, it is greatly in need of an endowment and is empowered by law to administer grants and funds of any kind.

CONTENTS

THE JOURNAL OF CHEMICAL PHYSICS Vol. 11, No. 3 MARCH, 1943

Vibrational Frequencies of the Isotopic Water Molecules; Equilibria with the Isotopic Hydrogens . . . . . W. F. LIBBY 101

Surface Recombination of H Atoms and OH Radicals . . . . . W. V. SMITH 110

Mechanical Properties of Polymeric Materials . . . . . ARTHUR TOBOLSKY AND HENRY EYRING 125

Diffusion of Air Through Metal Metal . . . . . H. S. COLEMAN AND H. L. YEAGLEY 135

Note Concerning I-Type Doubling in Linear Polyatomic Molecules . . . . . HARALD H. NIELSEN AND WAVE H. SHAFFER 140

Crystal Structure of Gadolinium Formate, Gd(OOCH)$_3$ . . . . . A. PABST 145

Electrostatic Influence of Substituents on Reaction Rates. IV . . . . . DONNA PRICE AND F. H. WESTHEIMER 150

Statistical Mechanics of Binary Mixtures . . . . . F. KOTHLER 153

Letters to the Editor:

Molecular Capacity of the Double Layer . . . . . W. G. EVERSOLE AND CHARLES E. REESE 156

LANCASTER PRESS, INC., LANCASTER, PA.